

Production and Characterization of Wheat Gluten Films

by
Jamie Lee Anne Cousineau

A thesis
presented to the University of Waterloo
in fulfilment of the
thesis requirement for the degree of
Master of Applied Science
in
Chemical Engineering

Waterloo, Ontario, Canada, 2012

© Jamie Lee Anne Cousineau 2012

Author's Declaration

I hereby declare that I am the sole author of this thesis. This is a true copy of the thesis, including any required final revisions, as accepted by my examiners.

I understand that my thesis may be made electronically available to the public.

Abstract

Biodegradable, edible wheat gluten films offer a renewable alternative to plastic food packaging or can be incorporated directly in the food product. Wheat gluten is a good option because it forms a fibrous network, lending strength and elasticity to films. The goal of this research project was to produce, with a water-based film formulation and methodology, smooth, homogeneous wheat gluten films with low water vapour permeability (WVP). The water-based film formulation also served to compare the FT Wonder wheat cultivar, grown in Ontario, to commercially produced wheat gluten and determine the effect of wheat source on the film properties, surface morphology, surface hydrophobicity, WVP, and film swelling in water for different pH, temperature and casting surface conditions. Fluorescence, SPR, and casting formulation viscosity provided preliminary information on the mechanism of film formation and on gluten protein structure induced by modifying the film formulation.

Films cast on a silicone surface were less hydrophobic than films cast on a glass surface coated with silicone grease (contact angles of 80.6° and 91.1° respectively). Examination of the top of the film surface by FTIR revealed the presence of silicone for the gluten films cast on the glass surface coated with silicone grease. Casting on a silicone surface resulted in smoother, more homogeneous films than the glass surface. Thus, the silicone surface was chosen for the wheat gluten films produced and characterized in this project.

The gluten solution temperature affected film surface hydrophobicity determined by water contact angle and surface morphology obtained by visual inspection when the temperature was varied between 70, 80 and 100°C. The highest surface hydrophobicity was observed at 70°C for films produced from old Wonder wheat (top and bottom contact angles of 68.5° and 93.1° respectively) and 80°C for the new Wonder wheat (top and bottom contact angles of 63.4° and 84.3° respectively). The most hydrophobic surface for ADM gluten films was obtained on the top film surface when the gluten solution was heated to 100°C (contact angle of 79.5°) but was most hydrophobic on the bottom surface when the gluten solution was heated to 80°C (contact angle of 92.0°). Surface morphology revealed a much more heterogeneous surface, containing protein aggregates, when films were produced from a gluten solution at 100°C, irrespective of gluten source. Intrinsic fluorescence spectroscopy measurements of the film surface revealed a blue shift for the tryptophan peak which increased with increasing gluten solution temperature, suggesting the occurrence of molecular structural changes as gluten solution temperature was increased. These results suggest that gluten proteins adopted different conformation in the dry film according to the gluten solution temperature.

Smoother more homogeneous surface morphology was observed for films cast from pH 11 gluten solutions compared to films produced from pH 4 gluten solutions. Lower water vapor permeability was also observed at pH 11 (average of 361 g.mm/(day.m².atm) for the three wheat sources) compared to pH 4 (averaged of 891 g.mm/(day.m².atm) for the three wheat sources) and was attributed to a higher degree of protein aggregation induced at pH 11. The lower degree of protein networking in the pH 4 film resulted in a higher water vapour permeability by producing a more heterogeneous, uneven film with higher content of voids and capillaries and larger surface area for vapour to contact. The larger surface area interfacing with the water vapour, as well as the looser protein network resulting from a lower degree of protein aggregation both combined to produce higher water vapour permeability in the pH 4 film compared to the pH 11 film. Higher surface hydrophobicity was observed for most films cast from the Wonder wheat source at pH 4 (average contact angles of 79° and 86° on top and bottom respectively) compared to pH 11 films (average contact angles of 64° and 86° on top and bottom respectively). The effect of pH on Wonder gluten was also observed by intrinsic fluorescence spectroscopy analysis which showed increased tryptophan peak intensity for pH 4 films (average intensity of 139 and 120 on top and bottom surfaces respectively) compared to pH 11 films (average intensity of 116 and 71 on top and bottom surfaces respectively), suggesting changes in protein conformation also occurred. SPR studies revealed a reduced attraction of gluten molecules to hydrophilic SAM surfaces for solutions at pH 11 compared to pH 7.7, suggesting that there exists a higher electrostatic repulsion between the negative charge on the amino acids of gluten in pH 11 solutions and the SAM surfaces. Gluten solution viscosity also increased with increasing pH, suggesting a higher degree of intermolecular penetration and aggregation of protein, which may explain the improved WVP for films prepared at pH 11.

Surface hydrophobicity of films was more consistent for films prepared with commercial gluten compared to laboratory produced gluten from Wonder wheat cultivar. The commercial gluten films had more hydrophobic surfaces for all gluten solution temperatures investigated (contact angle range of 76.4 - 79.5° on the top surface and 75.4 - 92.0° on the bottom surface). Intrinsic fluorescence spectroscopy measurements of commercial gluten films revealed 1.4 to 1.7 times higher tryptophan peak intensities compared to laboratory produced Wonder gluten films, suggesting molecular differences according to gluten preparation or gluten type. The surface morphology of films produced from laboratory prepared gluten of Wonder wheat was very different than for commercial gluten films. The laboratory prepared gluten films had dark flecks spread throughout and an irregular texture, whereas the commercial gluten films had no dark flecks and a much smoother surface texture.

For commercial and new Wonder gluten, conditions of pH 11 and 80°C produced the smoothest, most homogeneous and most hydrophobic gluten films with the lowest water vapour permeability (345 and 292 g.mm/(day.m².atm) respectively). Films prepared from old Wonder gluten produced the smoothest, most homogeneous and most hydrophobic gluten films with the lowest water vapour permeability (370 g.mm/(day.m².atm)) when the gluten solution conditions were pH 11 and 70°C.

This research provides an alternate use for some Ontario wheat cultivars based on their properties in films compared to commercial sources of gluten. As a result, using Ontario cultivars to prepare gluten film packaging material has potential as an alternate source of income for Ontario farmers. This research also defines the film properties for gluten films produced from aqueous solutions, helping to identify processing parameters that could bring gluten films on par with plastic packaging and make gluten films a viable alternative food packaging material. Finally, it was determined that the water vapour permeability of wheat gluten films was not correlated to film surface contact angle.

Acknowledgements

Thank you to my supervisors Christine Moresoli and Raymond L. Legge for all of their support during my time as a master's student. I would not have started, let alone finished, a masters degree without their guidance and encouragement over the course of the last few years.

I would like to acknowledge the financial support of the Ontario Ministry of Agriculture, Food and Rural Affairs (OMAFRA). Also, thank you to the Archer Daniel Muler (ADM) company for the ample supply of commercial grade wheat gluten.

I would like to acknowledge the work done by Dr. Chia of the University of Guelph in preparing wheat gluten from wheat grain for a large part of the Ontario cultivar gluten. I would also like to thank Dr. Chia and Dr. Pauls for lending me the use of their freeze dryer, Dr. Peldszus for the use of her Drop Shape Analysis (DSA) machine, and Dr. Simon for the use of his FTIR and optical microscope.

Special recognition and appreciation are extended to all of the members of the Legge-Moresoli lab group for their friendship and for all the knowledge and wisdom they shared with me in the lab and as I wrote my thesis. It has helped to shape my thesis as well as my personal outlook on life. Thank you to Ramila Peiris for his training on the fluorescence spectroscope and data processing assistance, to Barbara Guettler for training me on the FTIR, TGA, and DSA machines, and to Nick Ignagni for help preparing the SAM layer for SPR and training me on the SPR. I am grateful to Barbara Guettler, Katharina Hassel, Sarah Mercer-Meunier, and Rachel Campbell for their suggestions and guidance in data processing and thesis writing techniques. I would also like to thank Steven Reynaert for performing viscosity, UV-Vis, and total solids measurements, Eureka Choi for measuring the film swelling properties of my gluten films, and Ross Arnold for his help reviewing my thesis document for formatting errors.

I would like to express my deepest gratitude to my family, Lawrence, Pauline and Benjamin Durham, for their love, support, and enthusiasm in every aspect of life, which they have shared with me my whole life through. Finally I want to thank my husband, Jonathan Cousineau, from the bottom of my heart for his continual supply of love, support, and encouragement throughout the last 5 years of my life. You helped me through the tough times and brought me smiling and laughing through the great times.

Table of Contents

Author's Declaration	ii
Abstract	iii
Acknowledgements	vi
Table of Contents	vii
List of Figures	xi
List of Tables.....	xiii
List of Abbreviations.....	xv
List of Symbols	xvi
1 Introduction	1
1.1 Research Motivation.....	1
1.2 Research Objectives	2
1.2.1 Goal	2
1.2.2 Hypotheses	2
1.2.3 Objectives.....	2
2 Literature Review	3
2.1 Wheat	3
2.2 Wheat Flour to Wheat Gluten	4
2.2.1 Primary through Quaternary Structure of Wheat Gluten Proteins	6
2.3 Wheat Gluten Films.....	7
2.4 Techniques and Film Properties.....	11
2.4.1 Dynamic Thermogravimetric Analysis (TGA)	11
2.4.2 Surface Plasmon Resonance (SPR).....	12
2.4.3 Contact Angle and Surface Hydrophobicity	12
2.4.4 Water Vapour Permeability (WVP).....	14
2.4.5 Fluorescence Spectroscopy.....	15

2.4.6	Fourier Transform Infra-Red (FTIR)	15
3	Materials and Methods	18
3.1	Materials.....	18
3.2	Film Preparation	18
3.3	Film Thickness	19
3.4	Kjeldahl Analysis	19
3.5	Surface Plasmon Resonance (SPR).....	20
3.6	Viscosity.....	21
3.7	Thermogravimetric Analysis (TGA).....	21
3.8	Film Surface Investigation.....	22
3.9	Contact Angle (CA).....	22
3.10	Fourier Transform Infra-Red (FTIR) Spectroscopy	23
3.11	Fluorescence Spectroscopy	23
3.12	Water Vapour Permeability (WVP).....	24
3.13	Film Swelling	24
3.14	Statistical Analysis	25
4	Results and Discussion	26
4.1	Investigation of Film Ingredients.....	26
4.1.1	Analysis of Gluten Protein Content	26
4.1.2	Surface Plasmon Resonance (SPR).....	28
4.1.3	Kinematic Viscosity of Aqueous Wheat Gluten and Glycerol Solutions as a Function of pH and Solution Density	33
4.2	Thermal Stability of Wheat Gluten, Glycerol, and Wheat Gluten Films.....	37
4.2.1	Thermal Stability of Primary Film Ingredients: Wheat Gluten and Glycerol.....	37
4.2.2	Thermal Stability of Wheat Gluten Films	41
4.3	Film Surface Investigation.....	46

4.3.1	Film Surface Morphology - Effect of Modifying ADM Film Preparation Methodology	46
4.3.2	Film Surface Morphology - Effect of Wheat Gluten Source	50
4.3.3	Conclusions	58
4.3.4	Surface Film Hydrophobicity - Effect of Modifying ADM Film Preparation Methodology	60
4.3.5	Surface Film Hydrophobicity - Effect of Wheat Gluten Source and Contact Surface During Drying	66
4.3.6	Conclusions	71
4.4	Study of Protein Conformation by Fluorescence Spectroscopy on Top and Bottom Film Surface with Varying pH and Temperature of Casting Solution.....	73
4.5	Gluten Film Water Vapour Permeability	79
4.5.1	Effect of Modifying ADM Film Preparation Methodology	79
4.5.2	Effect of Wheat Gluten Source	82
4.5.3	Conclusions	84
4.6	Film Swelling	85
4.6.1	Conclusions	87
5	Conclusions	88
6	Future work	92
	References	94
	Appendix 1 – WVP Sample Calculation (metric units)	103
	Appendix 2 – Reported FTIR Peaks for Wheat Gluten, Glycerol, and Water	105
	Appendix 3 – Typical Amino Acid Sequences for Various Wheat Gluten Protein Classes	107
	Appendix 4 - Images of top and bottom surfaces of gluten film cast on a glass tray with a silicone release layer.....	109
	Appendix 5 - Gluten Preparation Method Comparison	110
	Appendix 6 - ADM Whetpro 80 Data Sheet.....	111
	Appendix 7 - Total Protein Content Sample Calculation for Kjeldahl Method	112

Appendix 8 - Viscosity Sample Calculation.....	115
Appendix 9 - TGA Estimating 1% Onset of Degradation.....	116
Appendix 10 - Film Swelling Sample Calculations	117

List of Figures

Figure 1 - Simplified Diagram of a Wheat Grain Cross-Section. Adapted from Wrigley et al. (Wrigley 2000)	4
Figure 2 - Wheat Flour and Wheat Protein Composition, Based on Information Gathered from Literature (Veraverbeke, Delcour 2002, Pareyt, Delcour 2008)	4
Figure 3 - Types of Glutenin Protein, Based on Information Gathered from Literature (Lafiandra et al. 2000). HMW and LMW Stand for High and Low Molecular Weight Respectively. B, C, and D type LMW Reflect Differences in Biochemical Characteristics. The sub-classes s, m, and i of B type LMW reflect the starting amino acids serine, methionine, and isoleucine, respectively, at the N-terminal.....	5
Figure 4 - Diagram of Water on Hydrophobic and Hydrophilic Surfaces with Contact Angle Location Designated by Theta.....	13
Figure 5 - SPR Sensorgram of Wheat Gluten in Milli-Q Water (1 mg/ml) at (A) pH 7.7 and (B) pH 11 on a Hydrophilic SAM (note the different scales for the ordinate axes)	28
Figure 6 - Kinematic Viscosity as a Function of Gluten-Glycerol Solution pH.....	33
Figure 7 - Density as a Function of Gluten-Glycerol Solution pH.....	34
Figure 8 - Kinematic Viscosity as a Function of Density for Gluten-Glycerol Solutions, Caused by pH Change	35
Figure 9 - Thermogravimetric (TGA) and Differential Thermogravimetric (DTGA) Curves Conducted in Nitrogen at a rate of 50 ml/min for Gluten from the Ontario Cultivars (A) Wonder, (B) Emmit, (C) Harvard, and (D) Norwell, as well as the Commercial Wheat Glutens (E) Sigma and (F) ADM Whetpro80.....	38
Figure 10 - Sample TGA and DTGA curves for Glycerol	41
Figure 11 - Thermogravimetric (TGA) and Differential Thermogravimetric (DTGA) Thermograms performed under Nitrogen with a flow rate of 50 ml/min for Gluten Films Containing Glycerol (A) ADM WP80 Film or No Glycerol and Cast at Varying Stages of the Film Solution Preparation: (B) NGT30pH7, (C) NGT30PH11, (D) NGT70pH11, (E) NGT70pH11sonicated.....	43
Figure 12 - Microscope Images of ADM Gluten Film Surface (Gluten solution at pH 11, 70°C) Cast on (A) Glass Surface with Silicone Release Layer and (B) Silicone Surface with no Release Layer. 46	
Figure 13 - Camera Images of ADM Gluten Films Cast from Solutions Heated to (A) 70 °C, (B) 80 °C, and (C) 100 °C. Arrow denotes an example of a raised bump.....	48
Figure 14 - Camera Images of ADM Gluten Films Cast from Gluten Solutions Adjusted to (A) pH 11 and (B) pH 4.....	50
Figure 15 - Terms Describing Key Features of Wheat Gluten Film Surface Morphology	51

Figure 16 - FTIR Spectra for Top Surface of Films Cast on Glass and Silicone Surfaces (arrows indicate positions characteristic for silicone)..... 61

Figure 17 - Fluorescence FEEM of the Black Background Surface before placing a gluten film: (A) 3D and (B) Contour. Example Fluorescence FEEM of New Wonder Wheat Gluten Film (70°C, pH 11) Top Surface: (C) 3D and (D) Contour. 73

Figure 18 - Kjeldahl Absorbance as a function of Concentrations..... 113

Figure 19 - Sample Data Set: TGA and DTGA curves for Wonder Wheat Gluten..... 116

Figure 20 - BSA Calibration Curve for Wheat Gluten Concentration Estimate (vertical error bars are shown on graph but are very small)..... 118

List of Tables

Table 1 – Estimated pI Values for Various Glutenin and Gliadin Types with a Known Amino Acid Sequence	10
Table 2 - Description of Each Phase of the SPR Response Curve	12
Table 3 - Common FTIR Peaks Characteristic of Protein, According to Barth et al. (Barth 2007)	16
Table 4 - Protein Content by Kjeldahl Analysis for Various Wheat Sources (Nitrogen to Protein Conversion factor of $n=5.7$)	26
Table 5 - Description of Each Phase of the SPR Sensorgrams	28
Table 6 - Key Characteristics of the SPR Sensorgrams Calculated for RU Signal Changes of Aqueous Wheat Gluten Solution	29
Table 7 - Wheat Gluten Proteins with Molecular Weight, Radius of Gyration, and Relative Contribution to Total Wheat Gluten Mass.....	32
Table 8 - Kinematic Viscosity and Density of Aqueous ADM Wheat Gluten and Glycerol Casting Solutions at Alkaline pH	33
Table 9 - Characteristics of the Thermogravimetric Analysis Conducted in Nitrogen at a Flow Rate of 50 ml/min for Glycerol and Gluten from Four Different Ontario Wheat Cultivars and Two Commercial Sources	39
Table 10 - Description of Gluten Film Preparation Conditions Without Glycerol.....	41
Table 11 - Characteristics of the Thermogravimetric Analysis Conducted under Nitrogen at a Rate of 50 ml/min for Gluten Films Cast With and Without Glycerol and at Varying Stages of Film Solution Preparation	44
Table 12 - Pictures of Gluten Films with Varying Wheat Gluten Source and Processing Temperature	52
Table 13 - Microscope Images (12.6 x) of Gluten Films for different Wheat Gluten Sources and Gluten Solution Processing Temperatures.....	54
Table 14 - Pictures of the Gluten Film Surface for Different Wheat Gluten Sources and Solution pHs	56
Table 15 - Microscope Images (12.6 x) of Gluten Films for Different Wheat Gluten Sources and Gluten Solution pHs	57
Table 16 - Contact Angles for ADM Gluten Films Cast on Silicone and Glass Surfaces (70°C, pH 11)	60
Table 17 - FTIR Peaks Associated with Silicone	60
Table 18 - Contact Angles for Wheat Gluten Films Cast with Commercial Wheat Gluten	62

Table 19 - Contact Angle of ADM Gluten Films at pH 11 according to Gluten Solution Heating Temperature	63
Table 20 - Contact Angle for Gluten Films made from Solutions Heated at 70 °C and Adjusted to pH 4 and pH 11	64
Table 21 - Effect of Varying Gluten Solution Temperature and Wheat Gluten Source on Film Surface Contact Angle. Silicone Casting Surface and pH 11 Solution.	66
Table 22 - Effect of the pH of the Gluten Solution and Wheat Gluten Source on Film Surface Contact Angle for Gluten Solutions Heated to 70 °C.	68
Table 23 - Emission Wavelengths and Associated Intensities (Average + Standard Error, n=2)) for Local Maxima at the 290 nm Excitation Wavelength from Fluorescence Spectra of the Top and Bottom Surface of Gluten Films for Preparation Method (Temperature and pH) and Wheat Gluten Source.	75
Table 24 - Shift of the Emission Wavelength from 333 nm (Reported for Viscous Wheat Gluten Dough, (Genot et al. 1992)) for Top and Bottom Gluten Film Surfaces Prepared at Varying Temperature and pH.....	76
Table 25 - WVP of ADM Gluten Films According to Casting Surface (gluten solution at 70 °C and pH 11).....	79
Table 26 - Literature WVP for Wheat Gluten Films Cast with Commercial Wheat Gluten	80
Table 27 - WVP of ADM Gluten Films Made from Gluten Solutions Heated to 70, 80, and 100 °C and pH 11	81
Table 28 - Average WVP of ADM Gluten Films Made from Gluten Solutions Adjusted to pH 4 and pH 11.....	82
Table 29 - WVP and Thickness of Gluten Films according to Gluten Solution Temperature, pH and Wheat Source	83
Table 30 - Swelling Ratios for Film Samples Soaked for One Hour or Twenty-Four Hours.....	85
Table 31 - Total Solids Content of the Film Soaking Water after 24 h (Dried at 100 °C).....	86
Table 32 - BSA Equivalent Total Protein Mass in Film Soaking Solution after 24 h using Absorbance at 280 nm.....	87
Table 33 – Major FTIR Gluten Protein Peaks according to Literature	105
Table 34 – Major FTIR Glycerol and Water Peaks of Gluten Films according to Literature.....	105
Table 35 – Major FTIR Peaks Characteristic of Proteins (Barth et al. ((Barth 2007)).....	106
Table 36 - Kjeldahl Standard Absorbances as a function of Concentrations	113

List of Abbreviations

ATR-FTIR	Attenuated total reflectance Fourier transform infra-red
BSA	Bovine serum albumin
CA	Contact angle (°)
DTGA	Derivative of TGA curve (rate of mass change over time)
EEM	Excitation-emission matrix
FTIR	Fourier transform infra-red
HMW	High molecular weight
HSA	Human serum albumin
LMW	Low molecular weight
MW	Molecular weight (kDa)
pI	Isoelectric point
RU	Response unit
SAXS	Small-angle X-ray scattering
SAM	Self-assembled monolayer
SPR	Surface plasmon resonance
TGA	Thermogravimetric analysis
WVP	Water vapour permeability (g.mm/ (day.m ² .atm))

List of Symbols

q	Swelling ratio
R_g	Radius of gyration (nm)
$\Delta W\%$	Change in weight percent
λ_{ex}	Excitation wavelength (nm)
λ_{em}	Emission wavelength (nm)
θ	Contact angle ($^\circ$)

1 Introduction

1.1 Research Motivation

Food packaging has become an integral part of food production and distribution in most of the developed world. Packaging food keeps freshness, avoids external contamination and can serve for marketing and as a source of information to consumers (Marsh, Bugusu 2007). One of the main packaging materials used today is plastic. Unfortunately, plastic films are much more difficult to identify and separate from waste compared to more rigid forms of plastic (Marsh, Bugusu 2007), with the result that significant quantities of plastic film from food packaging ends up as waste and far outlasts its use. Therefore, research into biodegradable and renewable alternatives for packaging materials is needed.

Gluten, the protein from wheat grain, is one such renewable and biodegradable alternative. Wheat gluten protein, a renewable resource, is capable of forming a fibrous network which lends strength, elasticity, and plasticity when formed into a film with glycerol (Shewry et al. 2002, Gontard, Guilbert & Cuq 1993). Research and characterization of wheat gluten protein films using Ontario wheat cultivars could lead to an alternative application for Ontario farmers and their crops, potentially increasing revenue at the farm gate.

Ethanol is a common solvent for lab scale preparation of wheat gluten films because of the solubility of gluten in ethanol, allowing for a homogeneous dispersion of wheat gluten to be obtained easily. However, at the industrial scale, green solvents are desired since environmental and health risks are significantly reduced. Therefore, environmentally friendly techniques for casting wheat gluten films from aqueous dispersions are needed.

The wheat gluten films investigated in this research project were designed to replace plastic wrap for the packaging of cookies. Nylon and polystyrene are some common choices for cookie packaging plastics and have water vapour permeabilities of 7.5 and 3.9 g.mm/(m².day.atm) respectively (Massey 2003). However, gluten films are known for their great gas barrier qualities, not their water vapour barrier qualities and have water permeability values in the hundreds instead of the tens (Olabarrieta et al. 2006). Ideally, water vapour permeability should be reduced below 20 g.mm/(m².day.atm) to provide food packaging with preservation times comparable to plastics. It is hoped that water vapour permeability in gluten films can be reduced by increasing surface smoothness and film homogeneity, tightening the protein network and increasing surface hydrophobicity. Due to the prevalence of gluten allergies and celiac disease, gluten films should be limited to wheat containing foods.

1.2 Research Objectives

1.2.1 Goal

Prepare water-based gluten films and investigate film properties and protein structure by modifying selected elements of the film formulation and preparation for two gluten types, Ontario wheat cultivar and commercial gluten.

1.2.2 Hypotheses

1. Changing the casting surface from a silicone grease coated glass tray to a flexible silicone tray should produce more uniform and homogeneous film, but may also increase the water vapour permeability of the film by eliminating contamination from the silicone grease coating.
2. Increasing the temperature of the heating stage during film preparation should improve film surface uniformity, increase film hydrophobicity and decrease film water vapour permeability (WVP).
3. Increasing the pH of the casting solution during film preparation should produce a more uniform film surface, increase film hydrophobicity, and decrease film water vapour permeability.
4. Selecting two gluten types, Wonder wheat gluten and ADM commercial gluten, should modify the gluten film properties.

1.2.3 Objectives

The objectives to test the above hypotheses are as follows:

1. Evaluate WVP, surface hydrophobicity, and surface appearance of films produced with a silicone grease coated glass tray and with a flexible silicone tray (no grease coating).
2. Examine the effect of gluten solution temperature to 80 and 100 °C on film properties.
3. Examine the effect of pH 4 and pH 11 gluten solutions on film properties.
4. Compare gluten film properties (WVP, surface hydrophobicity, surface appearance, structure) for two gluten types, laboratory scale gluten produced from Wonder wheat cultivar and commercially produced gluten.

2 Literature Review

2.1 Wheat

Wheat grain (botanical name "*Triticum aestivum*") provides a food staple for many people around the world. In Canada, wheat is grown most abundantly in the Prairie Provinces but is also grown locally in Ontario. To maximize the chances of a successful harvest, the type of wheat to grow can be selected to address climate challenges specific to the region.

Winter wheat is appropriate for cooler climates having sub-zero temperatures and low precipitation or moisture in the winter. It is sown in the fall, sprouts, and then lies dormant through the winter and continues its growth in the spring and can be harvested in the early summer. Winter wheat requires the cool winter period in order to grow to maturity (termed vernalization). In contrast, spring wheat is grown in regions where the summers are not too hot. The seeds are sown in the spring and harvested late in the summer (Skinner, Bellinger 2010, Wrigley 2000, Commodity Futures and Equity Analytics 2000).

Additionally, protein content affects the selection of a wheat type. The wheat grain can be classified as hard or soft and can have a kernel colour of red or white. Hard wheat tends to have a higher protein content than soft wheat, so that hard wheat is well suited to bread making (strong and extensible), while soft wheat is often used to make pastries (weak and extensible) (Wrigley 2000). The four Ontario wheat cultivars included in this study are Harvard, Emmit, FT Wonder, and Norwell. Harvard and Norwell are hard red winter wheat, whereas Emmit and FT Wonder are soft red winter wheat.

Wheat grain has an outer shell or hull made from cellulose, called bran (Figure 1). Endosperm comprises a large part of the wheat grain's interior. Wheat endosperm provides the flour commonly used for making bread, pasta, and pastries. At the semi-pointed tip (bottom of Figure 1), the inside of the grain is filled with wheat germ. In addition, there is a pigment strand in the grain crease, located on the end opposite to the germ (Wrigley 2000).

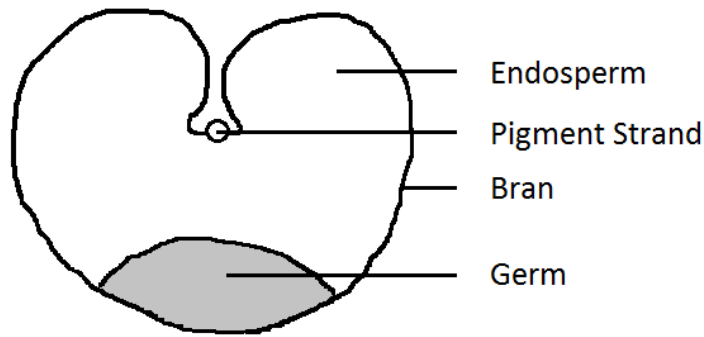


Figure 1 - Simplified Diagram of a Wheat Grain Cross-Section. Adapted from Wrigley et al. (Wrigley 2000)

2.2 Wheat Flour to Wheat Gluten

Wheat flour is obtained by crushing the wheat grain in a milling process and removing the bran and germ. Figure 2 shows that starch represents approximately 72 wt% of wheat flour while protein only accounts for 10 wt% of wheat flour (Veraverbeke, Delcour 2002, Pareyt, Delcour 2008).

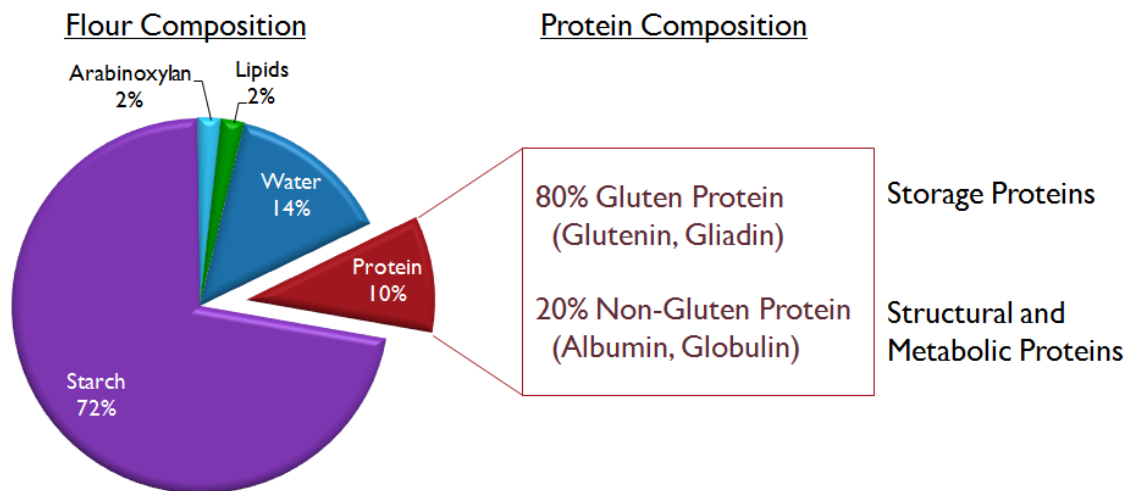


Figure 2 - Wheat Flour and Wheat Protein Composition, Based on Information Gathered from Literature (Veraverbeke, Delcour 2002, Pareyt, Delcour 2008)

Washing wheat flour removes the starch, leaving the protein. Figure 2 further shows that wheat protein is approximately 80 wt% gluten (storage) protein and 20 wt% non-gluten (structural and metabolic) protein (Veraverbeke, Delcour 2002, Pareyt, Delcour 2008). The two non-gluten proteins have mostly metabolic or structural purposes. They are the water soluble albumin and generally water

insoluble globulin. Glutenin and gliadin are storage proteins. These proteins are responsible for providing the strength and elasticity in applications such as bread dough and wheat gluten films (Veraverbeke, Delcour 2002). Glutenin is a polymeric protein, whereas gliadin is a monomeric protein (Lafiandra et al. 2000). There are various classes and sub-classes for glutenin proteins (Figure 3).

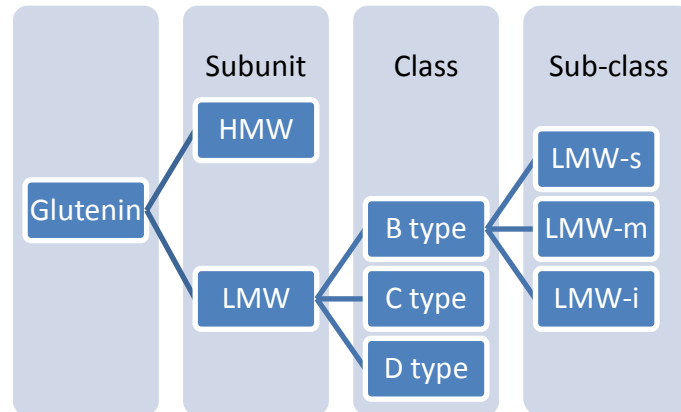


Figure 3 - Types of Glutenin Protein, Based on Information Gathered from Literature (Lafiandra et al. 2000). HMW and LMW Stand for High and Low Molecular Weight Respectively. B, C, and D type LMW Reflect Differences in Biochemical Characteristics. The sub-classes s, m, and i of B type LMW reflect the starting amino acids serine, methionine, and isoleucine, respectively, at the N-terminal.

Gliadin can be classified as α - β -, γ -, or ω -gliadin based on the N-terminal amino acid sequence (Lafiandra et al. 2000, Hernández-Muñoz et al. 2003). Cysteine is present in α - β -, and γ -gliadin, so disulphide bonds can form between different cysteine groups within the chain (intramolecular), whereas ω -gliadin contains no cysteine and thus cannot form disulphide bonds (Domenek et al. 2002).

Based on size, glutenin proteins are termed high (HMW) or low molecular weight subunits (LMW). The subunits are separate molecules, but they can be bound together by intermolecular disulphide bonds. The LMW subunit types B, C, and D reflect differences in LMW biochemical characteristics. The sub-classes in the B type LMW class reflect the amino acid located at the start of the N-terminal: serine for LMW-s, methionine for LMW-m, and isoleucine for LMW-i (Lambourne et al. 2010). The C type LMW shares similarities with γ -gliadin and the D type LMW shares similarities with ω -gliadin. (Lafiandra et al. 2000) Examples of the amino acid sequence for each type of wheat gluten protein are included in Appendix 3.

2.2.1 Primary through Quaternary Structure of Wheat Gluten Proteins

2.2.1.1 HMW Glutenin Structures

HMW glutenin subunits have the general structure: N-terminal domain | repetitive domain | C-terminal domain. The cysteine residues tend to be located near either end of the chain, and participate in disulphide bonds at the tertiary and quaternary levels of structure. The secondary structure of the repetitive domain is not certain for HMW glutenin. Potential conformations include β -reverse turns, β -turns organized to give a β -spiral structure, or γ -turns organized to give a different spiral structure (Shewry et al. 2002). Another suggested alternative is β -turns and β -sheets (Belton 1999).

The secondary structure of the non-repetitive, C- and N-terminal domains, are predicted to have different structures from each other and from the repetitive domain. A large amount of published work agrees that the N-terminal domain contains three to five cysteine residues, has a globular structure and contains one or more α -helices (Shewry et al. 2002, Kohler et al. 1997, Tatham, Shewry & Miflin 1984, Tatham, Miflin & Shewry 1985, van Dijk et al. 1998). The C-terminal domain contains only one cysteine residue and is believed to be α -helical (Tatham, Shewry & Miflin 1984, Bekkers et al. 1996).

The backbone of the HMW glutenin tertiary structure consists of polypeptides with cross-linking by means of covalent disulfide bonds between cysteine sulphur groups. However, hydrogen bonds also seem to contribute to tertiary structure. (Hamer, Vliet 2000) HMW subunits of glutenin have a significant amount of glutamine, and often a significant amount of glycine and proline as well. The three residues glutamine, glycine and proline appear to participate in large amounts of hydrogen bonding. It is believed that the repeating sequence sections of HMW subunits are linked together by means of many hydrogen bonds (Shewry et al. 2002, Belton 1999).

2.2.1.2 LMW Glutenin Structures

LMW glutenin subunits have been less extensively studied because they are smaller proteins and believed to have less of an impact on gluten protein structure. On the secondary structure level, the repetitive domain of LMW glutenin has an "extended conformation with an equilibrium between poly-L-proline II-like structure and type II' β -turns" (Lambourne et al. 2010). Poly-L-proline II is defined as "an extended left-handed helix with no intra-molecular hydrogen bonding along the polypeptide backbone; the amide groups of the backbone and glutamine side-chains being available for inter-molecular hydrogen bonding." (Tatham, Shewry 1995) On the other hand, the non-repetitive domains are more compact and globular, with many α -helices. Dynamic light scattering (DLS) suggests that repetitive and non-repetitive domains interact, creating more compact protein

conformations at the tertiary level of structure. The importance of LMW glutenin subunits to overall gluten properties may depend on the ratio of inter-chain to intra-chain hydrogen bonds in a particular type of wheat. (Lambourne et al. 2010)

2.2.1.3 Gliadin Structures

Recently, ultracentrifugation combined with UV absorption studies have been used to elucidate the shape of wheat gluten in solution (Ang et al. 2010). The types α -, γ -, and ω -gliadin were discernibly different but shape determination was still difficult. Gliadin had an asymmetric, extended structure, with α -gliadin being the most extended and γ -gliadin being the least extended. (Ang et al. 2010) The general shape of gliadin is supported by previous results with small-angle X-ray scattering (SAXS) (Thomson et al. 1999). In addition to the overall protein rod-like shape of gliadin in solution, Blanch et al. found that the repetitive domains of gliadin appear to be a mixture of poly-L-proline II and β -reverse turn structures, while the non-repetitive domains are rich in α -helical structures (Blanch et al. 2003). Blanch et al. specified that the C-terminal domain of α -gliadin contains α -helices and smaller quantities of poly-L-proline helices and β -structures. In contrast, ω -gliadin did not contain α -helices but did contain large amounts of poly-L-proline structure and some β -turns. (Blanch et al. 2003)

The rod-like extended structures observed for gliadin proteins indicates that neighbouring molecules would easily "stick" together by means of extensive hydrogen bonding and other non-covalent interactions, including van der Waals forces. These intermolecular interactions are expected to increase the viscosity of gluten solution especially since there are so many repetitive domains that are similar for all gliadin and because there are many sections of the gliadin protein that could interact with similar sections of neighbour proteins. Also, the asymmetry of gliadin repetitive domains should increase contact with neighbouring protein molecules (Ang et al. 2010).

2.3 Wheat Gluten Films

Research on the preparation and properties of wheat gluten films arose because of the excellent viscoelastic properties of wheat gluten. The two general methods used to prepare wheat gluten films are dry processing or solvent casting.

Gluten films obtained by dry processing are generally prepared with a small amount of plasticizer but very little water (<10%) compared to solvent cast films (Lagrain et al. 2010). Examples of the various dry methods used for preparing wheat gluten films include thermoforming (Angellier-Coussy et al. 2011), compression molding (Chen et al. 2012, Gällstedt et al. 2004), cold pressing (Song, Zheng 2008), and extrusion (Lagrain et al. 2010). Dry process gluten films are generally stronger than

solvent cast films (Lagrain et al. 2010) but are sometimes much thicker (Pommet et al. 2005, Kayserilioğlu et al. 2003).

Solvent cast gluten films often use an aqueous ethanol solvent to dissolve the gluten since gluten is soluble in ethanol (Olabarrieta et al. 2006). However, the industry trend towards greener solvents (Gu, Jérôme 2010, Kerton 2009) has encouraged efforts to prepare gluten films using water as the only solvent. In either case, the general procedure is to disperse the gluten and plasticizer in the solvent and then alter protein interactions in solution by methods such as pH adjustment, temperature, sonic or chemical treatments to cleave disulfide bonds (Lagrain et al. 2010, Gennadios, Weller & Testin 1993). The final gluten solution is cast and dried in a controlled environment (temperature, relative humidity) to remove the solvent and obtain a film. As the solvent evaporates, the gluten concentration in the film increases and facilitates intermolecular bond formation so as to produce the desired three dimensional gluten network (Lagrain et al. 2010).

In solvent cast gluten films, alkaline conditions above the isoelectric point of gluten, 7.5 (Gennadios, Weller & Testin 1993), tend to produce stronger films, likely because of increased gluten polymerization and cross-linking at higher pH (Lagrain et al. 2010, Olabarrieta et al. 2006).

The preparation of a gluten film by casting is believed to produce an open, loose protein network that is conducive to hydrophobic inter-chain bonding as well as cross-link formation when exposed to a heating and stirring step during film preparation (Lagrain et al. 2010, Jerez et al. 2005, Micard et al. 2001).

Typically glycerol and/or water are used as plasticizers because they are most effective (Lagrain et al. 2010). The purpose of a plasticizer, such as glycerol, is to improve film flexibility. Glycerol is a polar molecule, which breaks up some of the hydrogen bonds between protein chains. In the absence of glycerol, gluten would form a brittle film due to the high glutamine content in gluten (Shewry et al. 2002, Gontard, Guilbert & Cuq 1993, Belton 1999, Lagrain et al. 2010).

According to literature (Domenek et al. 2002, Angellier-Coussy et al. 2011, Schofield et al. 1983), heating wheat gluten encourages disulfide interchange reactions. Heating induces protein unfolding, which in turn exposes hydrophobic groups and cysteine residues that are usually hidden inside the protein molecule. (Domenek et al. 2002) The exposed cysteine residues react to re-stabilize the molecule by participating in disulphide interchange reactions with other cysteine residues. Although the total number of disulfide bonds in the system does not increase, the interchange of disulfide bonds throughout the protein shifts the bonds from intramolecular to intermolecular and locks the protein

into a more stable, less soluble network that remains even after cooling. (Angellier-Coussy et al. 2011, Schofield et al. 1983) The polymeric gluten protein, glutenin, begins disulfide interchange reactions at the lowest temperature (~ 60-70°C) due to its higher content of sulphur-containing cysteine groups (Angellier-Coussy et al. 2011). In contrast, the smaller monomeric gliadin proteins begin participating in disulfide interchange reactions only above 90°C and when the rate of disulfide interchange reactions slows for the glutenin molecules (Domenek et al. 2002). As one might expect, the cysteine deficient ω -gliadin does not participate in disulphide bond interchange reactions and remains soluble even after heating to 100°C (Schofield et al. 1983)

Ultrasound treatment of protein solutions has been investigated. The ultrasound treatment technique employs ultrasonic waves (Marcuzzo et al. 2010). Liu et al. reported that some ultrasound treatments of peanut protein isolate (PPI) casting solutions can have a detrimental effect on mechanical film properties (Liu, Tellez-Garay & Castell-Perez 2004). However, a 10 min ultrasound treatment of the PPI casting solution increased mechanical properties and water solubility of the PPI films (Liu, Tellez-Garay & Castell-Perez 2004). Marcuzzo et al. commented that in general, ultrasound treatments can be used to degas a protein casting solution (Marcuzzo et al. 2010). Marcuzzo et al. also reported that ultrasound treatment can improve gluten dispersion and improve film appearance in pH 4 films, which is believed to result from the breakdown of large protein aggregates at the mesoscopic level and not the breakdown of the gluten protein chains at the molecular level (Marcuzzo et al. 2010).

Wheat gluten films have excellent oxygen and carbon dioxide barrier properties compared to plastic films but have low water vapour barrier properties compared to plastic films (Olabarrieta et al. 2006, Gennadios, Weller & Testin 1993, Park, Chinnan 1995). A linear relationship between gluten film thickness and film barrier properties for oxygen and carbon dioxide gas was observed by Park et al. (Park, Chinnan 1995). Further, Olabarrieta et al. reported an increase in oxygen permeability for pH 4 wheat gluten films compared to pH 11 wheat gluten films, which could be attributed to reduced protein aggregation and a more heterogeneous wheat gluten film structure at pH 4 (Olabarrieta et al. 2006). Significant decrease of the water vapour permeability (WVP) for wheat gluten films has proven quite challenging to achieve and represents a major limitation in the application of wheat gluten films for food packaging materials (Angellier-Coussy et al. 2011).

Although the isoelectric point of wheat gluten occurs at pH 7.5, the two main constituents of gluten, glutenin and gliadin, have distinct isoelectric points, pH 7.1 and 8.1, respectively (Gennadios, Weller

& Testin 1993). Because of the differences in the amino acid sequences of gliadin and glutenin, pI values vary further depending on the specific glutenin or gliadin types (Table 1).

Table 1 – Estimated pI Values for Various Glutenin and Gliadin Types with a Known Amino Acid Sequence

	Gluten Component						
	α/β -Gliadin	γ -Gliadin	ω -Gliadin	HMW Glutenin	B-type LMW-s Glutenin	B-type LMW-m Glutenin	D-type LMW Glutenin
pI *	8.58	8.41	4.74	6.11	8.22	8.22	4.78

*pI was calculated using full sequences and a software program by Stothard (Stothard 2000)

Given that wheat cultivars probably contain different mixture ratios of glutenin and gliadin types, the overall gluten pI is expected to shift accordingly.

According to Domenek et al., covalent disulfide bonding can be viewed as an aggregation reaction because intermolecular bonding is formed (Domenek et al. 2004). Hydrophobic interactions and hydrogen bonds are the non-covalent interactions that connect different gliadin units together and to glutenin units (Lagrain et al. 2010, Ukai, Matsumura & Urade 2008). Wheat gluten is fairly insoluble in water because water is polar and the non-covalent interactions between protein segments are increased, causing aggregation at pH 7 (Day et al. 2009). Depending on the type of amino acid side groups, water will interact with neighbouring amino acid side groups by means of hydrophobic, van der Waals, and/or electrostatic interactions, as well as hydrogen bonds. Day et al. demonstrated the importance of these interactions for solubility by replacing the amide groups on many glutamine units of gluten with carboxyl groups and causing the water solubility to increase. The increased solubility was attributed to a reduction in the inter- and intra-molecular interactions in the wheat gluten because the modification of glutamine side groups removed the ability to form hydrogen bonds and increased electrostatic repulsion between gluten molecules (Day et al. 2009).

Ukai et al. reported that the addition of NaCl to gluten dough followed by washing with water, affected both interactions and distances between gluten units. Monomeric α/β - and γ -gliadin were released from the gluten network because of the NaCl addition increasing gliadin-gliadin interactions while disrupting gliadin-glutenin interactions. Further, when the extracted gliadin was exposed to NaCl, aggregation occurred (Ukai, Matsumura & Urade 2008). By studying the rheological properties of wheat gluten, van der Zalm deduced that NaCl addition can separate gluten from starch starting from flour as a result of the increased interactions between the gluten aggregates, which simultaneously draws the aggregates together and separates them from the flour (Zalm, Goot & Boom 2010).

In a study of hot-pressed wheat gluten films, the film swelling decreased and the shear modulus increased with increasing SDS-insoluble protein aggregation, suggesting that the primary cross-linking reaction in the system is disulfide bonding (Domenek et al. 2004). Further, the relationship between the shear modulus and protein aggregation content suggested that protein formed a network at the molecular scale and that gluten films consist of a mesoscale particle network having fractal inner structure (fractal dimension close to 3) (Domenek et al. 2004). Dynamic and retardation (creep and creep recovery) rheological experiments by Lefebvre et al. show that gluten viscoelastic behaviour over a large time or frequency scale exhibits a wide viscoelastic plateau and suggesting a transient type of network structure. Thus, Lefebvre suggested that aqueous gluten solution should be viewed as a particle network formed by aggregated particles connected by hydrogen bonds and hydrophobic interactions (Lefebvre et al. 2003)

2.4 Techniques and Film Properties

2.4.1 Dynamic Thermogravimetric Analysis (TGA)

There are two types of thermogravimetric analysis (TGA), dynamic (or scanning) and isothermal. In dynamic TGA, the temperature is increased at a constant rate and mass loss is recorded as a function of temperature. In isothermal mode, the temperature is kept constant and the mass loss is recorded as a function of time. Dynamic TGA allows one to measure mass loss (due to thermal degradation of the sample) as a function of temperature. Since sample constituents will undergo thermal degradation at its own specific temperature, the technique can be used to distinguish different constituents of a material and their weight percent relative to the total mass of the sample (Patnaik 2004, PerkinElmer 2010). In the case of wheat gluten films, the interactions of gluten proteins with glycerol and water can be analyzed by TGA according to temperature at which each constituent degrades relative to the temperature of degradation of the pure constituent (Gomez-Martinez et al. 2011).

TGA can be conducted in an inert nitrogen environment (pyrolysis) or in a reactive air or oxygen environment (oxidation). If an inert nitrogen environment is selected, we can expect higher residual mass at the end of the heating period. In the oxygen environment, most of the mass of an organic sample would degrade by oxidation such that lower residual mass will be obtained at the end of the heating period (PerkinElmer 2010).

The derivative of the TGA curve (DTGA) can be used to identify the regions of rapid thermal degradation. Low moisture content samples can be expected to exhibit a very small first DTGA peak in the range of 50 to 100°C, which is commonly attributed to water evaporation (Chiou et al. 2010).

According to Mohamed et al., gluten should have a maximum rate of thermal degradation near 300°C (Mohamed et al. 2008). On the other hand, pure liquid glycerol should undergo thermal degradation with a maximum at 168°C (Dou et al. 2009).

2.4.2 Surface Plasmon Resonance (SPR)

Surface plasmon resonance is a tool that can be used to study the interaction between molecules in solution and the coating on the SPR gold disk surface. Some coating options include biomolecules, polymers, or, as for the work presented in this thesis, a self-assembled monolayer (SAM). SPR measures change in resonance angle over time resulting from the following sequence of events: addition of running buffer to the cuvette and signal stabilization (baseline), addition of sample to cuvette and letting it sit (association), and washing and soaking the cuvette with running buffer to remove any loosely bound protein (dissociation) as outlined in Table 2 (Eco Chemie B.V. 2006).

Table 2 - Description of Each Phase of the SPR Response Curve

Phase	Component of Procedure
Baseline	Add running buffer to cuvette, wait for stable signal.
Association	Add sample to cuvette
Dissociation	Washed cuvette with running buffer. Injected more running buffer in cuvette and let sit 300 s

The amount of irreversibly/strongly bound protein can be measured by the SPR by comparing the signal after completing the dissociation phase to the signal at the start of the association phase (Barrett et al. 2005).

Wang et al. reported absorption of zein from an aqueous solution to a hydrophilic self-assembled monolayer (SAM) of 11-mercaptoundecanoic acid (Wang, Crofts & Padua 2003). A study of human serum albumin (HSA) protein absorption to different types of SAM layers over time, by Barrett et al., also showed differences in protein-to-SAM affinity can be measured successfully by the SPR technique (Barrett et al. 2005).

2.4.3 Contact Angle and Surface Hydrophobicity

Contact angle measurements represent the interior angle between a solid surface and a liquid droplet sitting on that solid surface (Figure 4) (KRÜSS GmbH. 2004).

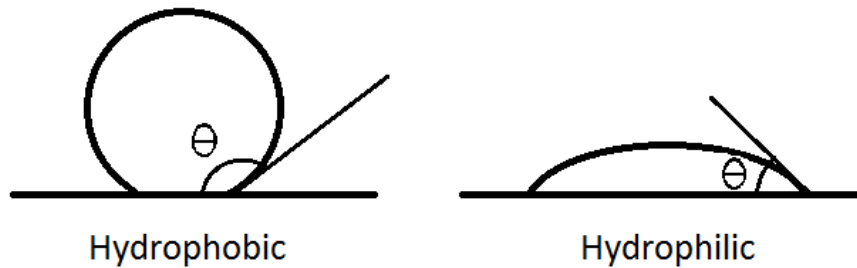


Figure 4 - Diagram of Water on Hydrophobic and Hydrophilic Surfaces with Contact Angle Location Designated by Theta

Static (sessile drop) contact angle measurements provide a means to study surface wettability (KRÜSS GmbH. 2004). Wetting occurs on a solid surface "when the work of adhesion W_{sl} between the solid surface and the liquid is greater than work of cohesion W_{ll} within the liquid" (KRÜSS GmbH. 2004). Complete wetting occurs when $\theta = 0^\circ$, good wetting at 15° , and poor wetting at 95° (KRÜSS GmbH. 2004). Wetting progressively decreases between 15° and 95° .

Although, the terms hydrophobic and hydrophilic are often treated like relative terms, for biomaterials, Volger et al. define a division point between hydrophobic and hydrophilic surfaces at a water contact angle of 65° (Vogler 1998). So a surface should be hydrophobic if the contact angle is above 65° , but hydrophilic if the contact angle is below 65° (Vogler 1998).

The water contact angles for different types of wheat gluten films tend to range between about 55° and 100° , with film formulation and preparation techniques having significant impact on the values reported. For example, ethanol solvent cast wheat gluten and glycerol films (with a 70°C heating step) prepared by Marcuzzo et al. exhibited a higher water contact angle (80°) when the casting solution was adjusted to pH 4, compared to a water contact angle of 55° when the solution was adjusted to pH 11 (Marcuzzo et al. 2010). The addition of a 10 min ultrasound step to pH 4 gluten solution reduced the film water contact angle to 54°C (Marcuzzo et al. 2010). A different formulation by Larre et al., where the enzyme transglutaminase was added to the gluten solution and heated to 70°C only while drying the casting solution into film form, resulted in a significantly higher water contact angle, 97° (Larré et al. 2000).

According to Marcuzzo et al., gluten film porosity and swelling can affect contact angle measurements (Marcuzzo et al. 2010). The effect of film swelling due to water absorption can be minimized by careful selection of the video frame that corresponds to the droplet just after water drop deposition (and stabilizing), and prior to any water absorption (Roman-Gutierrez 2001). Film

porosity, is more difficult to minimize. When film solvent casting is used, one can select the film surface that was in contact with the casting surface (smoother) to reduce standard deviation.

2.4.4 Water Vapour Permeability (WVP)

Water vapour permeability (WVP) of wheat gluten films depends on the protein network structure (including tightness) and the affinity of the film constituents for water (Gontard, Guilbert & Cuq 1993, Gennadios, Weller & Testin 1993, Park, Chinnan 1995). For example, not only composition but also bubbles, pinholes, or points of weakness due to material folding can increase water vapor permeability (Park, Chinnan 1995, Heiss 1959, Pascat 1986).

Although decreasing water vapor permeability in gluten films is a challenge, some inroads have been made. Gennadios et al. report that soaking wheat gluten films in a pH 7.5 (isoelectric point of gluten) aqueous solution increased tensile strength and reduced WVP by tightening the film structure (Gennadios, Weller & Testin 1993). Gennadios et al. also observed that WVP increased in gluten films when sodium sulfide was added to the formulation. Sodium sulfide cleaves disulfide bonds which is expected to increase chain mobility and bonding during film drying and reduce polypeptide chain length (Gennadios, Weller & Testin 1993). Gennadios et al. further reported that the addition of mineral oil and hydrolyzed keratin to the formulation reduced WVP of gluten films by 23 to 25% (Gennadios, Weller & Testin 1993). Mineral oil improved water barrier properties as a result of its non-polar and hydrophobic properties and also reduced the film tensile strength. The addition of keratin is believed to have improved WVP by forming links with gluten units (Gennadios, Weller & Testin 1993).

The effect of plasticizer content was studied extensively. Park et al. reports that increasing plasticizer content increases water vapor permeability for gluten films cast in aqueous ethanol and with ammonium hydroxide addition (Park, Chinnan 1995). Gontard et al. reported similar effects and attributed the addition of glycerol to the loosening of the protein network, lending flexibility but making the network less dense and more water permeable (Gontard, Guilbert & Cuq 1993). In addition, the hydrophilic nature of glycerol is also believed to improve water adsorption and water permeation (Gontard, Guilbert & Cuq 1993). Park et al. also indicated that as film thickness increases, WVP increases (Park, Chinnan 1995). The effect of film thickness on WVP was attributed to changes in structure or to film swelling (Park, Chinnan 1995, McHugh, Avenabustillos & Krochta 1993).

2.4.5 Fluorescence Spectroscopy

Luminescence is defined as the emission of light from any substance (Lakowicz 2006). Luminescence can occur quickly (fluorescence) or slowly (phosphorescence), depending on the nature of the original excitation state of the electrons. Fluorescence emission occurs from singlet excited states where the excited electron is paired by opposite spin to the electron in the ground-state orbital, such that return to ground state is spin allowed. Therefore, fluorescence emission occurs very quickly (Lakowicz 2006).

Fluorescence spectroscopy is a technique where light, in a pre-selected range of wavelengths, excites electrons to an excited state, followed by the emission of a photon and rapid return of the electron to ground state. The wavelength of the emitted photon will depend on the chemical structure of the fluorophores present in the material being studied and its surrounding environment. Therefore, excitation and emission wavelengths, along with associated intensities can provide information on the chemical structure and the environment of a substance (Lakowicz 2006).

Fluorescence properties of proteins are given by the fluorescence ability of their native amino acids. Fluorescing amino acids are those that contain aromatic side groups, tryptophan, tyrosine or phenylalanine. Tryptophan fluoresces at $\lambda_{\text{ex}} = 275$ nm and with λ_{em} range 330-350 nm. Tyrosine fluoresces at $\lambda_{\text{ex}} = 275$ nm and $\lambda_{\text{em}} = 305$ nm. Phenylalanine fluoresces at $\lambda_{\text{ex}} = 260$ nm and $\lambda_{\text{em}} = 282$ nm (Lakowicz 2006, Genot et al. 1992). Tyrosine and phenylalanine tend to transfer absorbed energy to tryptophan, making tryptophan the main peak in protein fluorescence spectra and masking tyrosine and phenylalanine fluorescence (Lakowicz 2006).

2.4.6 Fourier Transform Infra-Red (FTIR)

Infra-red (IR) spectroscopy provides information on the molecular vibrations and rotations associated with changes in the dipole moments of a molecule. IR spectrum will be produced when molecules possess electric dipole moments that change as the different functional groups of the molecules move (twists, stretches, vibrates, rotates). IR radiation is passed through the sample and the fraction of incident radiation absorbed at each wavenumber is recorded. The fraction of incident radiation absorbed at a specific wavenumber corresponds to the frequency of a specific molecular vibration or rotation within the molecule being studied. Peaks at a specific wavenumber correspond to the vibration frequencies of well-defined bonds or parts of the molecule. However, the vibration of one bond in the molecule typically impacts the vibrations in other bonds of the molecule. Therefore, each type of molecule will produce a slightly different IR spectrum, which can be viewed as a fingerprint (Stuart 2005).

Fourier transform IR technique, in particular, makes use of the interference of radiation between two light beams. The change in path length between the two beams produces a signal called an interferogram. Fourier transformation allows for the conversion of the signal (variation in power density as a function of the difference in path length) to the typical FTIR spectrum (variation in intensity as a function of wavenumber) (Stuart 2005).

ATR-FTIR (Attenuated Total Reflectance-FTIR) is a modification of conventional FTIR where the IR rays are aimed at the reflecting surface (with the sample material pressed against the surface) at an angle greater than the critical angle of incidence of the surface so that the rays undergo total internal reflection. However, the rays still penetrate the reflecting surface a fraction of a wavelength and lose energy at the absorbing wavenumbers of the sample material before reflecting back towards the detector. This means that at certain wavenumbers, the IR rays will be attenuated, again producing an IR spectrum with peaks at the wavenumbers corresponding to the molecular vibrations and rotations of the sample material (Stuart 2005). In this method, the sample does not have to be IR transparent which enables the analysis of intact films since no alteration of the film is required (Hofmann 2006).

Common characteristic FTIR peaks for proteins have been classified as described by Barth et al. in Table 3 (Barth 2007).

Table 3 - Common FTIR Peaks Characteristic of Protein, According to Barth et al. (Barth 2007)

Vibration Type	Wavenumber (cm ⁻¹)
Amide A: NH stretch	3300 (3310-3270)
Amide B: NH stretch	3070 (3100-3030)
Amide 1: C=O stretch, CN out-of phase stretch, CCN deformation, NH in plane bend	1650 (1600-1700)
Amide 2: Combined out of phase bends of the groups: NH in-plane bends, CN stretch, some CO in-plane bends, CC and NC stretch	1550
Amide 3: In-phase NH bending, CN stretching, and some CO in-plane bending and CC stretching	(1400-1200)

FTIR peaks reported for wheat gluten include amide 1 and amide 2 peaks. Olabarrieta et al. identify the amide 1 and 2 peaks at wavenumbers $1580\text{-}1720\text{ cm}^{-1}$ and 1535 cm^{-1} respectively for an ethanol solvent cast pH 11 wheat gluten film and a glycerol peak at 850 cm^{-1} since glycerol was added to the formulation (Olabarrieta et al. 2006).

When the intensity of a peak changes relative to its neighbouring peaks, information on changes in the protein conformation are obtained and can also reflect changes of the protein environment. Such changes were reported by Olabarrieta et al., where increased protein aggregation was measured for a pH 11 gluten film compared to pH 4 gluten film. Therefore, FTIR can be useful in the interpretation of the physical properties of gluten films (Olabarrieta et al. 2006).

3 Materials and Methods

3.1 Materials

Whetpro80 wheat gluten was obtained from ADM (Decatur, Illinois). ADM provided the following compositional information for Whetpor80: 80% protein, 8% moisture, 1% fat, 1% ash, and 10% non assigned. The University of Guelph (Guelph, Canada) provided wheat gluten from the Ontario wheat cultivar FT Wonder. Further, the University of Guelph obtained a protein content of 72% wt/wt (N=5.7) for FT Wonder wheat gluten using an NA2100 Nitrogen and Protein Analyzer (Thermo Quest, Milan, Italy). Old Wonder and new Wonder gluten refer to wheat glutes prepared in 2009 and 2011 respectively, from the Wonder Ontario wheat. Glycerol (item code GX0185-2), having a purity $\geq 99.5\%$, and sodium hydroxide, having a purity $\geq 95\%$, (item code SX0600-3) were obtained from EMD Chemicals Inc. (Darmstadt, Germany). Anhydrous calcium chloride pellets, with a 4-20 mesh size, was obtained from Fischer Scientific (item code C614-3, Fair Lawn, New Jersey, United States). Glacial acetic acid, having a purity $\geq 99.7\%$ was obtained from Fisher Scientific (item code A38 P212, Nepean, Ontario, Canada). Magnesium nitrate having a purity $\geq 98\%$ was obtained from Alfa Aesar (item code 11564, Ward Hill, MA, United States).

3.2 Film Preparation

Wheat gluten reference films were prepared as described by Kayserilioglu (Kayserilioglu et al. 2003). Using a molecular sieve (Collector, Tissue Sieve, Bellco Glass Inc., USA) with a 1.52 mm x 1.52 mm mesh size, 10% wt/wt wheat gluten (percent of total solution mass before pH adjustment) was added to Milli-Q water (Millipore) containing 2% wt/wt glycerol (percent of total solution mass before pH adjustment), under constant stirring. The solution pH was increased to pH 11 according to a SevenMulti pH meter (S47, Mettler Toledo, Schwerzenbach, Switzerland) with 1 M NaOH and stirred for 30 min. The solution was then placed in a water bath (150 x 75 mm crystallization dish, no. 3140, Pyrex, Germany) and heated at 2°C/min to 70°C. After reaching 70°C the solution was held at 70°C for an additional 10 min. The heated solution was placed in a Bransonic 52 (Branson Cleaning Equipment Company, Shelton, CT, United States) sonicating water bath for 10 min and the foam layer on the surface was carefully removed using a spoon and transfer pipette. The casting tray was placed in a Versatile Environmental Test Chamber (MLR-351H) from Sanyo Electric Co., Ltd. (Moriguchi, Osaka, Japan) and leveled. Then the final film solution was poured onto the casting tray. The film was placed in 50% relative humidity (RH) and 23°C for 20 - 30 h so that it was dry enough to peel up without deforming. Once the film was dry, the edges were loosened from the sides of the

tray and the film was peeled up. The film was then placed back in the environmental chamber (50% RH, 23°C) for 2 days of conditioning prior to testing.

In early research stages, films were cast on hand-made glass trays having a metal frame sealed around the edges of clear window glass. The dimensions of the casting surface were 0.295 m x 0.17 m (0.05015 m²). A release layer of silicone grease (Dow Corning High Vacuum Grease, Dow Corning Corporation, Midland, Michigan, United States) was evenly applied to the whole surface with Kimtech Science Kimwipes (Kimberly-Clark Inc., Mississauga, Ontario, Canada) prior to casting. In later research stages, films were cast on silicone trays (Professional Bakeware 9" Square Pans, supplied by the company Arts, China). The dimensions of the silicone tray surface were 0.215 m x 0.215 m (0.046225 m²).

3.3 Film Thickness

Film thickness was measured with an Electronic Digital Micrometer, from Marathon Watch Company Ltd. (Richmond Hill, Canada) to the nearest 2.5 µm. Average film thickness and standard deviation were determined from 15 thickness measurements for each prepared film.

3.4 Kjeldahl Analysis

Protein content in wheat gluten and wheat gluten constituents, glutenin and gliadin, was measured by microdetermination of Kjeldahl nitrogen as described by Lang (Lang 1958). Prior to the experiment, the Kjeldahl digestion solution was prepared by dissolving 40 g of potassium sulfate in 250 ml of Milli-Q water with heating and stirring on a magnetic stir plate. Next the solution was set to stir in an ice bath in the fume hood and 250 ml of sulfuric acid was added slowly, to avoid overheating. Finally, 2 ml of selenium oxychloride was added to the solution before storing it in the dark (in the cupboard below the fume hood) until needed.

Between 15 and 20 mg of each dry powder sample was weighed, recorded, and transferred to a 30 ml digestion flask. Likewise, 1 ml of standard solution of ammonium sulfate in Milli-Q water (4.714g/L) was transferred to a 30 ml digestion flask and subsequently treated like the dry powder protein samples. Next, 3 ml of the Kjeldahl digestion solution was added to each 30 ml digestion flask, and the flasks were placed on a digestion unit and brought to a boil for 3 to 4 hours. After the solution transitioned to brown and back to clear, the digestion was complete and the samples were left to cool for at least 1 hour. The cooled solutions were each diluted to 100 ml in a volumetric flask with Milli-Q water and used in a colorimetric assay. Note that, the dilution to 100 ml in the volumetric flasks gives a first dilution factor of 100 ($d_1=100$), to be used in the final calculation.

The standard solution of ammonium sulfate in Milli-Q water, that was digested alongside the samples, was diluted to four additional lower concentrations, to be used along with a blank as a calibration curve for the digested samples.

To bring the digested samples within the concentration range of the calibration curve, 200 μL of each sample was placed in a separate volumetric flask and mixed with 600 μL of Milli-Q water. Note that this dilution gives a second dilution factor of 4 ($d_2 = 4$), to be used in the final calculation.

Next, 50 μL of sample (or calibration curve standard, or water blank) was placed into separate wells on a 96 well plate, in triplicate. Then 150 μL of Milli-Q water was added to each well, followed by 50 μL of Nessler reagent. The plate was shaken for about 15 seconds using the shake function in the spectrophotometer (BioTek Instruments, USA) and then placed in the dark for 15 minutes for colour development. Finally, the plate was inserted back in the spectrophotometer, shaken another 15 seconds, and measured at 420 nm wavelength.

The nitrogen conversion factor to protein was 5.7, specific to wheat (Genot et al. 1992). A sample calculation is provided in Appendix 7.

3.5 Surface Plasmon Resonance (SPR)

Surface Plasmon Resonance (SPR) is a technique which allows the measurement of molecules on a planar surface. A change in SPR signal occurs when there is a change in the mass accumulated on the sensor surface. SPR signals were measured at room temperature ($\sim 23^\circ\text{C}$) on gold coated SiO_2 disks (Au- SiO_2 SPR disks, Metrohm, USA) coated with a self-assembled monolayer (SAM) using a cuvette-based AUTOLAB Springle system (Eco Chimie BV, Utrecht, Netherlands).

The gold coated SiO_2 disks were coated with SAMs and provided by Nicholas Ignagni according to the procedure detailed in his thesis (Ignagni 2011). The procedure involves washing the disks with 95% ethanol, followed by a rinse with Milli-Q water, and drying under a nitrogen stream. The disks were then immersed in an ethanol-based SAM forming solution (1 mM 11-mercaptoundecanoic acid) for 12 h. The disks were then washed with 95% ethanol, followed by a rinse with Milli-Q water, and dried under a nitrogen stream. All SPR experiments were performed on SAM coated disks prepared as just described.

ADM wheat gluten was dissolved in Milli-Q water at a concentration of 1 mg/ml with either no pH adjustment (pH 7.7) or pH adjusted to 11 using 1 M NaOH. Both were mixed for 20 h prior to the SPR measurements. Running buffers were prepared with 1 M NaOH to match the pH of each of the samples and also consisted of Milli-Q water. The experimental sequence was adapted from the

"Curve-SA-a full kinetic plot" (Autolab 2006) sequence provided in the Springle software Data Acquisition (version 4.2.2, Eco Chimie BV, Utrecht, Netherlands). At the start of the sequence, the sample delivery lines were flushed and replaced with running buffer. The recorded experiment started with the baseline phase: 50 μ l of running buffer was injected in the SPR cuvette and the baseline was recorded for 120 s. The association phase was then initiated with the injection of 50 μ l of the wheat gluten solution in the cuvette and the signal recorded for 400 s. Finally, the dissociation phase was initiated by washing loosely associated material from the surface with 500 μ l of running buffer. This was followed by the second dissociation phase when 50 μ l of running buffer was injected in the cuvette and the signal recorded for 300 s. If the same spot on the sensor surface was to be used for a new experiment, the surface was regenerated by cleaning with a regeneration solution of 0.01 M HCl. For the regeneration cycle, the cuvette was flushed with 200 μ l of regeneration solution and then an additional 50 μ l of regeneration solution was injected into the cuvette and left for 10 to 15 min. Following regeneration, the surface was flushed with running buffer and then the baseline was measured.

3.6 Viscosity

A Cannon-Fenske Routine Viscometer (Model 2707, size 100, Technical Glass Products Inc., Dover, NJ, United States) was used to measure the viscosity of an aqueous wheat gluten and glycerol solution at room temperature (\sim 23°C) as a function of pH. The solution was prepared using the same initial steps as for film preparation. Using a molecular sieve, 10% wt/wt wheat gluten was added to an aqueous solution of 2% wt/wt glycerol, under constant stirring. The solution pH was increased to the desired pH (9.5, 10, 10.5, or 11) with 1 M NaOH and stirred for 30 min. A 15 ml sample of the solution was poured through the molecular sieve and collected in a small beaker. Then the 15 ml sample was poured into the viscometer and six consecutive efflux times were obtained. A fresh gluten solution was prepared for each new pH. The kinematic viscosity (Cts) was calculated by multiplying the efflux time by the viscometer constant (0.01439 Cts/s). A sample calculation is provided in Appendix 8.

3.7 Thermogravimetric Analysis (TGA)

The thermal stability of wheat gluten films, liquid glycerol, as well as crude wheat gluten in powder form were characterized in TA Instruments Q500 Thermogravimetric Analyzer (New Castle, United States). Samples, each weighing a minimum of 9 mg, were heated at a rate of 10 °C/min from 30 °C to 600 °C. Samples were tested in a nitrogen environment with a flow rate of 50 ml/min. Before testing, samples were conditioned in an environmental chamber for at least 48 h at 23 °C and 50 %

RH. Relative mass change (Δw %) and rate of mass change over time (DTGA) were collected along with temperature and analysed for 1% onset degradation, temperatures of DTGA peak maxima, and change in weight percent for each major DTGA peak. The 1 % onset of degradation was estimated by considering the section of the TGA data after the evaporation of water mass, around 50 to 100°C (Chiou et al. 2010). The initial temperature used to calculate the 1% onset of degradation was defined as the temperature of the first DTGA minimum (located just after the water evaporation peak). The initial mass used to calculate the 1% onset of degradation was then set as the sample mass corresponding to the initial temperature. The 1 % onset was the temperature at which the sample mass decreased by 1% from the initial mass (see Appendix 9) and was calculated to provide a comparison between samples for the temperature at which the sample begins to degrade. Onset values are not consistent throughout literature and include values such as temperature at 1 and 5% onset (Ishida, Lee 2001, Song, Zheng 2009). TGA measurements presented here had the same trends for 1 and 5% onset. A 1% onset was selected to present in the results because it is closer to the temperature at which thermal degradation began. The mass loss ($\Delta w\%$) of a given peak represented the difference between the relative mass at the beginning of the peak and the relative mass at the end of the peak.

3.8 Film Surface Investigation

Macroscopic surface investigation was performed once films were dried and peeled from the casting trays. The films were visually inspected under good lighting for bubbles or other defects and all films were photographed with a regular camera, except the initial film cast on a glass tray with a silicone grease layer. Qualitative observations were recorded regarding film appearance. Images of wheat gluten films were obtained at 80x magnification (for ADM gluten films at early stages of research) or 12.6 x magnification (for films cast from different wheat gluten sources), according to the microscope optics, on the Leica MZ6 microscope using the Leica DFC 290 camera attachment and accompanying Leica Application Suite v. 2.6.0R1 software (Leica Microsystems, Wetzlar, Germany).

Samples were prepared by first applying two sided tape near the outer edges of a 0.02m x 0.02m (0.0004 m²) section on a glass microscope slide. Then a 0.0004 m² sample of film was placed on the tape. Imaging was done in the center of the sample.

3.9 Contact Angle (CA)

Sessile (static) drop measurements of contact angle for water in air on the film surface were obtained with a KRÜSS GmbH Drop Shape Analysis System DSA100 (Hamburg, Germany). The Tangent Method-1 was selected to determine the contact angle in the accompanying software DSA1 version 1.9 (KRÜSS GmbH., Hamburg, Germany). The software measures the left and right side of the liquid

drop separately and takes an average of the two angles to give the most consistent results across multiple drop measurements.

In earlier research stages, two film samples were cut from each prepared film and affixed, top side up, to a blank glass microscope slide (Pearl, China) with two sided tape. In later research stages, two additional film samples were cut from each film and affixed to blank glass microscope slides, bottom side up, to measure the contact angle of the bottom of the films. In all cases, the contact angle of a minimum of five different water drops were measured per film sample. Each water drop was delivered from the syringe of the DSA100 dosing system. The DSA100 dosing system controls the volume and rate of delivery for the liquid drop delivered to a sample. The 10 μL water drop volume was delivered at a rate of 240 $\mu\text{L}/\text{min}$. All film samples were held at 50% RH using supersaturated magnesium nitrate during the contact angle test period. Individual film samples were removed from the 50% RH environment prior to contact angle measurements. Measurements were conducted at room temperature ($\sim 23^\circ\text{C}$).

3.10 Fourier Transform Infra-Red (FTIR) Spectroscopy

Infrared (IR) spectra of wheat gluten films were measured on the Tensor 27 FTIR Spectrometer and accompanying OPUS v 4.2 software produced by Bruker Optik GmbH (Ettlingen, Germany). The ACCESS ATR attachment (Harrick Scientific Products Inc., Pleasantville, New York, United States) flattens the film samples against the FTIR-ATR crystal and holds the film in position during measurement. The films tested had an average thickness of $202 \pm 14 \mu\text{m}$. The scan range was $4000 - 550 \text{ cm}^{-1}$. Each FTIR spectra was obtained from 32 scans at a resolution of 4 cm^{-1} . Two film samples were measured and each film sample was measured twice without moving the sample.

3.11 Fluorescence Spectroscopy

Fluorescence spectra of the top and bottom of each film surface were collected using an Agilent Cary Eclipse Fluorescence Spectrophotometer (Mulgrave, Australia) equipped with a Fluorescence Optic Reflectance Probe. Excitation wavelengths in the range of 250 to 380 nm were scanned at increments of 10 nm. Emission intensity measurements were collected within the wavelength range of 275 to 600 nm. All spectra were measured at a medium scan speed of 600 nm/min and a photomultiplier voltage of 600 V. The excitation and emission slit widths were set to 5 nm.

The films were conditioned at 23°C and 50% RH and the spectra collected at room temperature ($\sim 23^\circ\text{C}$). It was not possible to control the relative humidity during testing. However, each film sample was individually removed from 50% RH conditions prior to measurement. The fluorescence

intensity data was graphed as 3D excitation-emission matrices (EEM) with MATLAB (m-file for 3D and contour plotting written by Ramila Peiris).

The flat bottom of a black 96-well plate (Nunc, Denmark) was placed underneath each film sample as the background since it was found to minimize interferences with the low intensity protein peaks.

3.12 Water Vapour Permeability (WVP)

WVP was measured following the ASTM standard D1653-03, Method A (Dry Cup Method), Condition A, which specifies environmental conditions of 23°C, 50% relative humidity (RH) (ASTM Standard D1653, 2003 (2008)). To do this, an aluminum dish was filled with calcium chloride desiccant and a film sample was sealed to the mouth of the dish with melted wax (Väghult candles, Inter IKEA Systems B.V., Germany), giving an internal relative humidity of 0% and an external relative humidity of 50%. The change in total mass over time was measured daily for 12 days. This provided the rate of water vapour permeation through the film ($\text{g}\cdot\text{mm}/\text{day}\cdot\text{m}^2\cdot\text{atm}$). A sample calculation is provided in Appendix 1.

The WVP of three distinct samples was measured for every film. Each film fixed on an aluminum dish containing desiccant was weighed daily to within 0.0001 g on a Sartorius 1801 scale (Sartorius GmbH Gottingen, Germany). The discs of film placed on top of the aluminum dish were 0.063 ± 0.002 m in diameter, giving a sample surface area of 0.0032 ± 0.0001 m². The films and aluminum dish were placed in an environmental chamber to maintain constant temperature at $23 \pm 1^\circ\text{C}$ and relative humidity at $50 \pm 3\%$.

3.13 Film Swelling

Film swelling in the presence of water was measured as a function of time over a 24 h period as follows. Sixteen, 0.0001m^2 , film samples were cut from a single wheat gluten film and their initial dry mass was recorded. Each film sample was immersed in a separate Petri dish containing 20 ml of Milli-Q water. After soaking during 0.25 h, two of the sixteen film samples were removed, held in the air with tweezers for one minute to allow excess water to drip off, and then weighed. At each of the other seven selected times during the 24 hour period, two film samples were removed from water, air dried for one minute, and weighed. The swelling of the film (q) was estimated as follows (Chiou et al. 2010, Yarimkaya, Basan 2007):

$$q = \frac{\text{mass}_{\text{swollen}}}{\text{mass}_{\text{dry}}} \quad (1)$$

The total protein content of the soaking water after 24 h was obtained from UV-vis measurements at 280 nm using a Spectronic Genesys 2 (Milton Roy Company, United States). Two replicate measurements were obtained for each sample of soaking water. In addition, the total solids content of the soaking water after 24 h was obtained using a convection oven method, as described in a Laboratory Analytical Procedure Manual entitled Biomass and Total Dissolved Solids in Liquid Process Samples (Sluiter et al. 2008). All film swelling related sample calculations are provided in Appendix 10.

3.14 Statistical Analysis

Unpaired, two sided t-tests were employed to compare the means of sample sets, using the case where the assumption that the population standard deviations are equal is not valid. A 95% confidence interval ($p=0.05$) was employed such that the difference between means was deemed significant when $t(\text{observed})$ values were greater than the $t(\text{critical})$ values. The t-test calculation followed the method outlined in Montgomery et al. (Montgomery 2009). Standard error was employed for data sets where $n \leq 2$, whereas standard deviation was employed for larger data sets.

4 Results and Discussion

4.1 Investigation of Film Ingredients

4.1.1 Analysis of Gluten Protein Content

Table 4 presents the protein content, determined by Kjeldahl analysis, for commercial ADM wheat gluten, and wheat gluten from four Ontario cultivars.

Table 4 - Protein Content by Kjeldahl Analysis for Various Wheat Sources (Nitrogen to Protein Conversion factor of n=5.7)

Wheat Source	Protein Content (wt %)	Error † (wt %)
ADM Whetpro75 Gluten *	61.8	1.6
ADM Whetpro80 Gluten *	73.7	1.6
Emmit Gluten grown in 2011 ‡	75.8	1.7
Harvard Gluten grown in 2010 ‡	60.2	3.7
Norwell Gluten grown in 2009 ‡	62.1	3.4
Wonder Gluten grown in 2011 ‡	75.0	1.8

† Error is calculated based on slope error of 0.02, balance error of 200 µg, standard deviation of 3 absorbance values and converted to percentage (sample calculation described in Appendix 7).

*Commercial wheat gluten.

‡ Gluten from Ontario wheat cultivars.

The Ontario cultivars divided very clearly into two levels of protein content. Harvard and Norwell gluten, from hard red winter wheat cultivars, had a lower protein content (60.2 to 62.1 wt%), compared to the Emmit and Wonder gluten, from soft winter wheat cultivars (75.0 to 75.8 wt%). This was not expected given that hard wheat tends to have a higher protein content than soft wheat (Wrigley 2000), and is hypothesized to be specific to the wheat cultivars selected for study.

ADM, the manufacturer of Whetpro75 and 80 wheat gluten, reports a protein content of 75% and 80% protein respectively for Whetpro75 and 80 (ADM 2012), with N=5.7 (Product Sheet in Appendix 6). The protein contents reported in Table 4 were low for the two ADM samples compared to the values reported by the manufacturer, using a FP-528 Nitrogen/Protein Determinator (Leco Corporation, MI, USA).

In comparison to the literature, the protein content for the wheat gluten in Table 4 was lower than expected. For example, Genot et al. reported 85.0 wt % protein content for commercial wheat gluten using a nitrogen-to-protein conversion factor of 5.7 (Genot et al. 1992). Given that both the ADM gluten and the Ontario cultivars display lower protein content compared to literature, it is

hypothesized that the Kjeldahl method resulted in a consistently lower estimation of the protein content due to a systematic error in approach used here.

4.1.1.1 Conclusions

In contrast to the literature, gluten extracted from the hard wheat cultivars in this study (Harvard and Norwell), had a lower protein content than gluten extracted from the soft wheat cultivars (Emmit and Wonder). The results for the four Ontario cultivars are hypothesized to be specific to the wheat cultivars selected for this study. Since the Kjeldahl results for gluten for both ADM and Ontario cultivars yielded lower protein content compared to literature, it is likely that the low protein content can be attributed to a systematic error in the approach used here for the Kjeldahl method.

4.1.2 Surface Plasmon Resonance (SPR)

The sensorgrams for aqueous wheat gluten solutions at pH 7.7 and 11 are presented in Figure 5.

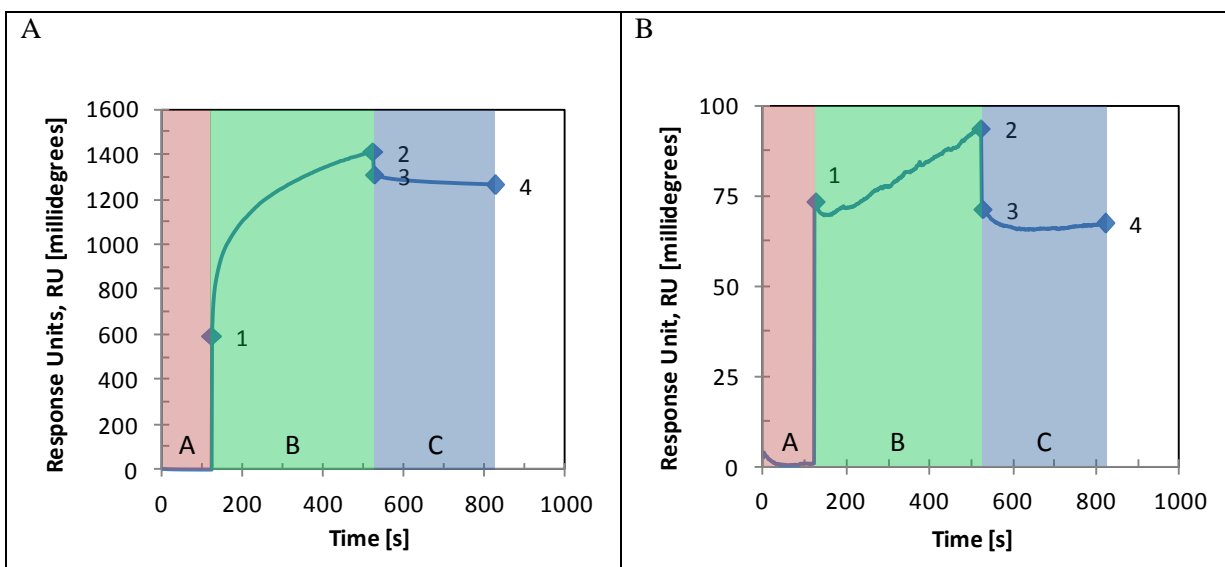


Figure 5 - SPR Sensorgram of Wheat Gluten in Milli-Q Water (1 mg/ml) at (A) pH 7.7 and (B) pH 11 on a Hydrophilic SAM (note the different scales for the ordinate axes)

Table 5 provides a description of the three phases of the SPR experiment for the two SPR sensorgrams of Figure 5.

Table 5 - Description of Each Phase of the SPR Sensorgrams

Phase	Description
Baseline (A)	pH 7.7 or 11 running buffer added to cuvette
Association (B)	pH 7.7 or 11 aqueous gluten sample added to cuvette (point 1 to 2)
Dissociation (C)	Running buffer wash (point 2 to 3) Additional running buffer in cuvette for 300 s (point 3 to 4)

In SPR experiments done by Barrett et al. with bovine and human serum albumin (BSA and HSA respectively) and their absorption to SAM surfaces, the washing step done at the beginning of the dissociation phase removed loosely bound protein from the surface such that the protein remaining on the surface was considered strongly (sometimes irreversibly) bound (Barrett et al. 2005). The same type of washing step as described by Barrett et al. was carried out in phase C (Dissociation), as described in Table 5.

Both the pH 7.7 and pH 11 running buffers resulted in flat baseline phases (after 50 s of stabilization) with very low noise (maximum variation of 0.8 m°), indicating that the system was stable before injecting the aqueous gluten samples. The flat baseline also indicates that no particulate matter in the running buffer was absorbing to the SAM surface confirming that there was no component in the running buffer contributing to the signal. However, following the addition of the aqueous gluten sample solution to the cuvette, the pH 7.7 and pH 11 aqueous gluten samples produced very different SPR curves. After the initial rapid rise in SPR signal (~600 RU), caused by changes in the solution refractive index in contact with the SPR disk (Ignagni 2011, de Bruijn et al. 1991), the signal for the pH 7.7 solution first displayed a rapid increase in RU, followed by a slower, almost linear increase in RU. Overall, the maximum change in RU, due to protein absorption to the surface, was 816 RU (Table 6).

Table 6 - Key Characteristics of the SPR Sensorgrams Calculated for RU Signal Changes of Aqueous Wheat Gluten Solution

Characteristic (position)	Aqueous gluten solution at pH 7.7 (RU)	Aqueous gluten solution at pH 11 (RU)
Max. Absorption (phase B: 2-1)	816	22
Irreversible Absorption (phase B and C: 4-1)	669 (82% of max.)	- 4 (-18% of max.)
Unbound molecules (phase B to C transition: 2-3)	102 (12.5% of max.)	24 (109% of max.)
Reversible Absorption (phase C: 3-4)	45 (5.5% of max.)	2 (9% of max.)

For the pH 7.7 aqueous gluten solution, washing the cuvette with running buffer resulted in an almost immediate decrease in the SPR signal by 102 RU (12.5% of the maximum change in RU due to association), suggesting that 12.5% of the gluten protein deposited on the SAM surface was not actually bound to the surface, or was bound very loosely according to the definition of loosely bound protein provided by Barrett et al. (Barrett et al. 2005). Between point 3 and 4, during the dissociation phase, the SPR signal dropped an additional 45 RU (5.5% of maximum change in RU), suggesting that 5.5% of the gluten protein that deposited on the surface dissociated from the surface while exposed to running buffer. The difference between the signal at the start of the association phase

(point 1 in Figure 5 A) and the signal at the end of the dissociation phase (point 4 in Figure 5A) was 669 RU (82% of maximum change in RU), indicating that 82% of the signal increase during the protein association phase was due to strong or irreversible binding to the SAM surface according to the definition of strongly bound protein provided by Barrett et al. (Barrett et al. 2005).

The association phase for the pH 11 aqueous gluten sample also exhibited an immediate increase in the SPR signal (~ 75 RU), due to the change of solution RI contacting the SPR disk (Ignagni 2011, de Bruijn et al. 1991). However, the magnitude of the jump was much less than at pH 7.7 supporting the effect of solution pH. During the association phase, the SPR signal decreased by 2 RU during the first 30 s, followed by a linear increase in the SPR signal of 24 RU throughout the remainder of the association phase. Note that due to the decrease in the SPR signal just after point 1 on Figure 5B, point 1 was not the lowest point in the association phase at pH 11, whereas it was for pH 7.7 (Figure 5A). However, the maximum absorption value was still defined to be 2-1 for the purposes of selecting a common basis for comparison of plot A and B and since the 2 RU difference is negligible. Washing with running buffer resulted in an immediate decrease in the SPR signal by 24 RU (109% of the maximum change in RU due to association), suggesting that very little of the gluten protein deposited on the surface during the association phase was strongly bound to the surface according to the definition of strongly bound protein provided by Barrett et al. (Barrett et al. 2005). Between points 3 and 4, during the dissociation phase, the SPR signal decreased an additional 2 RU, suggesting that the amount of protein in contact with the SAM surface only decreased a negligibly small amount. The difference between the signal at the start of the association phase (point 1 in Figure 5 B) and the signal at the end of the dissociation phase (point 4 in Figure 5B) was -4 RU. This suggests that none of the signal increase during the protein association phase was due to irreversible binding to the SAM surface.

Based on the contact angle measurements conducted by Barrett et al., a mercaptoundecanoic acid SAM layer creates a surface on the gold disk having a contact angle of 49° which the proteins can interact with when they come into contact with the disk surface (Barrett et al. 2005). In addition, Barrett et al. suggest that at the nearby pH of 7.4 the (SAM) 11-mercaptoundecanoic acid may have a negative charge enabling any positively charged protein side groups to participate in electrostatic interactions with the SAM surface (Barrett et al. 2005). The pI of glutenin and gliadin are 7.1 and 8.1 respectively (Gennadios, Weller & Testin 1993), so that at pH 7.7 it would be expected that the gluten will have a net charge near zero but still contain a substantial amount of protonated, positively charged amino acid side groups which can produce electrostatic interactions with the SAM. However, Barrett et al. point out that the pKa of carboxylic acid has been known to increase "in a tightly packed

SAM" environment and may undergo "strong ionic hydrogen bonding" such that protein interactions with the surface could be primarily hydrophilic/hydrophobic and not electrostatic. Barrett et al. further suggest that the SAM surface may exhibit a somewhat hydrophobic nature given the contact angle of 49°, which was higher than any of the other functionalized alkanethiol SAM's they studied (Barrett et al. 2005). The magnitude of the changes in SPR signal (Table 6) due to protein association on the SAM surface were much higher at pH 7.7 compared to pH 11. An increase in RU is associated with mass absorbing to the surface of the sensor disk (Eco Chemie B.V. 2006), which suggests that the gluten proteins at pH 7.7 had much higher affinity for the SAM surface compared to pH 11.

Based on Barrett et al., it is hypothesized that the differences in signal and initial shape of the absorption curves at pH 7.7 and 11 are due to differences in the hydrophobic and electrostatic interactions between the gluten proteins and the SAM surface and potentially some ionic interactions. At pH 7.7, the gluten proteins are believed to possess higher attraction to the SAM surface because of hydrophobic attractions between the SAM and hydrophobic regions of the proteins. There also exists the potential for a small amount of electrostatic attraction between positively charged amino acid side groups and the negatively charged SAM. Finally, the formation of "strong ionic hydrogen bond[s]" between the surface and the absorbed protein is also hypothesized to contribute to the production of irreversibly bound protein, as measured in the dissociation phase (Barrett et al. 2005). In contrast, at pH 11, the gluten proteins are believed to possess lower attraction to the SAM surface because of very strong electrostatic repulsion between the SAM and the proteins since the amino acid side groups and the SAM carboxylic acid groups would be highly negatively charged, resulting in repulsion.

It is possible to estimate the thickness of the protein layer absorbed to a SAM surface based on the molecular weight (MW) and radius of the protein combined with the measured increase in RU, as was done by Wang et al. with zein in a water-ethanol solution (Wang, Crofts & Padua 2003). However, in the case of a wheat gluten solution, the calculation would be a challenging because wheat gluten contains a mixture of proteins, some with very different sizes (Table 7).

Table 7 - Wheat Gluten Proteins with Molecular Weight, Radius of Gyration, and Relative Contribution to Total Wheat Gluten Mass

Protein Type	Sub-group	Shape	MW (kDa)*	Rg (nm)‡	Relative Mass Contribution (wt %)†
Glutenin	HMW	Globular	166-777	40-78	7-20
	LMW		5-35	< 10	30-43
Gliadin	alpha, gamma, omega	Extended	15-85	< 8 (monomeric)	30-35
Globulin & Albumin	-	-	25-75		15-20

* (Veraverbeke, Delcour 2002, Angellier-Coussy et al. 2011, Mendichi, Fisichella & Savarino 2008)

‡ (Mendichi, Fisichella & Savarino 2008, Stevenson et al. 2003)

† (Veraverbeke, Delcour 2002, Fu, Sapirstein 1996)

Given the ranges of molecular weights, radii of gyration and relative mass contribution of each gluten protein component, a quantitative value such as the total coating thickness or total mass of protein deposited on the SAM cannot be estimated accurately.

4.1.2.1 Conclusions

Aqueous gluten samples at two pH displayed very different SPR sensorgrams, indicating significant differences in the nature of the interactions of the gluten with its neighbour gluten and the SAM surface. At pH 7.7, the aqueous gluten solution exhibited a high affinity for the SAM surface believed to result from hydrophobic and electrostatic attractions between the protein and the SAM surface. The irreversible binding observed at pH 7.7 is believed to result from ionic interactions. At pH 11, the aqueous gluten solution exhibited very little affinity for the SAM layer because hydrophobic attractive forces appeared to be overpowered by electrostatic repulsion between the negative charge of the gluten proteins and the SAM surface. Since gluten consists of a mixture of proteins, estimation of the coating thickness absorbed to the SAM surface could not be obtained.

4.1.3 Kinematic Viscosity of Aqueous Wheat Gluten and Glycerol Solutions as a Function of pH and Solution Density

During the pH adjustment stage of casting solution preparation, a qualitative increase in viscosity was observed as the pH was adjusted to pH 11. To quantify these observations, the kinematic viscosity and density of aqueous wheat gluten and glycerol solutions over the range of pH 9.5 to 11 at room temperature were determined and are given in Table 8. The dynamic viscosity of the solution can be obtained from the product of kinematic viscosity and density (correct calculation units: cP = cSt x g/cm³)

Table 8 - Kinematic Viscosity and Density of Aqueous ADM Wheat Gluten and Glycerol Casting Solutions at Alkaline pH

pH	Kinematic Viscosity, n=6 (cSt)* (Average ± Standard Deviation)	Solution Density‡ (Error: ± 0.01) (g/cm ³)	Dynamic Viscosity † (cP)
9.5	1.5 ± 0.2	0.83	1.2
10.0	13.3 ± 0.4	0.95	13
10.5	16.4 ± 0.5	0.97	16
11.0	17.7 ± 0.6	0.97	17

*CentiStokes (cSt).

‡All densities at 10 % wt/wt wheat gluten (percent of total solution mass)

†CentiPoise (cP).

All of the kinematic viscosities were determined to be statistically significantly different from one another (p<0.05). The kinematic viscosity increased from 1.5 cSt to 17.7 cSt as the pH was increased from pH 9.5 to 11. At pH ≥ 10, the increase in viscosity began to plateau (Figure 6).

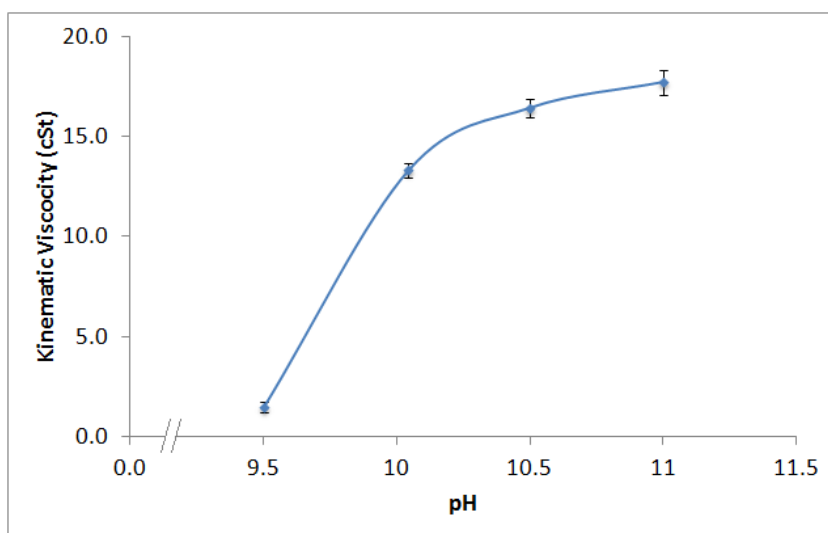


Figure 6 - Kinematic Viscosity as a Function of Gluten-Glycerol Solution pH

The density increased in a very similar manner over the same pH range, increasing from pH 9.5 to 10 and then plateauing as pH approached 11 (Figure 7).

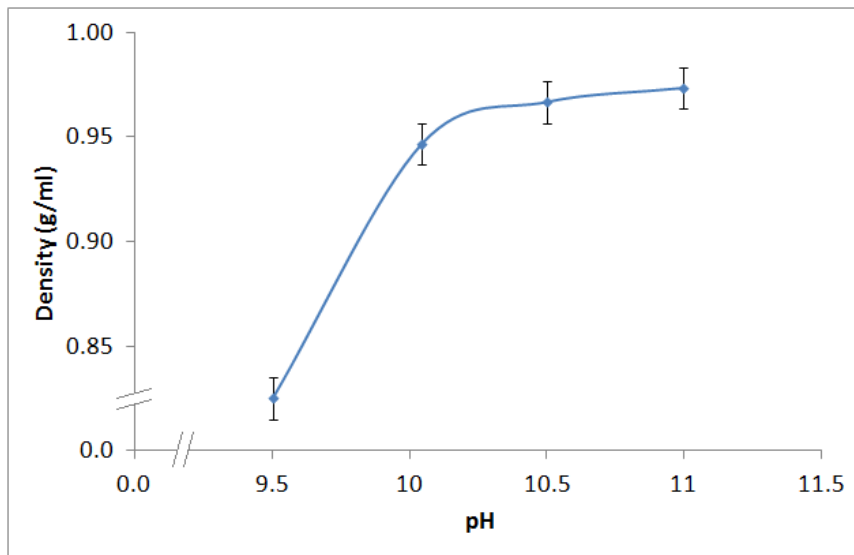


Figure 7 - Density as a Function of Gluten-Glycerol Solution pH

The increase in density reflects a more compact gluten solution at pH 10.0 compared to pH 9.5, confirming that significant changes in gluten water interactions occurred, likely caused by conformational changes of the gluten. In fact, kinematic viscosity and density are approximately directly proportional to one another within the range of pH 9.5 to 11, with a proportionality constant of 106 and R^2 equal to 0.9923 (Figure 8).

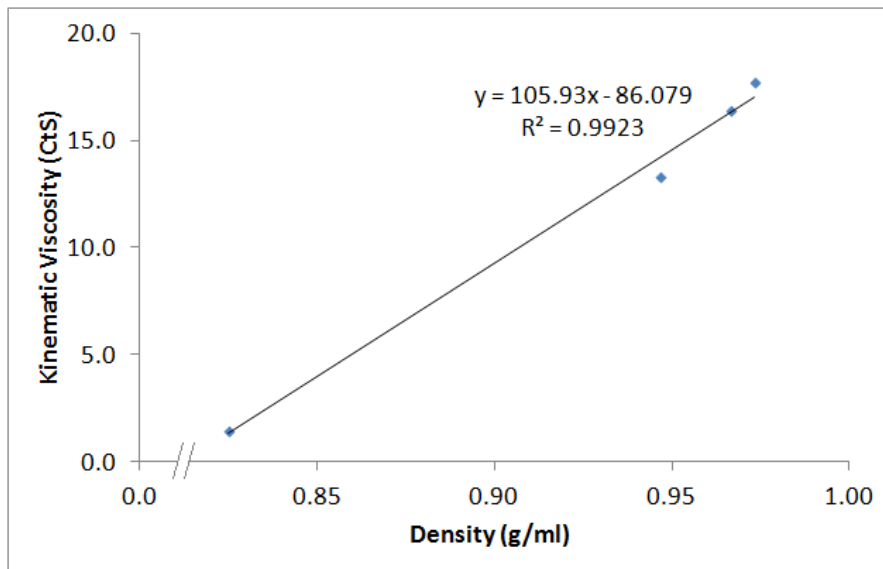


Figure 8 - Kinematic Viscosity as a Function of Density for Gluten-Glycerol Solutions, Caused by pH Change

The literature on the effect of pH and any type of protein solution viscosity is limited, and is even more limited or non-existent for basic pH solutions. Mastromatteo et al. reported that aqueous 10 wt% wheat gluten films containing 2 to 6 wt% glycerol and adjusted to pH 11 (also heated to 70°C for 15 min and cooled to 25°C for testing) are pseudoplastic ($n < 1$) non-Newtonian solutions (Mastromatteo et al. 2008). They also recorded a dynamic viscosity twice that of the pH 11 ADM gluten glycerol aqueous solutions studied here (40 cP compared to 17 cP). It is believed that the large difference between values reported in that literature and the pH 11 dynamic viscosity presented in Table 8 resulted from the different sample processing prior to testing. Mastromateo et al. heated and cooled the gluten solution but the results presented in Table 8 did not include a heating step. Heating a gluten solution allows for intra-molecular disulphide bonds to break and reform as inter-molecular disulphide bonds, thus strengthening the network (Angellier-Coussy et al. 2011, Schofield et al. 1983) and likely producing the higher dynamic viscosity for the gluten solutions reported by Mastromateo et al.

Despite the limited literature on the viscosity of aqueous protein solutions, the literature viscosity data suggests that the relationship between solution viscosity and pH is not consistent for all types of proteins dispersed in solution nor for all pH ranges. For example, in a study of a semi-dilute mucin glycoprotein solution (1 wt%), Maleki et al. observed an increase in zero-shear viscosity from pH 1 to

2 but a nearly linear decrease in viscosity from pH 2 to 7 (Maleki et al. 2008). In comparison, the viscosity of aqueous dispersions of the polysaccharide pectin (1 wt%) decreased approximately linearly by 2 cSt as the pH was increased from pH 3 to 6 (Guimarães, Coelho Júnior & Garcia Rojas 2009). Further, unlike the positive linear viscosity to density trend observed for the wheat gluten in Table 8 and shown in Figure 8, the relationship between kinematic viscosity and density was non-linear for the 1 wt% aqueous pectin solutions (Guimarães, Coelho Júnior & Garcia Rojas 2009).

The effect of pH on solution viscosity and density in Table 8 may be better understood by considering the literature on wheat gluten films and molecular protein interactions in aqueous solutions. Olabarrieta et al. determined that for gluten-glycerol films (~11 wt% wheat gluten and ~4 wt% glycerol) prepared with a 75°C heating step, there is an increase in the level of intermolecular interactions for dried pH 11 films compared to pH 4 films, based on SE-HPLC results, indicating that pH 11 films have a lower fraction of SDS soluble protein compared to pH 4 films (Olabarrieta et al. 2006). Olabarrieta et al. further concluded that a higher degree of denaturation was present during the preparation of pH 11 films (Olabarrieta et al. 2006). In a study of acidic aqueous zein protein solutions, Li et al. suggested that at high zein concentrations (above 43mg/ml), the protein molecules come into contact facilitating intermolecular interactions and intermolecular penetration occurs (Li et al. 2011). It is also known that the pI of wheat gluten is 7.5 (Gennadios, Weller & Testin 1993) and thus increasing the pH of an aqueous wheat gluten solution from 9.5 to 11 will increase the number of negative charges on the wheat gluten molecules (Lehninger, Nelson & Cox 2004). The increase in number of negative charges with increasing pH would likely contribute to wheat gluten denaturation and rearrangement, resulting in a new stable conformation in the alkaline environment. Therefore, the increase in viscosity and density as pH was increased suggest the wheat gluten was increasingly denatured as reflected in the viscosity.

4.1.3.1 Conclusions

The viscosity of aqueous glycerol gluten solutions increased significantly when pH was increased from 9.5 to 10. When the pH of the aqueous glycerol gluten solution was further increased from pH 10 to pH 11.0, the magnitude of the viscosity increase was smaller. The increase in viscosity suggests that most of the changes in the gluten solution occur in a narrow pH range and could be associated with wheat gluten denaturation, intermolecular penetration and a resulting increase of intermolecular interactions. The approximately parallel increase in density with increasing pH, supports the hypothesis that increasing the pH increases solution viscosity due to wheat gluten denaturation, intermolecular penetration, and increasing intermolecular interactions.

4.2 Thermal Stability of Wheat Gluten, Glycerol, and Wheat Gluten Films

4.2.1 Thermal Stability of Primary Film Ingredients: Wheat Gluten and Glycerol

Sample TGA and DTGA plots for the gluten of four different Ontario wheat cultivars and two commercial wheat glutes are shown in Figure 9. The properties of the TGA curves for wheat gluten film ingredients are summarized in Table 9.

The characteristics of the gluten TGA and DTGA curves reported in Figure 9 are consistent with TGA and DTGA results reported by Mohamed et al. for commercial vital wheat gluten (Mohamed et al. 2008). Mohamed et al. reported a primary DTGA peak occurring around 310°C, with a shoulder to the right of the primary DTGA peak similar in size and location to the shoulder observed for the Wonder, Emmit and Sigma wheat gluten main DTGA peaks. The wheat gluten TGA and DTGA results of Mohamed et al. also included a minor peak, occurring around 60°C, and a residual mass of approximately 22% at 595°C (Mohamed et al. 2008).

For the gluten analyses presented in Figure 9, the primary thermal decomposition peak (largest peak on the DTGA curve, and largest drop in the TGA curve) for all the wheat gluten samples covered the range between 250 and 400°C, with the peak maximum always near 300°C (between 294 to 318°C for all samples). In Table 9, the primary peak for gluten DTGA thermograms is labeled Peak 3. According to TGA and DTGA curves for wheat gluten presented by Mohamed et al., this primary peak can be attributed to wheat gluten (Mohamed et al. 2008).

A shoulder also appeared to the right side of this main DTGA peak occurring near 400 - 450°C for all of the samples. However, the Emmit, Wonder, and Sigma samples did not have as large of a shoulder as the Norwell, Harvard, and ADM Whetpro80 samples. TGA studies of gluten constituents by Gomez-Martinez et al., show that gliadin undergoes thermal decomposition before glutenin and degrades more rapidly and at a lower temperature than glutenin, which is characterized by a sharp gliadin DTGA peak and a short broad glutenin DTGA peak (Gómez-Martínez et al. 2011). Therefore, the “sharp” character of the largest DTGA peak for the glutes in Figure 9 is believed to be the gliadin component of gluten while the shoulder on the right of the peak is believed to result from the slightly later thermal degradation of glutenin. The proximity of the temperatures for thermal degradation for glutenin and gliadin mean that the gliadin and glutenin thermal degradation peaks merge so it is difficult to differentiate between them (Figure 9 A through F).

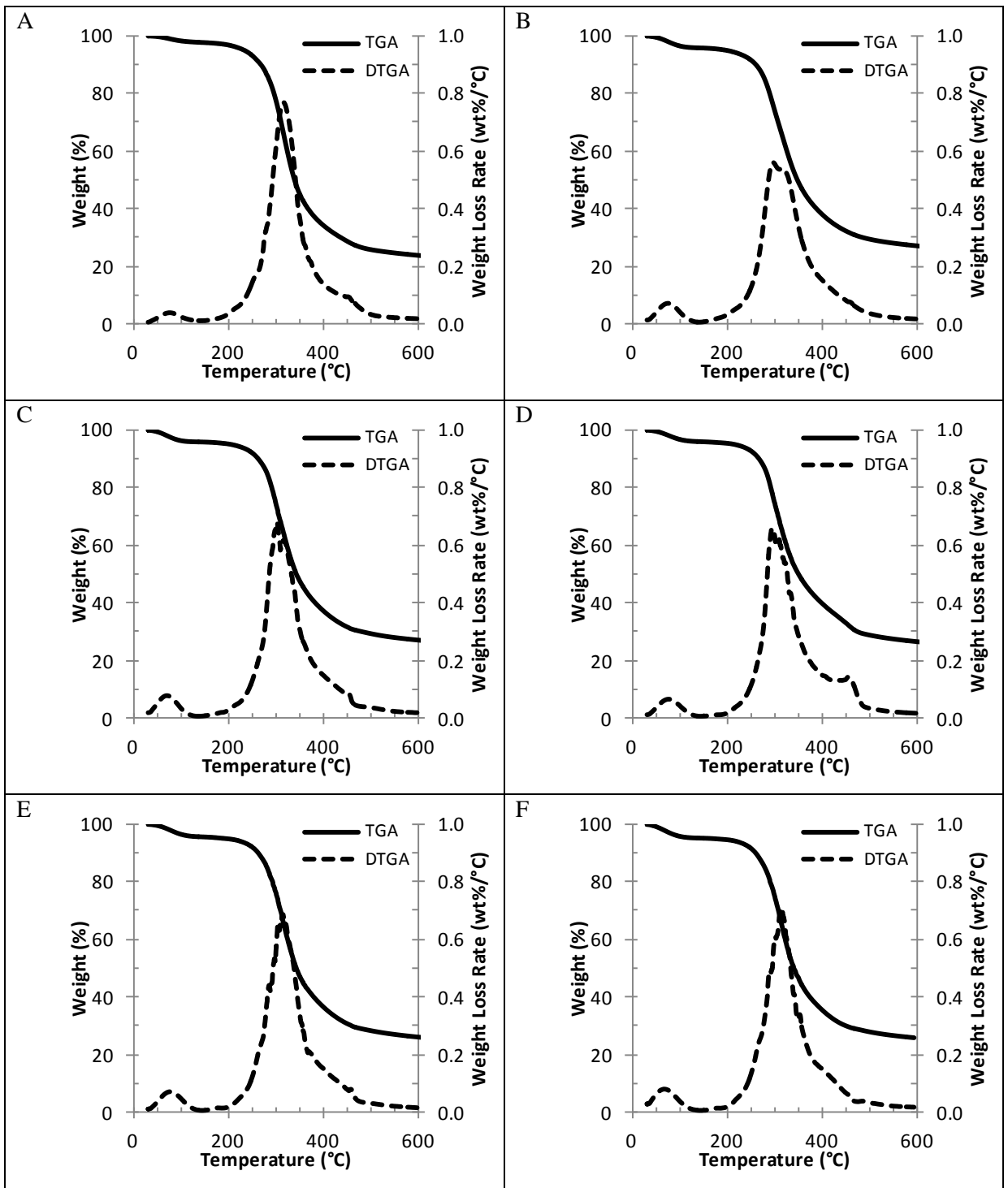


Figure 9 - Thermogravimetric (TGA) and Differential Thermogravimetric (DTGA) Curves Conducted in Nitrogen at a rate of 50 ml/min for Gluten from the Ontario Cultivars (A) Wonder, (B) Emmit, (C) Harvard, and (D) Norwell, as well as the Commercial Wheat Glutens (E) Sigma and (F) ADM Whetpro80.

Table 9 - Characteristics of the Thermogravimetric Analysis Conducted in Nitrogen at a Flow Rate of 50 ml/min for Glycerol and Gluten from Four Different Ontario Wheat Cultivars and Two Commercial Sources

Sample	Test Date (D-M-Y)	1% Onset of Degradation (°C)	Peak 1		Peak 2		Peak 3		Residual Mass at 595 °C (%)
			DTGA (°C)	ΔW (%)	DTGA (°C)	ΔW (%)	DTGA (°C)*	ΔW (%)	
Wonder Gluten	12-Jan-11	203.0	76.0	3.2	N/A	N/A	316.4	73.3	23.5
	10-Aug-11	206.9	63.0	7.4	N/A	N/A	317.5, (295.4)	69.8	22.8
Emmit Gluten	12-Jan-11	203.3	74.1	5.2	N/A	N/A	297.0, (318.3)	67.9	26.9
	10-Aug-11	208.8	66.2	7.0	N/A	N/A	318.6	70.2	22.8
Harvard Gluten	12-Jan-11	209.3	69.7	5.2	N/A	N/A	302.6, (315.2)	68.2	26.7
Norwell Gluten	12-Jan-11	217.0	76.0	4.9	N/A	N/A	294.5, (308.3, 322.7)	68.6	26.5
Sigma Gluten	12-Jan-11	212.9	75.4	5.4	N/A	N/A	315.1	68.7	25.9
	09-Aug-11	213.4	59.8	8.4	N/A	N/A	313.2, (265.8)	69.9	21.8
ADM Whetpro 80 Gluten	09-Aug-11	216.9	67.3	6.7	N/A	N/A	315.3, (301.3)	68.1	25.3
	02-Feb-12	219.0	85.6	2.5	N/A	N/A	317.7 (301.5)	75.1	22.5
Glycerol	10-Aug-11	124.6	63.0	2.1	238.9	97.9	N/A	N/A	-0.02
	02-Feb-12	149.7	72.7	0.46	275.7	99.4	N/A	N/A	0.13

*Numbers in brackets are the temperatures for the second highest neighboring DTGA peak maximum.

For TGA studies of wheat gluten films by Chiou et al. a small DTGA peak around 100°C was attributed to water evaporation (Chiou et al. 2010). It is believed that the small secondary DTGA peak observed below 100°C in Figure 9, with a peak maximum between 60 and 76°C for all the wheat gluten samples, can be attributed to water evaporation. The residual mass at 595°C was quite large, ranging between 22 and 27% of the mass for the various wheat gluten samples.

The similarity in peaks shared between Ontario and commercial wheat gluten in Figure 9, as well as with literature results by Mohamed et al., is a good indication that wheat gluten was indeed obtained

when washing Ontario wheat cultivar flours to remove starch. Further, the similarities observed support the expectation that all the wheat gluten samples have similar compositions.

As mentioned earlier, the gluten from hard red winter wheat (Norwell and Harvard cultivars), had a larger shoulder to the right of the primary DTGA peak, compared to the gluten from soft red winter wheat (Wonder and Emmit cultivars). The larger shoulder in the Harvard and Norwell DTGA thermograms is attributed to a component in the hard red winter wheat gluten present in smaller quantities in the soft red winter wheat gluten and to a larger proportion of hard red winter wheat gluten being more thermally stable than soft red winter wheat. In addition, if the trend holds true for all types of wheat gluten, Sigma commercial wheat gluten is from a soft winter wheat while ADM Whetpro80 commercial wheat gluten is a hard winter wheat (information not available from either ADM or Sigma-Aldrich).

The effect of Test Date (Table 9) on the TGA of the gluten from Wonder, Emmit, Sigma, and ADM Whetpro80 was obtained by conducting the analysis on two different dates. Despite the variation in lab humidity conditions that might be expected to occur during the summer and winter months, there is only a small amount of variation in temperature for the peak 1 and 3 DTG maxima for a given type of gluten sample. By comparing the peak 1 DTGA temperatures for a given type of gluten sample along with their associated relative mass change (ΔW), it is observed that the rate of water evaporation reaches a maximum at a lower temperature for a more humid gluten powder sample (higher ΔW_1).

The 1% onset of thermal degradation listed in Table 9 are slightly higher for the commercial wheat glutens Sigma and Whetpro80 compared to the gluten from Ontario wheat cultivars, with the exception of Norwell wheat gluten. The gluten sources with higher 1% onset of degradation suggest that they are slightly more thermally stable samples.

The 1% onset of thermal degradation for glycerol (a liquid at room temperature) are also listed in Table 9 and are much lower and more variable than for wheat gluten powder, indicating that glycerol is less thermally stable than wheat gluten powder. The TGA and DTGA curves for glycerol are shown in Figure 10.

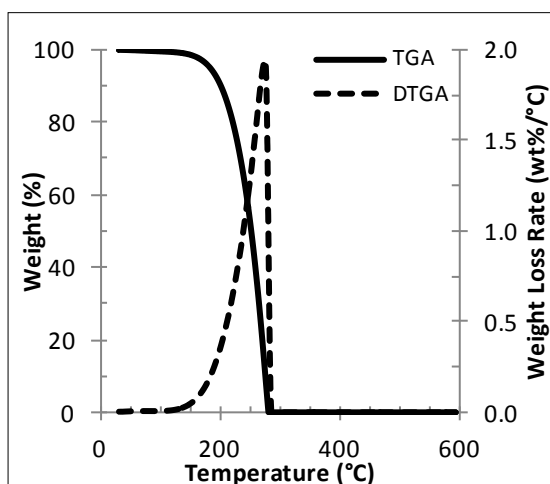


Figure 10 - Sample TGA and DTGA curves for Glycerol

The main DTGA peak temperature (peak 2) for glycerol from Table 9, at 239 or 276°C was also quite inconsistent between the two test dates compared to the gluten peak temperatures, suggesting that the thermal stability of glycerol may be very sensitive to environmental conditions or may change gradually over time. The glycerol used in this study had a higher thermal stability than in a thermogravimetric study by Dou et al. for pure glycerol (heated at 10°/min in a nitrogen environment), where a maximum rate of mass loss was observed at 168°C, and a final mass loss temperature of 237°C was observed (Dou et al. 2009).

4.2.2 Thermal Stability of Wheat Gluten Films

Table 10 provides the film solution conditions without glycerol that were used to prepare the gluten films at each stage of the film casting procedure.

Table 10 - Description of Gluten Film Preparation Conditions Without Glycerol

No Glycerol Gluten Film Label	Casting pH	Temperature of Solution Heat Treatment (°C)	Sonication? Yes/No
NGT30pH7	7	30	No
NGT30pH11	11	30	No
NGT70pH11	11	70	No
NGT70pH11 sonicated	11	70	Yes

Figure 11 shows sample TGA and DTGA plots for wheat gluten films cast using ADM Whetpro80 gluten with glycerol and gluten films without glycerol where the casting solution was adjusted according to pH, temperature, and sonication prior to casting the film (described in Table 10). The characteristics of the TGA curves of ADM Whetpro80 wheat gluten films with and without glycerol are summarized in Table 11.

From Figure 11, all the films exhibited a primary DTGA peak accounting for the thermal degradation of 50 to 71% of the sample mass and with a maximum between 291 and 315°C (peak 3 of Table 11). The maximum for peak 3 of the DTGA for ADM WP80 gluten powder (Table 9), also occurred between 301 and 318°C, indicating that the temperature of peak 3 for the wheat gluten films is also associated with thermal degradation of wheat gluten. The DTGA of the films also exhibited the same shoulder characteristic to the right of peak 3, suggesting that glutenin still degrades over a longer temperature range and with a slightly higher temperature for maximum rate of degradation compared to gliadin (Gómez-Martínez et al. 2011). Therefore, the sharp character of the largest DTGA peak for the gluten films (Figure 11) is believed to be the gliadin component of gluten while the right shoulder of the peak is believed to result from the thermal degradation of glutenin that occurs at a higher temperature. The proximity of the temperatures for thermal degradation for glutenin and gliadin result in a thermal degradation peak that is partially merged as seen in Figure 11 A through E.

According to the TGA studies for wheat gluten films by Gomez-Martinez et al., the presence of glycerol reduces intermolecular forces in the three-dimensional protein network of the film, thus increasing protein chain mobility (Gómez-Martínez et al. 2011). Therefore, the lower 1% onset of thermal degradation observed for film T70pH11SR with glycerol compared to the film with no glycerol (NGT70pH11sonicated) is believed to occur because glycerol creates chain mobility between protein molecules in the T70pH11SR film with glycerol. The multiple DTGA peaks contained in peak 2 (Table 11) for the T70pH11SR film with glycerol are believed to be associated with glycerol evaporation (Gómez-Martínez et al. 2011) and are suspected to occur because the protein matrix hinders glycerol release.

The ADM Whetpro80 films (T70pH11SR) with glycerol prepared and tested on August 2011 and February 2012 exhibited a fair bit of difference for the DTGA peak 1 temperature and the 1% onset of degradation temperature, with the August 2011 film having the higher temperature. However, for peaks 2 and 3 (associated with glycerol and wheat gluten peaks, respectively), the film prepared and tested in the winter term (Feb 2012) had higher peak temperatures and thus is believed to be more

thermally stable. The most likely cause for the improved thermal stability of the Feb 2012 film is from differences in ambient humidity during film preparation.

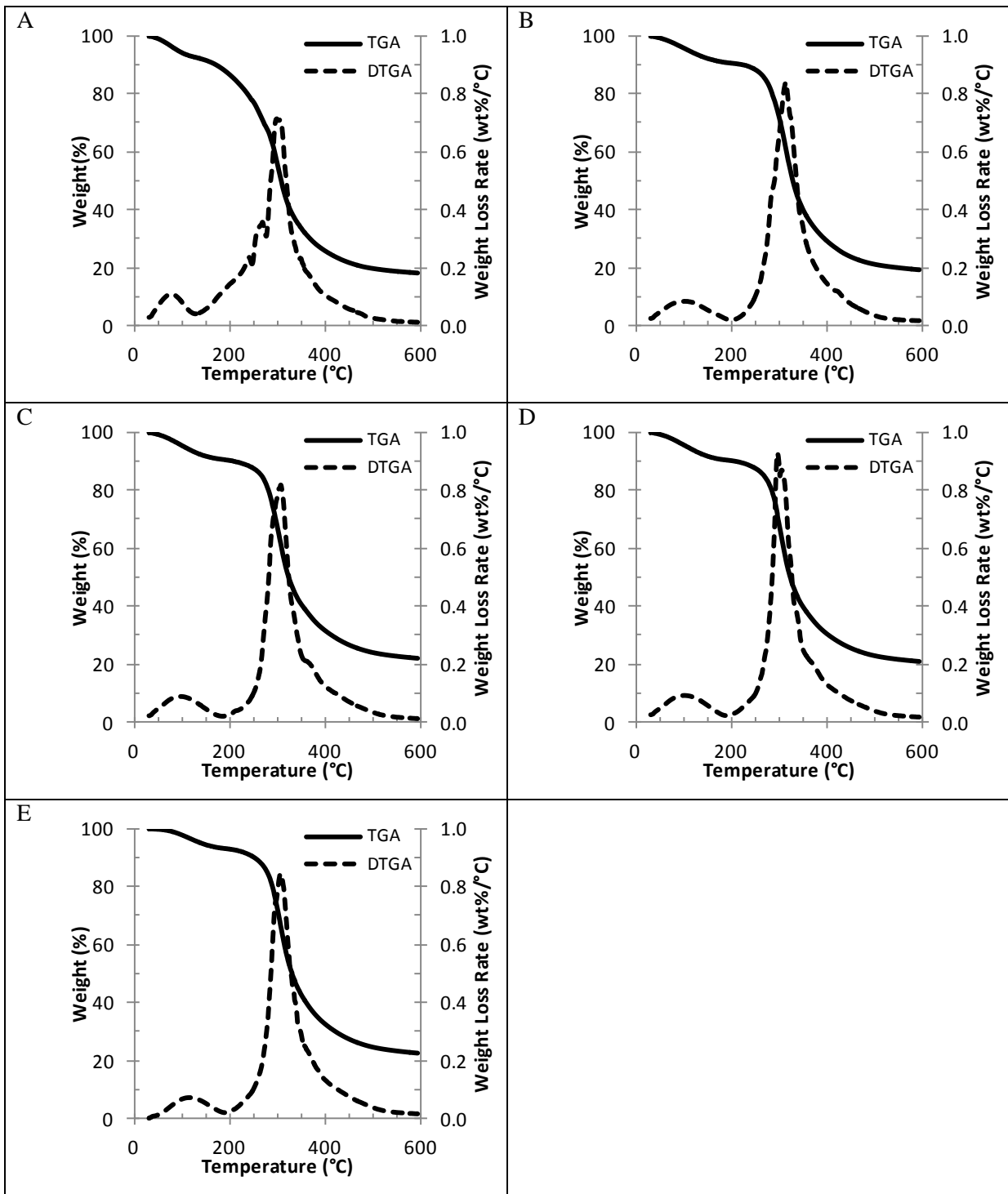


Figure 11 - Thermogravimetric (TGA) and Differential Thermogravimetric (DTGA) Thermograms performed under Nitrogen with a flow rate of 50 ml/min for Gluten Films Containing Glycerol (A) ADM WP80 Film or No Glycerol and Cast at Varying Stages of the Film Solution Preparation: (B) NGT30pH7, (C) NGT30pH11, (D) NGT70pH11, (E) NGT70pH11sonicated.

Table 11 - Characteristics of the Thermogravimetric Analysis Conducted under Nitrogen at a Rate of 50 ml/min for Gluten Films Cast With and Without Glycerol and at Varying Stages of Film Solution Preparation

Sample	Test Date (D-M-Y)	1% Onset (°C)	Peak 1		Peak 2		Peak 3		Residual Mass at 595°C (%)
			DTGA (°C)	ΔW (%)	DTGA (°C)	ΔW (%)	DTGA (°C)	ΔW (%)	
T70pH11SR Film with Glycerol	10-Aug-11	186.6	101.2	9.0	255.6, (242.7)	13.4	291.1, (301.3)	57.3	20.4
	03-Feb-12	150.2	75.9	8.0	269.0 (241.2)	24.0	298.9 (306.3)	49.9	18.1
NGT30pH7	03-Feb-12	234.3	98.2	9.9	N/A	N/A	314.7 (325.2, 285.7)	70.9	19.2
NGT30pH11	03-Feb-12	218.7	97.5	9.9	N/A	N/A	307.5 (292.5)	68.3	21.8
NGT70pH11	03-Feb-12	224.6	101.4	10.0	N/A	N/A	297.5 (306.3)	69.0	20.9
NGT70pH11 sonicated	03-Feb-12	223.4	118.8	9.3	N/A	N/A	306.7 (296.6)	70.0	21.7

Several changes in TGA curve characteristics can be observed for the films prepared with no glycerol and cast at progressive stages of the regular film casting procedure. Increasing the pH of the solution from pH 7 to pH 11 decreased the 1% onset temperature by 15.6°C but subsequent heating of the film solution to 70°C increased the 1% onset temperature of the NGT70pH11 film by 5.9°C compared to the NGT30pH11 film. The increase in pH from pH 7 to 11 also appeared to decrease the temperature of the peak 3 DTGA maximum, suggesting that wheat gluten is slightly less thermally stable at pH 11 compared to pH 7 (in the absence of glycerol). Finally, adding a sonication step at the end of the film solution preparation resulted in an increase in the temperature for the maximum DTGA peak of water moisture in the film, suggesting that the sonication step may allow the film to retain more moisture. Marcuzzo et al. reported that wheat gluten films prepared with a sonication step in the casting procedure may result in a breakdown of large protein aggregates at the mesoscopic level, potentially creating a slight plasticizing effect in the film due to the smaller molecular weight gluten fragments. Therefore, here it is believed that, the NGT70pH11sonicated film may retain more moisture due to a more open structure (Marcuzzo et al. 2010).

4.2.2.1 Conclusions

Wheat gluten undergoes thermal decomposition between 250 and 400°C with a maximum rate of degradation around 300°C that is fairly constant for gluten in powder or film form and whether or not the film contained glycerol. The shoulder on the right side of this primary DTGA peak may be

attributed to glutenin which degrades at slightly higher temperatures and more gradually than gliadin, and was observed for gluten powder and gluten films. The small DTGA peak below 100°C was attributed to evaporation of water from the sample.

For gluten powder, an inert nitrogen environment resulted in a relatively high residual gluten mass of 22 to 27% at 595°C. The height of the shoulder on the right of the primary DTGA peak was larger for the hard red winter wheat compared to the soft red winter wheat. The testing environment did not impact curve characteristics as much as expected but the higher the moisture content of a gluten powder sample was at the outset, the lower the temperature of the maximum DTGA peak associated with water evaporation. The commercial wheat gluten samples tended to have a higher 1% onset of thermal degradation compared to the Ontario wheat cultivars, except for Norwell gluten, suggesting a greater thermal stability in the commercial gluten samples and the Norwell gluten. Glycerol had a much lower 1% onset of thermal degradation, a much lower water content and the primary DTGA peak occurred at a lower temperature compared to gluten samples, suggesting that glycerol is less thermally stable than gluten.

The presence of glycerol in wheat gluten films is believed to reduce intermolecular forces between protein chains, resulting in a lower 1% onset of thermal degradation for glycerol containing films compared to with no glycerol (NGT70pH11sonicated). A larger temperature range for glycerol evaporation in films compared to pure glycerol is believed to result from protein matrix interactions with glycerol hindering its escape.

Films prepared with no glycerol and cast at pH 11 had a lower onset temperature than when cast at pH 7. However, heating the film solution to 70°C increased the 1% onset temperature partially again. The increase in pH from pH 7 to 11 also appeared to decrease the temperature of the peak 3 DTGA maximum, suggesting that wheat gluten is slightly less thermally stable at pH 11 compared to pH 7 (in the absence of glycerol). Finally, adding a sonication step at the end of the preparation of the film solution resulted in an increased temperature for the maximum DTGA peak of water moisture in the film, suggesting that the sonication step may allow the film to retain more moisture in it due to a more open structure.

4.3 Film Surface Investigation

4.3.1 Film Surface Morphology - Effect of Modifying ADM Film Preparation Methodology

4.3.1.1 Effect of Film Casting Surface

Top surface microscope images of gluten films cast on a glass surface with a silicone release layer and on a silicone surface with no release layer are shown in Figure 12. The top film surface is defined as the surface exposed to air.

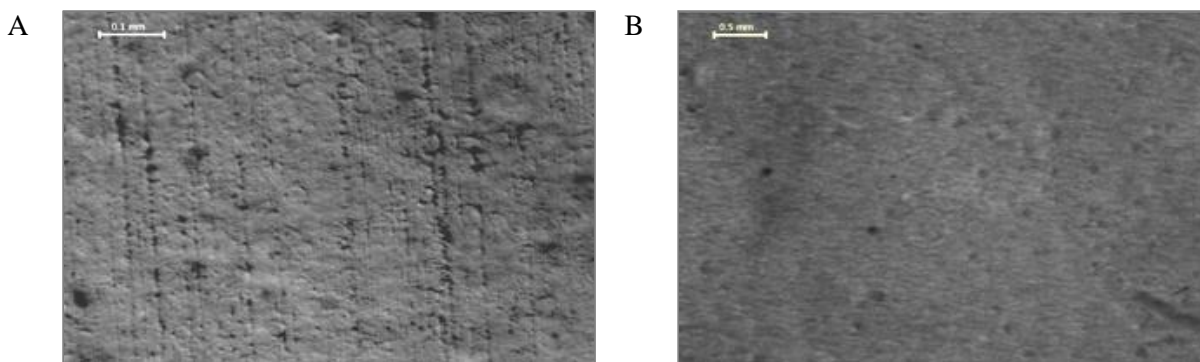


Figure 12 - Microscope Images of ADM Gluten Film Surface (Gluten solution at pH 11, 70°C) Cast on (A) Glass Surface with Silicone Release Layer and (B) Silicone Surface with no Release Layer.

Microscope images of the film top surface revealed 8 to 12 μm wide parallel grooves in the gluten film cast on a glass surface. However, inspection of the glass casting surface after the application of a silicone grease release layer and before film casting, revealed parallel ridges in the silicone grease layer, like those seen under the microscope. Therefore, it was determined that the silicone grease release layer applied to the glass casting surface produced the parallel ridges seen in the microscope image in Figure 12A. Subsequent inspection of the top and bottom surface of the film cast on the glass surface (Appendix 4) showed a very smooth top surface but a bottom surface covered with very small parallel lines. It was concluded that microscope images of the top surface of the wheat gluten films also captured features from the bulk of the film and bottom film surface due to the semi-transparent nature of wheat gluten films. The semi-transparent nature of wheat gluten films is fairly well documented in the literature (Sánchez et al. 1998, Cho, Gällstedt & Hedenqvist 2010, Gontard, Guilbert & Cuq 1992). The similar lines present on the bottom film surface and the casting surface suggests that the wheat gluten film solution conforms to the casting surface and maintains the form as it dries. This conformation of the gluten film to the casting surface would be an ideal property for dip

coating applications as demonstrated by Tanada-Palmu et al. with wheat gluten casting solutions (Tanada-Palmu, Grosso 2005).

The film cast on a silicone surface (Figure 12B) had a relatively featureless, homogeneous appearance with a few dark (black or grey) spots spread across the surface, possibly submerged in the film bulk. The homogeneous appearance of the film cast on a silicone surface agrees with observations during film solution preparation where the film casting solution also appeared homogeneous. The indistinct outline of several small circle structures also appeared in the microscope images of both films (Figure 12). These circle structures could not be identified and have not been reported in literature. By changing the focal length of the microscope, it was determined that the rims of these circles protruded out of the film surface while the centers remained at the same height as the film outside the circles.

Given that the top surface of the film cast on the glass surface (Figure 12A) could not be properly captured (Figure 12A and Appendix 4), a more detailed visual inspection was also carried out on the two films. The visual inspection revealed that the gluten film cast on the silicone surface was more homogeneous and had a smoother surface than the film cast on the glass surface. It is suspected that the film cast on the glass surface was not as homogeneous because the spreading of silicone on the casting surface was done manually affecting the uniformity of hydrophobicity across the surface. Since proteins can respond to the hydrophobic surface because they are made up of both hydrophobic and hydrophilic regions (Davis, Copeland 2000), one might expect that the distribution of the gluten proteins during film casting would be affected by the hydrophobicity of the casting surface. Furthermore, since the water evaporates exclusively from the air-solution interface during drying, the components in the lower part of the film surface will have more time to rearrange in solution (Marcuzzo et al. 2010) and, in the case of the glass surface, the rearrangement will be affected by the uneven degree of hydrophobicity of the casting surface. The uneven distribution of hydrophobic silicone grease is believed to make the film cast on the glass surface more heterogeneous than with the uniform surface of the silicone surface. In addition, it is suspected that the heterogeneous distribution of the protein in the bulk of the film could affect the top surface of the film too, reducing the surface smoothness of the film cast on the glass surface compared to the silicone surface.

As gluten films cast on glass surface stuck to the glass during drying, making it very difficult to peel the dried film (results not shown), a layer of silicone vacuum grease was applied to the glass surface before film casting to prevent films from sticking to the surface excessively and help with their removal. However, the use of silicone grease also introduced a source of contamination to the film

(details presented in chapter 4.3.4 Film Surface Hydrophobicity). Alternatives to eliminate the addition of silicone grease while being able to remove the dried films relatively easily was obtained by casting the films on the silicone surface. The use of a smooth casting surface having no release layer eliminates a potential source of contamination and error in studying the film properties, as well as producing a smoother film. Therefore, a silicone surface was adopted and films produced on this surface will be discussed in the remaining sections of this chapter.

4.3.1.2 Effect of Heating Temperature for ADM Gluten Films

The gluten solutions prepared by heating at temperatures of 70 and 80°C were all homogeneous before and during casting, containing no protein aggregates. However, the gluten solution prepared at 100°C contained aggregates or clumps. After drying, the ADM gluten films appeared as shown in Figure 13.

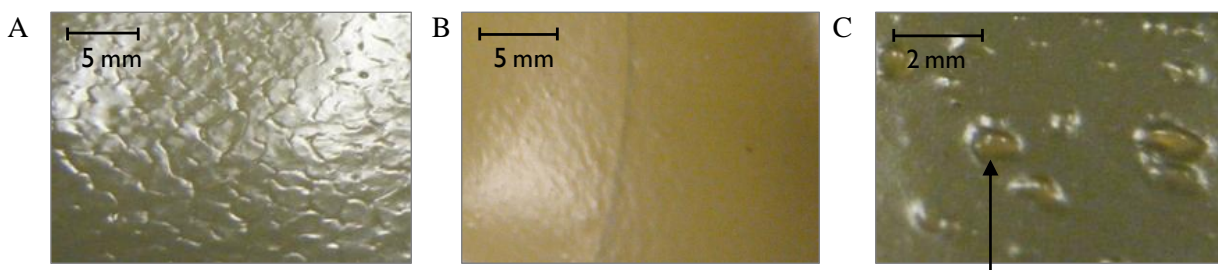


Figure 13 - Camera Images of ADM Gluten Films Cast from Solutions Heated to (A) 70 °C, (B) 80 °C, and (C) 100 °C. Arrow denotes an example of a raised bump.

The gluten film solutions prepared at 70°C produced beige, semi transparent, very homogeneous and fairly smooth films (Figure 13A). However, close inspection showed small channels/grooves spread across the surface of the films, but which did not pass through the films. These small grooves are the lines seen all over the film surface in Figure 13A, giving the film a slightly rippled appearance. The gluten solution prepared at 80°C produced an extremely smooth and homogeneous film (Figure 13B) that was slightly more opaque than the 70 °C gluten films but very similar in colour. The gluten solution prepared at 100°C produced a film slightly darker than the 70 °C films but with raised bumps (Figure 13C) of a slightly lighter colour than the rest of the film, making it a quite heterogeneous film. The flat areas of the film, between the raised bumps were smooth like the whole 80 °C film, with no grooves/channels formed on the surface. The bumps on the surface were determined to be solid, and not air bubbles.

The differences in surface morphology may be related to the size of gluten proteins when exposed to different temperatures. For example, Domenek et al., investigated the SDS-soluble gluten protein

fraction of wheat gluten films moulded at different temperatures by SE-HPLC (Domenek et al. 2002). Domenek et al. reported that the high molecular weight wheat gluten constituent, glutenin, is most reactive and participates in disulfide interchange reactions at lower temperatures (beginning ~60-70°C), while the lower molecular weight wheat gluten constituent, gliadin, is less reactive and only participates at higher temperatures (beginning ~90°C) (Domenek et al. 2002). Angellier-Coussy et al. observed that as the heating temperature is increased, more of the glutenin molecules are able to participate in disulfide interchange reactions, which should improve the protein network (Angellier-Coussy et al. 2011). Therefore, it is believed that increasing the heat treatment temperature from 70 to 80 °C allowed more of the glutenin molecules to participate in disulfide interchange reactions, creating a more complete protein network with better inter-molecular cross-links. The value of increasing the protein network is in the type of cross-linking formed by disulfide interchange reactions when wheat gluten is heated. Before heat treatment, intra-molecular disulfide bonds exist between glutenin subunits in a single glutenin unit. Increasing the temperature unfolds the proteins so that glutenin (and gliadin at temperatures above 90°C) participate in disulfide interchange reactions between exposed groups (inter- and intra-molecular), locking the protein into a three-dimensional network (Domenek et al. 2002, Angellier-Coussy et al. 2011). Therefore, an increased three-dimensional protein network at 80°C is believed to be associated with the improved surface smoothness and homogeneity observed by increasing the temperature from 70 to 80°C.

In contrast to the film cast from a gluten solution at 80°C, the appearance of clumps observed in the film for the gluten solution heated to 100 °C suggests that too many disulfide interchange reactions occurred at 100°C. Recall that above 90 °C, both gliadin and glutenin participate in disulfide interchange reactions (Domenek et al. 2002). Since distinctive bumps appeared across the surface of the very smooth film, it is believed that the participation of gliadin in disulfide interchange reactions produced excessive cross-linking. The solid appearance of the distinctive bumps and the consequence of disulfide interchange reactions which polymerizes proteins (Schofield et al. 1983), suggest that the distinctive bumps are protein aggregates.

4.3.1.3 Effect of Solution pH for ADM Gluten Films

When the pH of the gluten solution was adjusted to pH 4, the dried gluten film was very bumpy, with 1 to 2 mm diameter indentations relatively uniformly distributed across the film surface, as shown in Figure 14A.

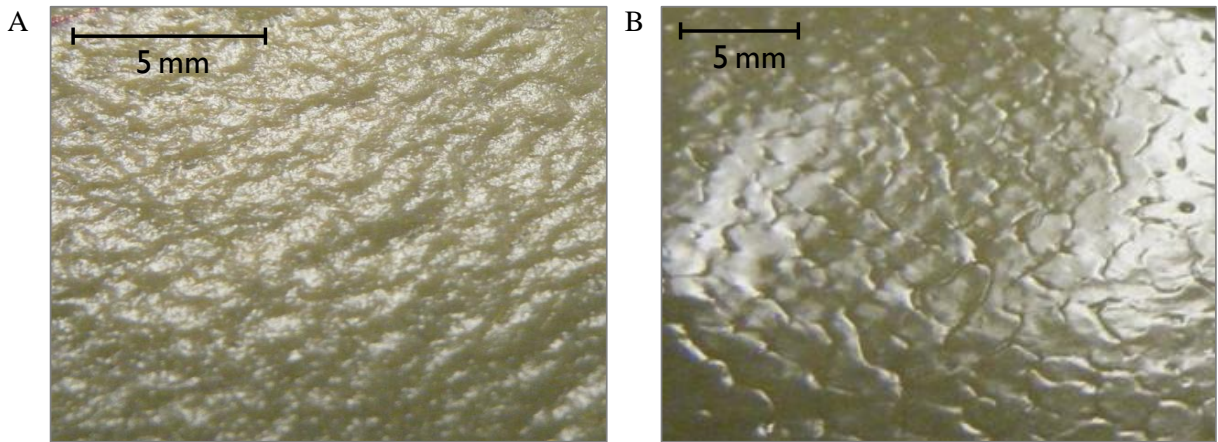


Figure 14 - Camera Images of ADM Gluten Films Cast from Gluten Solutions Adjusted to (A) pH 11 and (B) pH 4

In addition, the film contained clear, transparent sections interspersed with beige opaque sections in a heterogeneous manner. In contrast, when the gluten solution was adjusted to pH 11, the resulting film was much smoother as shown in Figure 14B. The pH 11 film did have some non-uniformity, in the form of channels/grooves that spread across the surface, but they were much shallower. The pH 11 film was also homogeneous and semi-transparent.

The homogeneous and smooth appearance of the pH 11 film surface and the heterogeneous and uneven character of the pH 4 film surface are consistent with the literature and have been attributed to higher and lower degrees of protein network formation, respectively (Olabarrieta et al. 2006, Marcuzzo et al. 2010, Cho, Gällstedt & Hedenqvist 2010). The formation of a better protein network is believed to also be at the root of the superior surface properties seen in Figure 14 for the pH 11 film, relative to the pH 4 film.

4.3.2 Film Surface Morphology - Effect of Wheat Gluten Source

In order to simplify the discussion of film features in the following section, the key features of the gluten films are presented in Figure 15.

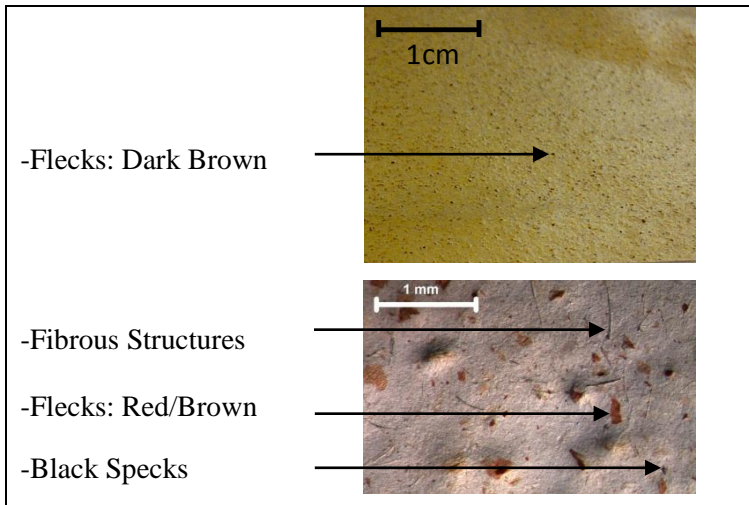


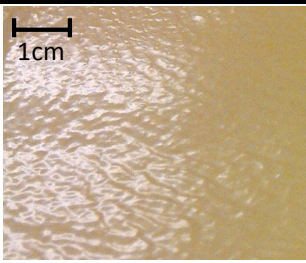
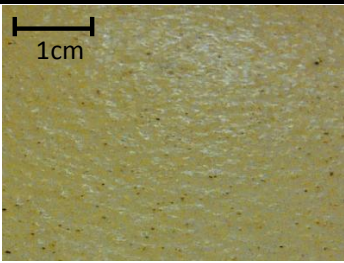
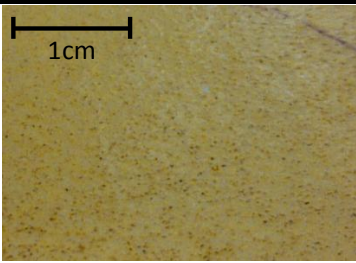
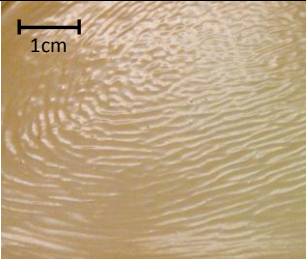
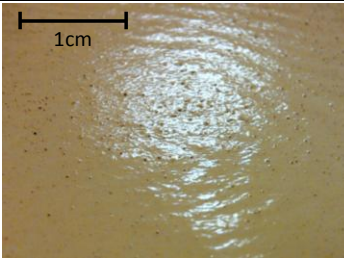
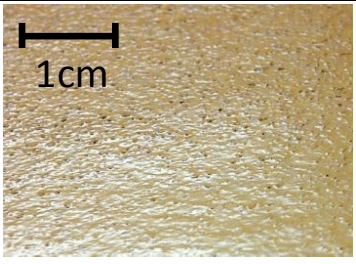
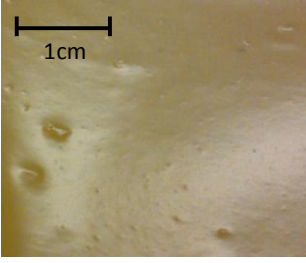
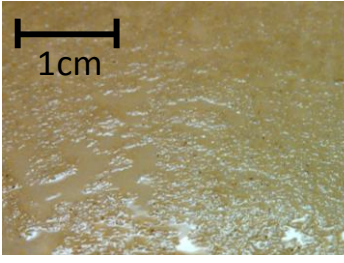
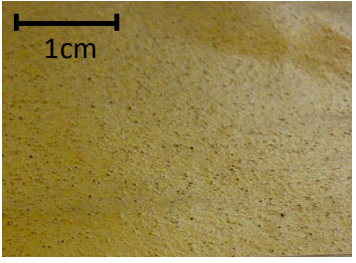
Figure 15 - Terms Describing Key Features of Wheat Gluten Film Surface Morphology

One key feature was the "flecks" that appeared "dark brown" in low magnification images and "red/brown" in higher (12.6 x) magnification images. Flecks were always jagged around the edges and varied in size even within one microscope image. Another key feature was the "fibrous structures" that looked like small, un-branched twig segments. The third key feature identified was "black specks" only visible under higher magnification. The black specks were generally half the size or smaller than the jagged dark brown flecks.

4.3.2.1 Effect of Temperature and Wheat Gluten Source on Film Appearance

Pictures of gluten films, in relation to the heating temperature of the gluten solution, are shown in Table 12.

Table 12 - Pictures of Gluten Films with Varying Wheat Gluten Source and Processing Temperature

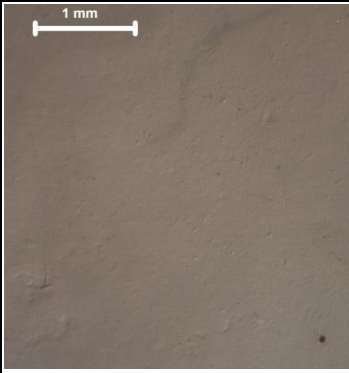
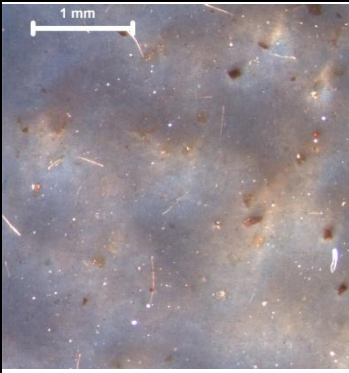
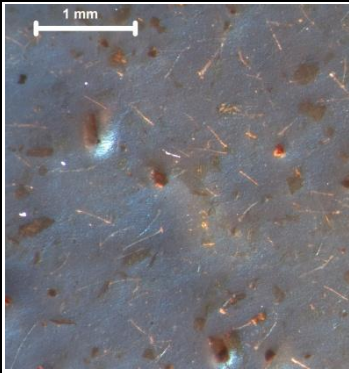
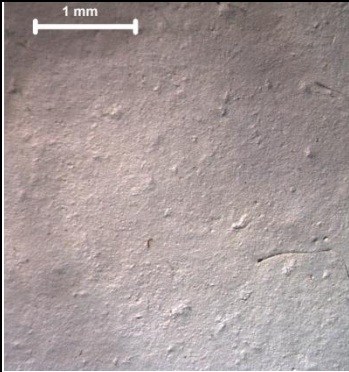
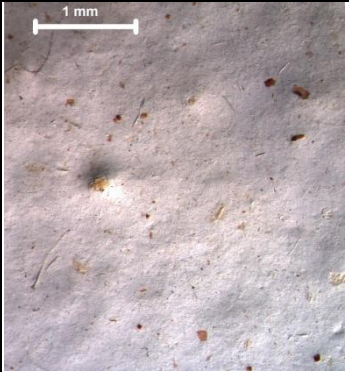
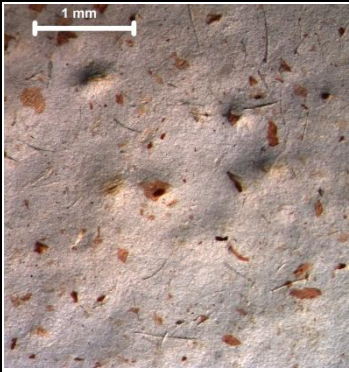
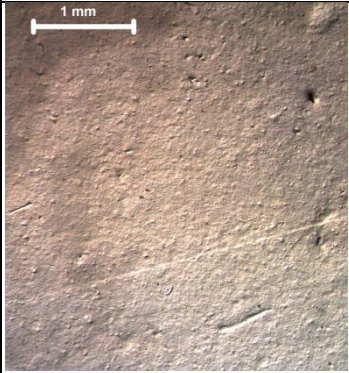
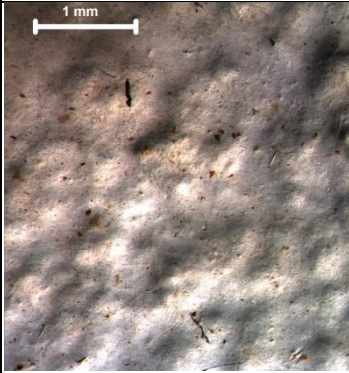
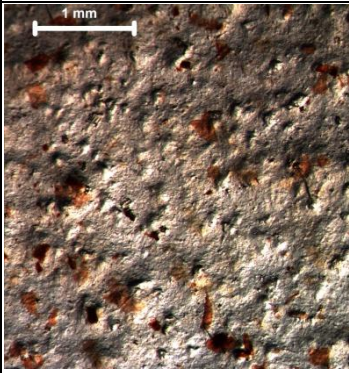
Temperature (°C)	Wheat Source		
	ADM	New Wonder	Old Wonder
70			
80			
100			

There are two distinctive differences in appearance for films produced from different gluten sources: surface roughness/smoothness and frequency of dark flecks. The old and new Wonder refer to the age of the gluten and potential differences in their composition resulting from the gluten being isolated by different individuals. The old Wonder and new Wonder wheat glutes were prepared in 2009 and 2011, respectively. Although both batches of Wonder cultivar grain were ground with the same mill, the wheat flour was washed by two different operators communicating the procedure by e-mail, which could have affected the consistency of the preparation method. In particular, a Kitchen-aid mixer and dough hook attachment were used to knead the new Wonder batch (in water) to reduce the amount of starch in the final gluten. After kneading, what appeared portions of the seed coat remained at the bottom of the water of the mixing bowl (gluten preparation detailed in Appendix 5). The Wonder wheat cultivar had dark flecks in both the new and old sources. In the old Wonder films, the dark flecks tended to gather in one area and didn't distribute evenly across the film when pouring the casting solution and during drying. In contrast, there were fewer dark flecks, and they were evenly

distributed across the film surface, in the new Wonder films. It is believed that either gluten age, gluten preparation, or a combination of the two factors affected the concentration and distribution of the dark flecks in Wonder films. The mechanized kneading step for the new Wonder could account for the decrease in fleck concentration in the new Wonder films compared to the old Wonder films.

The Wonder cultivar films were also quite rough and many of the bumps were topped by dark flecks. The ADM films were smoother, with wide gentle waves or ripples on the surface with very few and smaller dark flecks, visible only by microscopy (Table 13).

Table 13 - Microscope Images (12.6 x) of Gluten Films for different Wheat Gluten Sources and Gluten Solution Processing Temperatures

Temperature (°C)	Wheat Source		
	ADM	New Wonder	Old Wonder
70			
80			
100			

ADM Whetpro 80 wheat gluten is a commercial wheat gluten product (ADM 2012), whereas the Wonder cultivar wheat gluten was prepared with a small scale mill and so the gluten likely underwent a less refined seed coat and flour separation process. Therefore, it is believed that the "flecks" are pieces of seed coat (Cho, Gällstedt & Hedenqvist 2010) that were not removed during processing.

Based on the film appearance and magnified images presented in Table 12 and Table 13, the ADM wheat gluten films possessed relatively smooth but wavy surfaces until the gluten solution was heated to 100°C, when a few more bumps on the film surface were observed. The films from old and new Wonder cultivar had a rough surface even when the gluten solution was heated to 70°C. However, the 70 and 80°C Wonder films maintained relatively consistent appearances, while the 100°C Wonder films showed a marked increase in surface roughness.

The surface for the film prepared from new Wonder at 100°C (Table 12) is an example of the heterogeneous nature of localized sections of the film (approximately one third of the film). There are large sections of smooth film surrounded by bumpy raised film sections. Visual inspection of the film revealed that the smooth sections are clear and transparent, while the raised bumpy sections are beige and opaque. It is suspected that the significant differences in the appearance of the new Wonder 100°C film compared to the other two types of gluten films is caused by variation in the preparation methodology. During the preparation of the new Wonder 100°C film, after stirring 30 min, the gluten solution was placed in the water bath at a temperature between 40 and 45°C instead of room temperature before the heating stage was initiated, which had the potential to induce different conformational changes than normal. However, the temperature gap between the temperature during 30 min of stirring and the 40-45°C water bath was not as large as expected because heat generated by turning on the plate motor (during the 30 min stirring) was found to heat up samples to ~32°C during the 30 min stirring step in preparation of all films. Therefore, the temperature changed less than expected for the proteins when going from the 30 min of stirring to the 40-45°C water bath.

The surface roughness observed in the images of the ADM film prepared at 80°C (Table 12 and Table 13) may be a more accurate depiction of the 80°C film morphology. It was discovered that the 80°C film (discussed in chapter 4.3.1, Figure 13B) was accidentally heated for 18 minutes instead of 10 minutes, whereas the 70 and 100°C films (Figure 13A and C) were heated for 10 minutes and actually resemble the ADM films prepared at 70 and 100°C from Table 12 and Table 13. However, the difference in appearance of the 80°C film heated for a longer time (Figure 13B), compared to any of the 70, 80, or 100°C films heated for 10 minutes (Table 12 and Table 13 and Figure 13 A and C), raises the possibility that holding the film solution at 80°C for a longer period of time may improve the protein network and the resulting film morphology.

4.3.2.2 Effect of Gluten Solution pH and Wheat Gluten Source on Film Morphology

The pictures of the film surface and 12.6 x microscope images for the gluten films prepared from gluten solutions at pH 4 and pH 11 and different wheat gluten sources are shown in Table 14 and Table 15.

Table 14 - Pictures of the Gluten Film Surface for Different Wheat Gluten Sources and Solution pHs

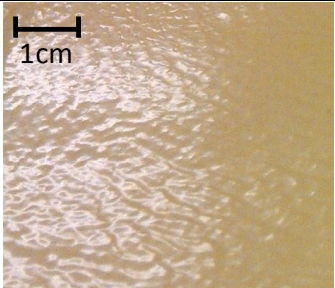
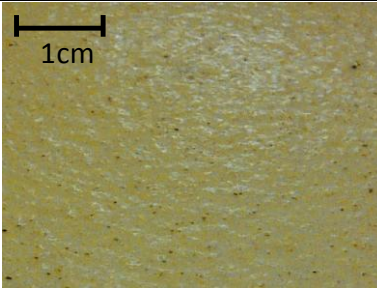
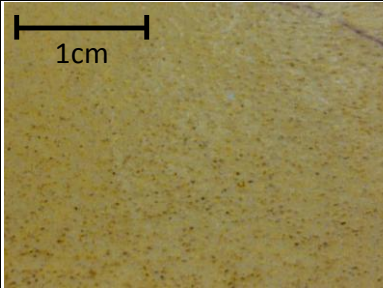
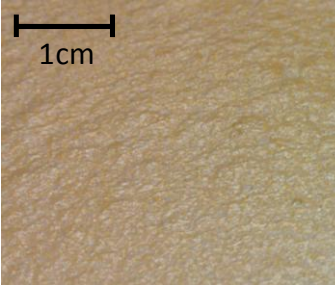
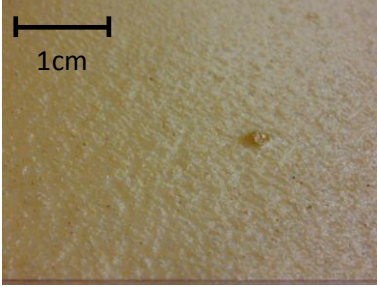
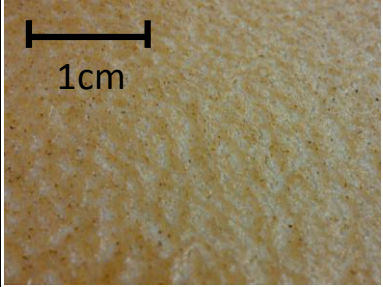
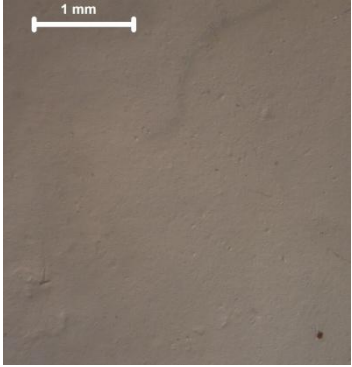
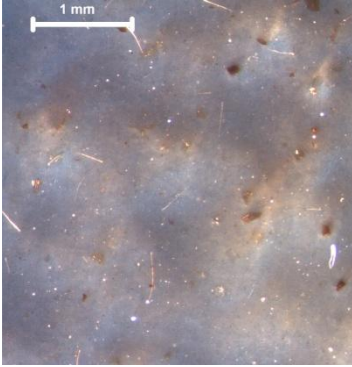
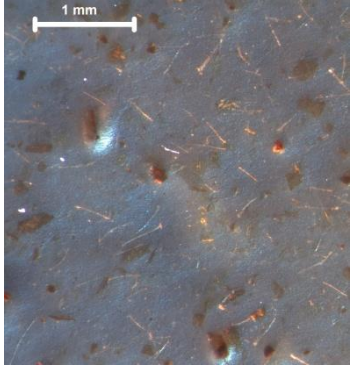
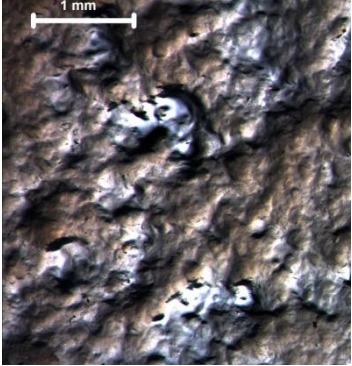
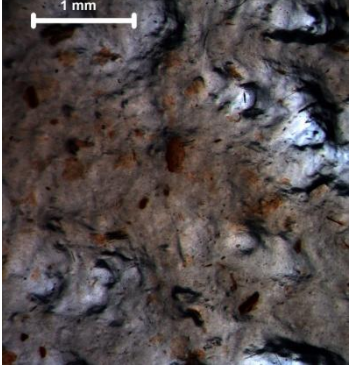
pH	Wheat Source		
	ADM	New Wonder	Old Wonder
11			
4			

Table 15 - Microscope Images (12.6 x) of Gluten Films for Different Wheat Gluten Sources and Gluten Solution pHs

pH	Wheat Source		
	ADM	New Wonder	Old Wonder
11			
4			

The surface images of the pH adjusted old Wonder films exhibited a larger number of flecks non-uniformly distributed on the film surface compared to the pH adjusted new Wonder films, where the flecks were more evenly distributed and not as numerous (Table 14). The difference in fleck distribution and concentration may be attributed to either the difference in Wonder wheat gluten age or gluten preparation procedure or a combination of the two factors (as seen previously for the temperature adjusted films of Table 12).

An increased separation between clear and beige patches was observed in the pH 4 old Wonder film compared to the pH 4 new Wonder film (Table 14). Cho et al. and Olabarrieta et al. reported that a more heterogeneous, uneven solvent cast wheat gluten film surface was associated with a lower degree of protein network formation (Olabarrieta et al. 2006, Cho, Gällstedt & Hedenqvist 2010). Therefore, it is hypothesized that protein degradation due to aging of the old Wonder wheat gluten and/or the gluten preparation procedure may have reduced the degree of protein network formation in old Wonder pH 4 films, thus resulting in the increased separation between the clear and beige sections observed for the pH 4 old Wonder films.

The ADM gluten film surface changed from a smooth homogeneous and wavy surface at pH 11 to a heterogeneous and bumpy surface with no waves at pH 4. These changes in surface morphology for films between pH 4 and 11 is consistent with observations reported by Olabarrieta et al. and Cho et al. for cast wheat gluten films (Olabarrieta et al. 2006, Cho, Gällstedt & Hedenqvist 2010). Olabarrieta et al. attributed the more homogeneous film structure observed at pH 11, to increased protein "aggregation and polymerization" (Olabarrieta et al. 2006). Cho et al. also suggested that the transparent regions are probably gliadin-rich, while the beige regions are believed to be glutenin-rich (Cho, Gällstedt & Hedenqvist 2010). Therefore, the pH 11 films shown in Table 14 and Table 15 are likely smoother and more homogeneous in terms of surface morphology than the pH 4 films due to increased protein aggregation and intermolecular network formation.

The manufacturer of ADM Whetpro 80 gluten advertises that one of the benefits of their product is for "food systems requiring improved binding strength, increased ingredient carrying capacity and restructuring" (ADM 2012). The most drastic change in surface morphology due to pH adjustments occurred with films from this commercially processed (and likely more standardized) wheat gluten source (Table 15), demonstrating how sensitive pH induced changes are to the molecular make-up of the gluten source. Although, the pH 4 and 11 ADM gluten films exhibited the largest change in surface morphology, they still had a more homogeneous morphology on a large scale compared to the Wonder cultivars. It is hypothesized that the "improved binding strength" that ADM wheat gluten is advertised to possess (ADM 2012), provided the ADM wheat gluten films with a more homogeneous morphology at a large size scale.

4.3.3 Conclusions

The microscope images of the top surface of wheat gluten films captured features found in the bulk of the film and on the bottom film surface due to the semi-transparent nature of the wheat gluten films. Pictures of the film surface and low magnification images (12.6 x instead of 80 x) were preferred for revealing difference in the film surface morphology. The uneven distribution of hydrophobic silicone grease on the glass casting surface is believed to be the reason for the more heterogeneous film surface compared to the very smooth and uniform film surface obtained with the silicone tray. The film heterogeneity induced in the bulk is also believed to have translated into a more heterogeneous film surface.

Increasing the temperature of the gluten solution from 70 to 80 °C may have resulted in a higher level of glutenin participation in disulfide interchange reactions, improving the three-dimensional protein network and correspondingly the film surface smoothness and homogeneity. In contrast, the

appearance of bumps in the film from gluten solutions heated to 100 °C suggests that the participation of gliadin in disulfide interchange reactions produced excessive protein cross-linking, adversely affecting the film surface morphology. It is also believed that the distinctive bumps seen on the 100°C films are protein aggregates. The improvement of the protein network is believed to also be at the root of the superior surface properties seen for the pH 11 films, relative to the pH 4 films.

The wheat gluten source had a noticeable impact on the film surface morphology. Old Wonder films had more flecks than new Wonder films and the flecks were not distributed evenly across the film surface. The difference may be attributed to the age of the Wonder wheat gluten, its preparation or a combination of the two factors. ADM gluten films had very few flecks. It is believed that the "flecks" are pieces of seed coat.

Variations in surface roughness were visible in the films for gluten solutions heated at temperatures between 70 and 100°C. The Wonder cultivar films were quite irregular, while the ADM films were smoother, with wide, gentle waves or ripples on the surface. However, all of the 100°C films showed a marked increase in surface roughness compared to the 70 and 80°C films. Adjusting the pH of the gluten solution resulted in the most noticeable changes to film surface morphology, irrespective of the wheat gluten source. Further, the age or gluten preparation method of the old Wonder wheat gluten contributed to an increased separation between clear and beige sections in all three wheat sources.

4.3.4 Surface Film Hydrophobicity - Effect of Modifying ADM Film Preparation Methodology

4.3.4.1 Effect of Film Casting Surface

The hydrophobic character of the films cast on a glass surface (coated with a silicone grease layer) compared to a silicone surface were obtained from contact angle measurements on the top of the films (Table 16). A higher contact angle means a higher degree of hydrophobicity.

Table 16 - Contact Angles for ADM Gluten Films Cast on Silicone and Glass Surfaces (70°C, pH 11)

Film Casting Surface	Contact Angle (°) (Average ± Standard Deviation)	Number of Measurements, n
Silicone Tray	80.6 ± 2.9	46
Silicone Grease Coated Glass Tray	91.1 ± 5.1	86

The films prepared on a silicone surface had statistically significantly lower contact angle ($p < 0.05$) than when prepared on a glass surface. It is believed that the hydrophobic silicone grease from the release layer of the glass casting surface contaminated the film, thus increasing its hydrophobic character on the top surface. Since Infra-Red (IR) only penetrates a few micrometers into the film surface (Olabarrieta et al. 2006), FTIR spectra on the top surface of the films were examined for any indication of silicone grease, according to Table 17. FTIR spectra confirmed the presence of silicone at the surface of the film cast on the glass surface coated with silicone grease, as indicated by the 1261 cm^{-1} peak associated with bending and symmetric deformation of Si-CH₃ and the 799 cm^{-1} peak associated with Si-C stretching and CH₃ rocking. The two silicone-related peaks were absent for the film cast on the silicone tray (Figure 16).

Table 17 - FTIR Peaks Associated with Silicone

Vibration Type	Wavenumber (cm ⁻¹)	Reference
Stretching of CH ₃	2800-3100	(Kaali et al. 2010, Exova 2012)
CH ₃ asymmetric deformation of Si- CH ₃ or Si-Ph	1513, 1453, 1415-1412	
Bending /symmetric deformation of Si- CH ₃ *	1258-1261	
Si-O-Si stretching vibrations (polymer backbone)	1008 -1091	
S- CH ₃ Rocking Vibrations*	864	(Kaali et al. 2010)
Si-C stretching vibration and CH ₃ rocking	787-799	(Kaali et al. 2010, Exova 2012)

*Identified in gluten film cast on glass tray (Figure 16)

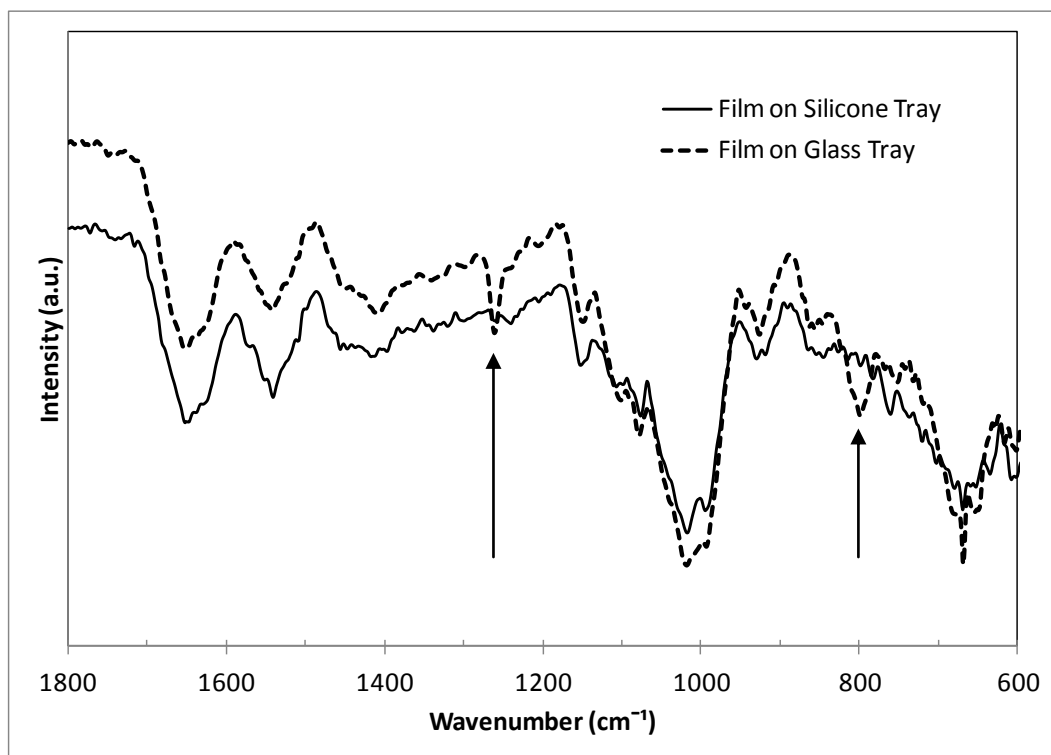


Figure 16 - FTIR Spectra for Top Surface of Films Cast on Glass and Silicone Surfaces (arrows indicate positions characteristic for silicone)

Other silicone related peaks listed in Table 17 could not be identified due to overlap with glycerol, water and protein peaks (Appendix 2). It is hypothesized that silicone grease reached the film surface during the casting and drying stage. Audic et al. reported that for the surface of caseinate protein films coated with silicone grease, the silicone layer partially solubilised in water with stirring since the silicone is not covalently bound to the protein film (Audic, Chaufer 2010). The casting solution for the films prepared here was aqueous and around 60°C when poured in the glass tray. It is suspected that the heating of the solution and long drying time (~1 day) helped to dissolve some silicone grease in the casting solution and alter the film surface hydrophobicity. Therefore, it is believed that eliminating the hydrophobic silicone layer reduced hydrophobicity for the gluten film cast on the silicone tray.

Table 18 presents literature contact angles for wheat gluten films produced with commercial wheat gluten.

Table 18 - Contact Angles for Wheat Gluten Films Cast with Commercial Wheat Gluten

Step	Parameter	Reference				
		(Tunc et al. 2007)	(Larré et al. 2000)	(Marcuzzo et al. 2010)		
Film Formulation	Gluten Type	Amylum	Amylum	Commercial: Sigma-Aldrich		
	Type of Casting Solution	Aqueous	Aqueous	Ethanol		
	Gluten (g/100g solution)	25	10	10		
	Additives	Acetic Acid (pH); Glycerol; Sodium sulfite	Tris-HCl (for pH); Glycerol; Transglutaminase	HCl (for pH); Glycerol	HCl (for pH); Glycerol	NaOH (for pH); Glycerol
	pH Adjustment	4	~8	4	4	11
	Mixing / Heating / Duration	Rest 30 min; Degassed 1 h; Mix 15 min; No heating	25000 rpm mixing; 15 min of 1000g centrifuging; Incubated 4 h at 37°C	Mixed 15 min at 70°C; 10 min ultrasound treatment	Mixed 15 min at 70°C;	Mixed 15 min at 70°C;
Film Preparation	Method	Cast	Cast	Cast		
	Drying Conditions	25°C and 70%RH	70°C, unknown RH	25°C and 40%RH		
	Aging Conditions	None	None	None		
Film Characterization	Contact Angle (°)*	76.13 ± 2.30	96 ± 7	54 ± 5	80 ± 7	55 ± 4

*Measurement method: initial contact angles for water droplets on the leveled film surface.

Clearly, the contact angles can vary drastically based on formulation and preparation techniques for the films. Marcuzzo et al. prepared gluten films at similar temperature and pH to the reference films prepared in this research (70°C and pH 11) with the difference that ethanol was added to their formulation. The ethanol-based solution decreased the gluten film contact angle by ~25°. Larre et al. prepared an aqueous gluten film around pH 8 with a different formulation procedure (lower

temperature) and preparation techniques (heating at a high temperature during the drying stage). None the less, the contact angle for this pH 8 gluten film is only ~16° higher than for the films cast on a silicone tray and falls within standard deviation for the gluten films cast on a glass tray.

4.3.4.2 Effect of Gluten Film Solution Temperature

The contact angle for the gluten films prepared at different heating temperature for the film solutions and cast using a silicone surface, are shown in Table 19.

Table 19 - Contact Angle of ADM Gluten Films at pH 11 according to Gluten Solution Heating Temperature

Gluten Solution Heating Temperature (°C)	Contact Angle (°) (Average ± Standard Deviation)	Number of Measurements, n
70	80.6 ± 2.9	46
80	97.3 ± 0.6	17
100	82.6 ± 6.0	13

The gluten solution heated to 80 °C produced a film with significantly higher hydrophobicity ($p < 0.05$) than for the gluten solutions heated to either 70 or 100°C. According to literature (Domenek et al. 2002, Angellier-Coussy et al. 2011, Schofield et al. 1983), heating wheat gluten encourages disulfide interchange reactions. Heating induces protein unfolding, which in turn exposes hydrophobic groups and cysteine residues that are usually hidden inside the protein molecule (Domenek et al. 2002). The exposed cysteine residues react to re-stabilize the molecule by participating in disulfide interchange reactions with other cysteine residues. Although the total number of disulfide bonds in the system does not increase, the interchange of disulfide bonds throughout the protein shifts the bonds from intramolecular to intermolecular and locks the protein into a more stable, less soluble network that remains even after cooling (Angellier-Coussy et al. 2011, Schofield et al. 1983). The polymeric gluten proteins, glutenins, begin disulfide interchange reactions at the lower temperature (~ 60-70°C) because it has the highest content of sulphur-containing cysteine groups (Angellier-Coussy et al. 2011). In contrast, the smaller monomeric gliadin proteins begin participating in disulfide interchange reactions only above 90°C and when the rate of disulfide interchange reactions slows for the glutenin molecules (Domenek et al. 2002). As one might expect, the cysteine deficient ω -gliadin does not participate in disulfide bond interchange reactions and remains soluble even after heating to 100°C (Schofield et al. 1983).

It is therefore believed that the higher hydrophobicity of the film produced from the solution heated to 80°C compared to the films produced from the solution heated to 70°C was the result of a higher proportion of hydrophobic groups exposed during heating and locked into place with disulphide bonds (Domenek et al. 2002, Angellier-Coussy et al. 2011, Schofield et al. 1983). Thus, in the cooled state, it is reasonable that more exposed hydrophobic regions were located at the surface of the film and increased the surface hydrophobicity. Further, for films prepared at 80°C, a much smaller standard deviation than those prepared at 70 and 100°C, is reflected in its superior homogeneous surface appearance (described in chapter 4.3.1 Film Surface Morphology). It is suspected that the film homogeneity impacts the contact angle standard deviation because each contact angle measurement is taken at a new location on the film. If the film hydrophobicity varies drastically with location across the film, then the average contact angle should have a higher standard deviation.

The film produced from a solution heated to 100°C did not increase significantly in surface contact angle compared to the one produced from a solution heated to 70°C. It is hypothesized that heating the gluten solution to 100°C exposed too many hydrophobic groups and destabilized the system because gliadin had also begun participating in disulphide interchange reactions at this temperature (Domenek et al. 2002, Angellier-Coussy et al. 2011). This hypothesis is further supported by the observations presented in the Film Surface Morphology chapter (4.3.1). The film surface showed solid raised bumps spread throughout the film which resembled protein aggregates or insoluble protein. It has been previously reported that the aggregation of excess hydrophobic groups helps to stabilize aqueous wheat protein (Day et al. 2009). Therefore, it is suggested that this aggregation of excess hydrophobic groups in the aqueous wheat protein solution reduces the surface hydrophobicity of the dried wheat protein film.

4.3.4.3 Effect of Gluten Film Solution pH

The contact angle for water on the gluten film surface was significantly higher ($p < 0.05$) when the pH of the gluten solution was adjusted to pH 4, compared to pH 11 (Table 20).

Table 20 - Contact Angle for Gluten Films made from Solutions Heated at 70°C and Adjusted to pH 4 and pH 11

pH of Gluten Solution	Contact Angle (°) (Average ± Standard Deviation)	Number of Measurements, n
11	80.6 ± 2.9	46
4	86.1 ± 4.3	16

The gluten film surface was more hydrophobic when the gluten solution was adjusted to pH 4 than 11. Olabarrieta et al. attributed pH 11 ethanol cast wheat gluten films with a more complete protein network than at pH 4, based on FTIR measurements and film protein solubility (Olabarrieta et al. 2006). In addition, Cho et al. attributed a more open protein structure, identified in FTIR studies, to a lower degree of intermolecular interactions in pH 4 ethanol cast wheat gluten films compared to at pH 11 (Cho, Gällstedt & Hedenqvist 2010).

Here it is hypothesized that the degree of protein network formation in pH adjusted gluten films is also reflected in the gluten film surface hydrophobicity. The higher contact angle of the pH 4 water cast gluten film surface suggests that a lower degree of protein networking results in a film with more hydrophobic regions exposed at the film surface. Whereas, the lower contact angle seen for water gluten films cast at pH 11 suggests that a higher degree of protein networking produces a film with less hydrophobic regions exposed to the surface.

Marcuzzo et al. also reported that the surface of ethanol cast gluten films produced at pH 4 were more hydrophobic than those produced at pH 11 (Marcuzzo et al. 2010), although the choice of an ethanol casting solvent appears to create a much larger spread in surface hydrophobicity (Table 18). Marcuzzo et al. also reported challenges in contact angle measurements of the pH 4 ethanol cast gluten films due to the surface roughness, suggesting that film surface morphology can affect surface hydrophobicity measurements (Marcuzzo et al. 2010).

4.3.5 Surface Film Hydrophobicity - Effect of Wheat Gluten Source and Contact Surface During Drying

In section 4.3.4, sections of the films were selected randomly for contact angle measurements. In this subsequent analysis, all contact angle specimens were selected from sections of the film with similar visual appearance to obtain more consistent readings. In the previous study (section 4.3.4), contact angles were not determined immediately following each water drop, possibly allowing the film sample to dry out by the time the subsequent contact angles were measured. Therefore, in this analysis, all water drops were captured one right after the other and the videos were analyzed afterwards. This was expected to improve the consistency of the contact measurements for each sample.

4.3.5.1 Effect of Gluten Casting Solution Temperature and Wheat Gluten Source

The contact angle of wheat gluten films prepared by varying the gluten solution temperature at pH 11, using the silicone casting surface, and for different wheat gluten sources are shown in Table 21.

Table 21 - Effect of Varying Gluten Solution Temperature and Wheat Gluten Source on Film Surface Contact Angle. Silicone Casting Surface and pH 11 Solution.

Heating Temperature (°C)	Wheat Source	Contact Angle (°) with n= 10 (Average ± Standard Deviation)		Contact Angle (CA) Difference (°) [CA(bottom)-CA(top)]
		Top Surface	Bottom Surface	
70	ADM	76.4 ± 2.5	90.6 ± 4.1	14.2
	Old Wonder	68.5 ± 2.7	93.1 ± 2.8	24.6
	New Wonder	58.5 ± 1.1	66.7 ± 1.8	8.2
80	ADM	77.2 ± 1.5	92.0 ± 1.3	14.8
	Old Wonder	55.6 ± 4.9	76.2 ± 1.7	20.6
	New Wonder	63.4 ± 3.0	84.3 ± 4.0	20.9
100	ADM	79.5 ± 0.9	75.4 ± 3.2	-4.1
	Old Wonder	57.6 ± 3.7	68.9 ± 3.8	11.3
	New Wonder	48.7 ± 2.4	65.1 ± 2.1	16.4

The bottom surface of the gluten film was significantly more hydrophobic ($p < 0.05$) than the top surface for all gluten sources and temperatures except the film prepared with ADM gluten and the solution heated to 100°C. Olabarrieta et al. reported glycerol migration in ethanol cast wheat gluten films (pH 11 adjustment and 75°C heating of gluten solution) after comparing FTIR spectra of the top and bottom film surfaces (Olabarrieta et al. 2006). In addition, glycerol is hydrophilic (Lens et al. 2003). Therefore, the contact angle differences between the top and bottom surface of the films

suggest different film structure arrangements at the top surface compared to the bottom surface that may be attributed to a combination of glycerol migration and protein rearrangement during film drying, as well as to the hydrophobic nature of the silicone casting surface.

The ADM gluten films exhibited a higher contact angle than the gluten films from the new and old Wonder cultivars for the top surface and the bottom surface with the exception of the bottom surface of the ADM gluten and old Wonder gluten produced with the solution heated to 70°C. Further, the contact angle properties of the films prepared with the ADM gluten showed less variation across temperature than the films prepared with the two sources of Wonder gluten (except for the bottom surface from the solution heated to 100°C). The ADM gluten Whetpro80 is a commercially prepared vital wheat gluten. The term vital means that the wheat gluten still has functionality and can therefore form a viscoelastic network (Van Der Borgh et al. 2005). However, as commercially prepared wheat gluten, one of the treatment steps during gluten preparation, such as drying, may impact the film forming properties of Whetpro80. In particular, ADM reports that Whetpro80 is useful in “food systems requiring improved binding strength, increased ingredient carrying capacity and restructuring” (ADM 2012), suggesting that one or more special treatment steps may have been included in its preparation. The observed sensitivity to lower temperature of the ADM wheat gluten and the higher contact angle of the ADM gluten films suggests that the industrial production of the ADM Whetpro80 has exposed hydrophobic regions of the gluten and locked it in place (Domenek et al. 2002) so that 70 and 80°C heating does not impact protein network formation significantly ($p > 0.05$ for ADM films surfaces when solution is heated to 70 and 80°C).

In contrast, the old and new Wonder gluten were more sensitive to changes in heating temperature, as indicated by the more pronounced differences in the contact angles for different heating temperatures. The Wonder wheat cultivar was grown in Ontario and the gluten was manually extracted at a small scale. Therefore, extraction conditions were well controlled. It is hypothesized that the gluten proteins of the Wonder cultivar are more sensitive to heating temperature because the gluten proteins were not denatured or significantly altered during the wheat gluten extraction stage (prior to film preparation) (Van Der Borgh et al. 2005).

Films from all three gluten sources, cast from solutions heated to 100°C, exhibited smaller differences between their respective top and bottom surface contact angles than when the solution was heated to 70 or 80°C, except the 70°C new Wonder film (Table 21). The smaller differences suggest that heating to 100°C induced a higher degree of network formation throughout the film, locking the protein into place in a more uniform manner (Angellier-Coussy et al. 2011, Schofield et al. 1983) that

is less sensitive to the hydrophobic nature of the casting surface. The reduced difference in contact angle measured on the top and bottom surfaces was more pronounced for the ADM film. The ADM film produced from the solution heated to 100°C possessed a more hydrophobic top surface and a more hydrophilic bottom surface, the opposite effect to all eight other film types. Therefore, it is believed that the temperature of the solution altered the ADM wheat gluten protein network significantly (Angellier-Coussy et al. 2011, Schofield et al. 1983).

The top and bottom film surface contact angles were highest for the old Wonder wheat gluten films when the solution was heated to 70°C. The contact angle of the film surface decreased with increasing heating temperature ($p < 0.05$), except on the top surface of the film produced from the solution heated to 80 and 100 °C. The contact angle of the top and bottom film surfaces was highest for the new Wonder wheat gluten when the solution was heated to 80°C. The contact angle of the top film surface was highest for the ADM gluten films when the solution was heated to 100°C. However, the ADM gluten film with the highest contact angle for the bottom surface was obtained from the solution heated to 80°C. The temperature sensitivity of the wheat gluten indicates that each of the wheat gluten sources responded differently to heating. Further, the age or operator's manipulations of the wheat gluten can alter its response to heat treatment as can be seen by comparing the contact angle of the top and bottom film surface of old Wonder (3 years old) and new Wonder (1 year old) for a given heating temperature.

4.3.5.2 Effect of pH of the Gluten Film Solution and Wheat Gluten Source

The contact angle of wheat gluten films prepared with solution at two pHs and with different gluten sources are shown in Table 22.

Table 22 - Effect of the pH of the Gluten Solution and Wheat Gluten Source on Film Surface Contact Angle for Gluten Solutions Heated to 70 °C.

pH	Gluten Source	Contact Angle (°), with n= 10 (Average ± Standard Deviation)		Contact Angle (CA) Difference (°) CA(bottom)-CA(top)
		Top Surface	Bottom Surface	
11	ADM	76.4 ± 2.5	90.6 ± 4.1	14.2
	Old Wonder	68.5 ± 2.7	93.1 ± 2.8	24.6
	New Wonder	58.5 ± 1.1	66.7 ± 1.8	8.2
4	ADM	75.0 ± 4.2	84.1 ± 3.1	9.1
	Old Wonder	77.9 ± 4.3	89.5 ± 2.2	11.6
	New Wonder	80.6 ± 2.9	82.9 ± 1.7	2.3

As with temperature adjusted solutions (section 4.3.5.1), the bottom film surface was more hydrophobic than the top film surface for the two pHs (Table 22). Here again, the contact angle differences between the top and bottom surface of the films for the two different pHs suggest different film structure arrangements at the top surface compared to the bottom surface, believed to result from a combination of glycerol migration and protein rearrangement during film drying, as well as to the hydrophobic nature of the silicone casting surface (Olabarrieta et al. 2006).

All three films produced from pH 4 gluten solutions displayed smaller contact angle differences between their respective top and bottom film surfaces compared to pH 11 (Table 22). At pH 4, gluten films have been reported to have a lower degree of protein denaturation and a lower degree of inter-molecular bond formation than at pH 11 (Olabarrieta et al. 2006). Since the isoelectric point (pI) of wheat gluten is 7.5 (Gennadios, Weller & Testin 1993), gluten proteins in a pH 4 solution will have a positive net charge (Lehninger, Nelson & Cox 2004). The smaller contact angle difference between the top and bottom film surface observed for the gluten film at pH 4 indicates that the top and bottom surface hydrophobicity were more similar and suggests that wheat gluten protein rearranged more easily during drying when it had a positive net charge and a lower degree of inter-molecular bond formation. The uneven surface morphology of films prepared from the pH 4 solution (chapter 4.3.1 Film Surface Morphology) suggests that these films are also not homogeneous from top to bottom compared to the films prepared from the pH 11 solution. Cho et al. also reported an uneven distribution of glycerol, glutenin and gliadin in pH 4 films and found that it produces a looser protein network (Cho, Gällstedt & Hedenqvist 2010). It is believed that the uneven distribution of film constituents observed here also produced a looser protein network, resulting in the localization of the hydrophilic regions of the proteins in the core domain of the film, away from the top and bottom film surfaces.

As seen for the temperature effect on the film contact angle measurements (chapter 4.3.4), the Wonder gluten displayed a more pronounced variation in surface contact angle than the ADM gluten films when the pH was adjusted to pH 4, supporting the hypothesis of higher pH sensitivity for gluten extracted in cold water by hand washing and kneading (detailed procedure in Appendix 5). Films produced from solutions adjusted to pH 4 with Wonder gluten had significantly higher ($p < 0.05$) or statistically equivalent ($p > 0.05$) top and bottom surface contact angles relative to the ADM gluten films. ADM gluten films, with their very low variability ($p > 0.05$) in top surface contact angles and relatively low variability ($p < 0.05$) in bottom surface contact angle when comparing films from solution at pH 11 and pH 4, indicates that the industrial gluten extraction conditions may have

significantly affected the gluten properties such that the effect of pH adjustment on protein conformational changes was reduced.

The contact angle of the top and bottom film surface increased significantly ($p < 0.05$) for Wonder gluten films (except for old Wonder gluten bottom film surface) produced at pH 4. Contact angle values reported by Marcuzzo et al. (Table 18) for ethanol cast gluten films (no ultrasound treatment), agree well with the surface properties of the Wonder gluten. In particular, the new Wonder gluten film top surface contact angles match perfectly, after accounting for the standard deviation. The higher top and bottom contact angles, associated with higher hydrophobicity, for the films produced from the pH 4 solutions suggests a more open protein structure due to a lower degree of intermolecular interactions (Olabarrieta et al. 2006, Cho, Gällstedt & Hedenqvist 2010) and a film with more hydrophobic protein regions exposed at the film surfaces. In contrast, the lower contact angle for the films produced from the pH 11 solution suggests a higher degree of protein networking and a film with fewer hydrophobic regions exposed at the film surface.

The contact angle of old Wonder gluten films was higher on the top surface when the pH was adjusted to 4 ($p < 0.05$), but higher on the bottom surface when the pH was adjusted to 11 ($p < 0.05$). The contact angle of the top and bottom surfaces was higher for the new Wonder gluten films produced from the pH 4 solution, compared to pH 11 ($p < 0.05$). The contact angle for the ADM gluten was higher for the bottom film surface ($p < 0.05$) and equivalent for the top film surface ($p > 0.05$) for the pH 11 solution, compared to pH 4. Clearly the wheat gluten source responded differently in conformation and to varying degrees according to the pH of the solution. Further, the operator or age of the wheat gluten played a role in its response to pH conditions of the solution as seen when comparing the contact angle of the top and bottom film surface for the old Wonder gluten (3 years old) to the new Wonder gluten (1 year old) at a given solution pH.

A final observation is the range of the contact angle for pH 4 films and the three wheat sources, 5.6° (75.0° to 80.6°) for the top film surface and 6.6° (82.9° to 89.5°) for the bottom film surface. The respective ranges for the top and bottom film surfaces of the pH 4 films are smaller than for either the pH 11 film or the films prepared with varying casting temperatures (Table 21). The bottom surface of the films produced from the 100°C solution also have a small contact angle range, 10.3° , with the remaining films having ranges between 15 and 30° . Adjusting the pH of the solution to pH 4 creates a looser protein network (Olabarrieta et al. 2006). Further, since the three different gluten sources were all obtained from wheat they should still share strong conformational similarities when cast as a film by the same method. Therefore, it is believed that the protein molecules rearrange more easily during

film drying at pH 4, to assume more similar conformations in the dry film according to wheat sources, and that this is reflected in the more similar contact angles observed between wheat sources in pH 4 films compared to pH 11.

4.3.6 Conclusions

The effect of varying film casting procedure on contact angle was first explored with the commercial ADM wheat gluten (Whetpro80). ADM gluten films cast on a silicone surface were more hydrophobic than gluten films cast on a glass surface coated with silicone grease. FTIR spectra of the top of the gluten film surfaces revealed that silicone grease contaminated the gluten film cast on the glass surface, thus increasing its surface hydrophobicity.

The ADM film solution heated to 80°C produced a more hydrophobic film surface than when solutions were heated to 70 or 100°C. It is believed that hydrophobic groups of the gluten were exposed during heating and locked into place near the film surface with disulphide bonds. The gluten films prepared at 80°C, possessed a more homogeneous appearance, and this homogeneity was reflected in a reduced standard deviation for their contact angles. Heating the ADM gluten solution to 100°C may expose more hydrophobic groups, destabilizing the system because gliadin also participated in disulphide interchange reactions at this temperature. The increased contact angle at pH 4 could be due to the lower degree of protein networking taking place and producing a film with more hydrophobic regions exposed at the film surface.

When the three different wheat sources (ADM, new Wonder, and old Wonder) were examined, the bottom film surface was more hydrophobic than the top surface for all gluten films, at all temperature and pH conditions except for the ADM film produced at 100 °C at pH 11. The smallest variations of the contact angle between the top and bottom film surfaces were achieved for the films produced at 100°C and pH 4.

Each wheat gluten source responded to heating and pH adjustments differently. ADM gluten films exhibited the highest contact angles for all solution temperature adjustments at pH 11 but not when pH was adjusted to pH 4. The ADM gluten also exhibited a relatively constant contact angle for all temperatures and pH conditions investigated. The Wonder gluten was more sensitive to changes in solution temperature and pH (observed as higher change in contact angle). However, in the case of pH 4, the contact angle of the Wonder gluten film was similar or higher than for the ADM gluten films. The differences were attributed to the method of gluten extraction, which was done in cold water by hand washing and kneading for the Wonder gluten but likely done by an automated process

for the ADM gluten. The Wonder gluten films also responded differently to pH and temperature treatments according to age of the material.

Films produced from solutions adjusted to pH 4 at 70°C exhibited smaller contact angle variation between gluten sources compared to all other solution temperatures and pH 11.

4.4 Study of Protein Conformation by Fluorescence Spectroscopy on Top and Bottom Film Surface with Varying pH and Temperature of Casting Solution

Gluten films were placed on a smooth black surface for the collection of fluorescence spectra in the form of fluorescence excitation-emission matrices (FEEM), the intensity at combinations of emission and excitation wavelengths. Figure 17A and B show the 3D and contour plots, respectively of FEEM of the black background surface. Figure 17C and D present the 3D and contour plots of FEEM for the new wonder gluten film prepared at 70°C and pH 11 as an example.

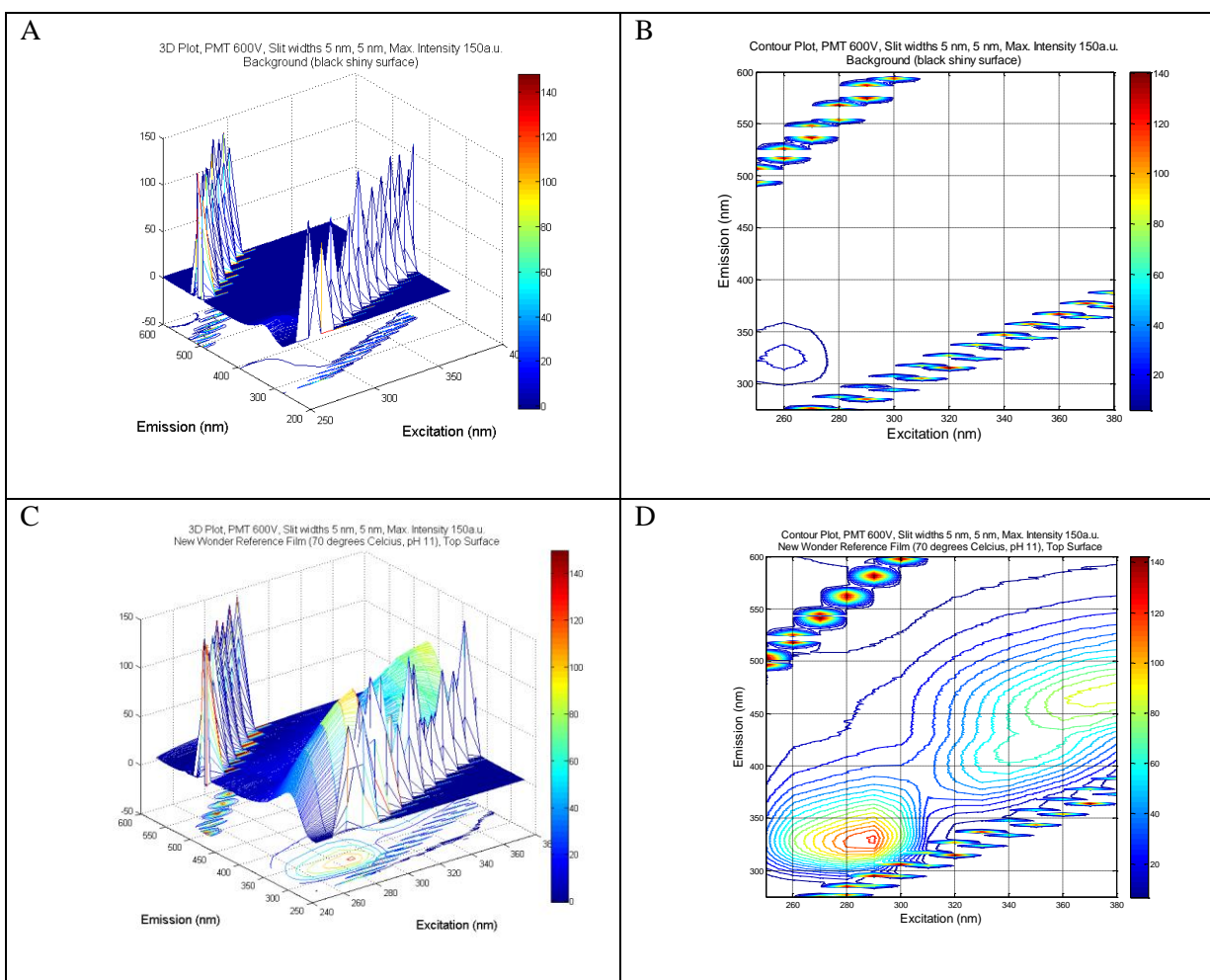


Figure 17 - Fluorescence FEEM of the Black Background Surface before placing a gluten film: (A) 3D and (B) Contour. Example Fluorescence FEEM of New Wonder Wheat Gluten Film (70°C, pH 11) Top Surface: (C) 3D and (D) Contour.

The high intensity peaks that form two lines across the excitation-emission plane for both the background and the film spectra are first and second order Rayleigh scattering, respectively referred to as FORS and SORS. FORS occurs where emission wavelength equals excitation wavelength

($\lambda_{\text{ex}}=\lambda_{\text{em}}$). SORS occurs where emission wavelength is twice the excitation wavelength ($2\lambda_{\text{ex}}=\lambda_{\text{em}}$) (Peiris et al. 2010). The intensity along these two lines actually saturates the detector, surpassing the instrument's maximum of 1000 a.u. (full intensity not shown in graph). Since Wyatt et al. report that these light scattering regions can provide information about the particulate/colloidal matter in water samples (Wyatt 1993) it is believed that solid surfaces studied by fluorescence spectroscopy would innately have very high levels of scattering in these regions purely due to the nature of the sample. Therefore, the background itself or the solid nature of the sample may explain the SORS and FORS peaks seen in the background spectra (Figure 17 A and B) and the film spectra (Figure 17 C and D).

In Figure 17 D, a broad peak is spread across $\lambda_{\text{ex}} = 340 - 350$ nm and $\lambda_{\text{em}} = 410 - 430$ nm. Zandomeneghi et al. reported a similar peak at $\lambda_{\text{ex}} / \lambda_{\text{em}} = 350$ nm/430 nm for powder rice flour samples using similar fluorescence techniques (Zandomeneghi 1999). The peak was attributed to either a "nonradiative energy transfer mechanism" (Zandomeneghi 1999) or to flour fluorophores after partially re-absorbing the 335 nm wavelength emissions from protein. Zandomeneghi et al. further commented that cereals contain 4-aminobenzoic acid, pyridoxine, and tocopherols amongst other species, which could be responsible for the observed 430 nm emission (Zandomeneghi 1999).

The aromatic nature of the amino acids tryptophan, tyrosine, and phenylalanine make them intrinsically fluorescent (Lakowicz 2006). Wavelength emission peaks for the three amino acid residues are 282 nm for phenylalanine, 303 nm for tyrosine, and 350 nm for tryptophan (Lakowicz 2006). Both tryptophan and tyrosine have an excitation λ_{ex} of 280 nm, whereas phenylalanine exhibits a maximum excitation wavelength at 260 nm (Genot et al. 1992). Therefore, a peak for phenylalanine is not seen in most protein samples because it is not excited at the commonly used 280 nm excitation wavelength. Furthermore, an excitation wavelength between 295 and 305 nm is reported to excite tryptophan without exciting tyrosine (Lakowicz 2006). Finally, both tyrosine and phenylalanine tend to transfer absorbed energy to the tryptophan residues so that tryptophan is often the main fluorescence peak seen in spectra, while emission intensities are absent for tyrosine and phenylalanine (Lakowicz 2006).

In a study of fluorescence and wheat gluten dough, Genot et al. reported that the expected fluorescence for phenylalanine was not observed, even for its maximum excitation wavelength of 260 nm. The peak at $\lambda_{\text{ex}}/\lambda_{\text{em}} = 275$ nm/330 to 350 nm was associated with the fluorescence of tryptophan residues, while the peak at $\lambda_{\text{ex}}/\lambda_{\text{em}} = 275$ nm/305 nm was associated with tyrosine residues (Genot et al. 1992). From a review of peaks reported by Lakowicz et al and Genot et al., it is believed that the peak with a maximum intensity at $\lambda_{\text{ex}}/\lambda_{\text{em}} = 290$ nm/331.5 nm in Figure 17C and D represents

tryptophan residues known to be present in wheat gluten amino acid sequences (Sugiyama et al. 1985, Arentz-Hansen et al. 2000). However, the oval shape peak intensity located in the tryptophan excitation/emission intensity range (Figure 17C and D), suggests that the multiple tryptophan residues in the gluten film had overlapping wavelengths, and resulted in a wider tryptophan FEEM peak. The oval shape peak intensity also suggests that the multiple tryptophan residues in the gluten films were excited to varying degrees at different excitation wavelengths (260-300 nm) but all emitted near a narrower wavelength region (~330-345 nm). Due to the absence of FEEM peaks for tyrosine and phenylalanine residues, it is also believed that the tyrosine and phenylalanine transferred absorbed energy to the tryptophan residues, contributing to an increase in the tryptophan peak intensity (Lakowicz 2006).

Since the emission wavelength of tryptophan residues is said to be "highly dependent upon polarity and/or local environment" (Lakowicz 2006), shifts in the emission wavelength at 290 nm excitation were investigated. Table 23 shows the emission wavelength and associated intensity at which the fluorescence had the highest intensity (local maximum) at the 290 nm excitation wavelength for the top and bottom surface of gluten films for different preparation methods (temperature and pH) and wheat source.

Table 23 - Emission Wavelengths and Associated Intensities (Average \pm Standard Error, n=2)) for Local Maxima at the 290 nm Excitation Wavelength from Fluorescence Spectra of the Top and Bottom Surface of Gluten Films for Preparation Method (Temperature and pH) and Wheat Gluten Source.

Gluten Solution Conditions	Gluten Type*	Top Film Surface		Bottom Film Surface	
		λ_{em} (nm)	Intensity	λ_{em} (nm)	Intensity
70°C, pH 11	ADM	332.5 \pm 0.5	161.8 \pm 7.2	331.5 \pm 2.5	115.3 \pm 0.4
	OW	331.0 \pm 1.0	113.3 \pm 3.9	331.5 \pm 0.5	64.7 \pm 2.9
	NW	331.5 \pm 1.5	118.0 \pm 4.5	330.5 \pm 0.5	78.0 \pm 1.8
80°C, pH 11	ADM	332.1 \pm 1.0	162.1 \pm 2.0	332.0 \pm 0.0	118.9 \pm 2.5
	OW	330.1 \pm 1.0	106.1 \pm 2.7	330.0 \pm 0.0	65.4 \pm 0.7
	NW	329.5 \pm 2.5	105.3 \pm 2.6	331.5 \pm 0.5	76.8 \pm 2.9
100°C, pH 11	ADM	328.5 \pm 0.5	155.7 \pm 0.3	328.1 \pm 1.0	131.7 \pm 2.2
	OW	328.5 \pm 1.5	98.9 \pm 1.4	328.5 \pm 1.5	75.2 \pm 0.0
	NW	330.1 \pm 1.0	109.4 \pm 0.7	329.5 \pm 0.5	87.3 \pm 0.9
70°C, pH 4	ADM	329.0 \pm 1.0	224.7 \pm 0.1	331.1 \pm 0.0	210.0 \pm 1.4
	OW	332.1 \pm 1.0	130.2 \pm 6.1	331.0 \pm 1.0	106.4 \pm 0.3
	NW	330.5 \pm 1.5	147.0 \pm 0.9	331.5 \pm 1.5	133.8 \pm 0.7

*OW = Old Wonder; NW = New Wonder

As a point of comparison, Genot et al. studied the fluorescence spectra region of amino acids for viscous hydrated wheat gluten dough (with the sample pressed between two quartz plates) and reported a peak at $\lambda_{ex}/\lambda_{em} = 275 \text{ nm}/333 \text{ nm}$ (Genot et al. 1992). Table 24 shows the shift in λ_{em} between the top and bottom gluten film surfaces of this study (Table 23) compared to the 333 nm literature value.

Table 24 - Shift of the Emission Wavelength from 333 nm (Reported for Viscous Wheat Gluten Dough, (Genot et al. 1992)) for Top and Bottom Gluten Film Surfaces Prepared at Varying Temperature and pH

Gluten Solution Conditions	Gluten Type*	Emission Wavelength Shift from 333 nm	
		Top Surface (nm)	Bottom Surface (nm)
70°C, pH 11	ADM	0.5	1.5
	OW	2.0	1.5
	NW	1.5	2.5
80°C, pH 11	ADM	0.9	1.0
	OW	2.9	3.0
	NW	3.5	1.5
100°C, pH 11	ADM	4.5	4.9
	OW	4.5	4.5
	NW	2.9	3.5
70°C, pH 4	ADM	4.0	1.9
	OW	0.9	2.0
	NW	2.5	1.5

*OW = Old Wonder; NW = New Wonder

Although the gluten dough is more hydrated in the work of Genot et al., the emission wavelength of 333 nm is quite close to the measured values (Table 23). Further, the 333nm emission wavelength provides a good point of comparison by means of which blue-shifts can be compared for the gluten film produced in this study. The magnitude of blue shift in the vicinity of 333 nm emission for the top and bottom gluten film surface increased with increasing gluten solution temperature, except for the bottom surface of the gluten film prepared at 80°C with the ADM and NW wheat sources. Also, the magnitude of blue shift increased for the film prepared at pH 4 compared to pH 11 on both top and bottom film surface. Lakowicz et al. state that the peak for tryptophan "in water [...] is highly dependent upon polarity and/or local environment" (Lakowicz 2006). In particular, Lakowicz states that changing the solution pH can affect the protein conformation and cause a shift in the amino acid peak (Lakowicz 2006). Therefore, based on the increased shifts in the amino acid peak of fluorescence spectra, it is believed that the increases in temperature or pH in the film preparation method effects protein conformation in the gluten films.

The measured intensities of the fluorescence peaks (Table 23) varied according to the gluten source and according to preparation methods. Difference in the fluorescence spectra were expected according to wheat cultivar and preparation method since Zandomeneghi report differences in fluorescence spectra of wheat flour according to wheat cultivar (Zandomeneghi 1999), while Lakowicz report differences in fluorescence spectra as pH is changed (Lakowicz 2006). Most of the variations in fluorescence intensity related to wheat gluten source were similar for the top and bottom film surfaces. First, the fluorescence peak intensity on the top and bottom film surface was statistically significantly higher ($p < 0.05$) for all the ADM wheat gluten films compared to the Wonder gluten films, suggesting that the wheat source had a much more significant impact on fluorescence than the age of the wheat since the peak intensities were not significantly different between the old and new Wonder cultivars for a given condition ($p > 0.05$), except for the top and bottom film surface of the 100°C film and the bottom film surface at pH 4. Similar fluorescence peak intensity of the old and new wonder wheat gluten films was expected since amino acid composition should not change over time within the same wheat cultivar. The fact that the differences occurred at the highest heating temperature, 100°C at pH 11 and pH 4 suggests that pH and more extreme heating conditions can alter protein conformations for different ages of wheat gluten and possibly reflects protein degradation. However, the absence of statistical difference of the FEEM between old and new wonder gluten films for 70 and 80°C suggests that as the gluten ages, the tryptophan interactions with other amino acids do not change and would not contribute to film structural changes.

The fluorescence peak intensity of the bottom film surface was significantly higher ($p < 0.05$) for pH 4 films compared to pH 11 films for a given wheat gluten source. Such differences were reflected in the morphological differences observed between pH 4 and 11 films (chapter 4.3.1 Film Surface Morphology).

Bonomi et al. report higher fluorescence peak intensities when wheat flour is hydrated (Bonomi et al. 2004). Since gluten films were all conditioned for two days on a filter paper support with the top surface exposed to 50% RH, it is proposed that the higher fluorescence peak intensity recorded for the top film surface compared to the bottom film surface may be caused by a higher degree of film hydration on the top surface.

4.4.1.1 Conclusions

First and second order Rayleigh scattering peaks were observed for both the background fluorescence spectra (Figure 17 A and B) and the fluorescence spectra for all the wheat gluten films prepared in this work, suggesting that they are characteristic of fluorescence spectra of solid film samples or the

background itself. The fluorescence peak in the region $\lambda_{\text{ex}} = 340 - 350 \text{ nm}$ and $\lambda_{\text{em}} = 410 - 430 \text{ nm}$ was attributed to a non-radiative energy transfer mechanism or re-absorption of fluorophores at the 335 nm wavelength emissions. The fluorescence peak around $\lambda_{\text{ex}} = 290 \text{ nm}$ and $\lambda_{\text{em}} = 330 \text{ nm}$ was attributed to tryptophan fluorescence. Further, the observed increased shifts in the tryptophan peak region at increasing gluten solution temperature and pH 11 or at 70°C and pH 4, support the notion that there are changes in protein conformation due to changes in film preparation method. Comparing the tryptophan fluorescence peak intensities, the ADM wheat gluten films had higher intensities than the Wonder cultivar films suggesting that the wheat source can be differentiated based on tryptophan peak intensity. With only a few exceptions, there were no statistically significant differences between old and new Wonder films suggesting that the protein only changed slightly as it aged 2 years. The bottom film surface also showed a difference in tryptophan peak intensity between the pH 4 and pH 11 films, which is suspected to reflect the morphological changes as previously discussed (chapter 4.3.1 Film Surface Morphology). Increased tryptophan peak intensity observed for the top film surface compared to the bottom film surface may result from a higher degree of film hydration on the top surface due to the methods of storage prior to analysis.

4.5 Gluten Film Water Vapour Permeability

4.5.1 Effect of Modifying ADM Film Preparation Methodology

4.5.1.1 Effect of Gluten Film Casting Surface

Table 25 compares the water vapour permeability (WVP) of gluten films according to the casting surface.

Table 25 - WVP of ADM Gluten Films According to Casting Surface (gluten solution at 70°C and pH 11)

Film Casting Surface	WVP (g.mm/ (day.m ² .atm)) (Average ± Standard Deviation)	Number of Measurements, n
Silicone Tray	341 ± 55	16
Silicone Grease Coated Glass Tray	322 ± 33	14

There was no statistically significant difference in film WVP resulting from the two different casting surfaces ($p > 0.05$). However, the large standard deviation seen for both casting surfaces, suggests that either the WVP estimation method or the film casting method (or both) may not be accurate enough to examine the effect of film casting surface on WVP. As such, the large standard deviation may mask the effect of protein conformation on WVP.

This lack of difference between casting surfaces is surprising since WVP literature (Table 26) shows that WVP can vary drastically according to many other elements of film formulation, film preparation method, and WVP characterization method. However, the ASTM D1653-03, states that temperature, relative humidity and film thickness must be the same in order to reliably compare WVP estimates (ASTM Standard D1653, 2003 (2008)). Consequently, here and in many published studies on wheat gluten films (where film casting techniques are investigated) an adjusted WVP value is employed, such that thickness variations are accounted for. Further, room temperature is an extremely common choice of temperature at which to conduct WVP, so that temperature can also be excluded from the situation. This leaves the relative humidity that creates the water vapour gradient which changes from publication to publication and is not standardized. Therefore, the humidity gradient may be the largest contributing factor to the large differences in the WVP values presented in Table 26.

Table 26 - Literature WVP for Wheat Gluten Films Cast with Commercial Wheat Gluten

Step	Parameter	Reference		
		(Gennadios, Weller & Testin 1993)	(Lens et al. 2003)	(Hager, Vallons & Arendt 2012)
Film Formulation	Gluten Supplier/ Type	ADM Arkady	Amylum	Sigma-Aldrich
	Type of Casting Solution	EtOH	Aqueous	Aqueous
	Gluten (g/100g solution)	11	unknown	7.3
	Additives	Ammonium Hydroxide (base)	N/A	Acetic Acid (for pH)
	pH adjustment	basic	5	4
	Mixing / heating / duration	Stirred 10 min; Added water and base. Final solution temp: 75-77°C. Let stand 2-3 min before casting	Add glycerol to aqueous WG dispersion. Heat to 80°C, stirring time 187 min.	Add glycerol to ethanol/WG. Adjust pH, Add water; heat to 70°C for 10 min.
Film Casting Preparation	Drying Conditions	32°C, unknown RH	50 °C, 50% RH	40°C, unknown RH
	Aging Conditions	23°C, 11%RH	20 °C, 60% RH	22°C, 60%RH
Film WVP Characterization	WVP [g.mm/(m².day.atm)]	490 ± 26	90.6 ± 1.5	23.3 ± 0.96
	WVP Gradient (%)	11.1	85	60
	WVP method	ASTM meth F 1249 - 89	silica in bottles, film clamped on opening	silica in bottles, film clamped on opening
	Film Thickness (µm)	127 ± 11	~ 350	16.5 ± 0.73 µm/g film forming solution*

*Not enough information to convert value to µm units.

A silicone casting surface was adopted for all remaining films prepared in this project in order to take advantage of the uniformity of the film and the elimination of silicone grease contamination (chapter 4.3.1 Film Surface Morphology).

4.5.1.2 Effect of Heating Temperature of the ADM Gluten Solution

The water vapour permeability of the gluten films in response to the temperature of the gluten solution is given in Table 27.

Table 27 - WVP of ADM Gluten Films Made from Gluten Solutions Heated to 70, 80, and 100 °C and pH 11

Temperature of Heating Stage (°C)	WVP (g.mm/ (day.m ² .atm)) (Average ± Standard Deviation)	Number of Measurements, n
70	341 ± 55	16
80	306 ± 36	3
100	389 ± 51	3

Variations in the water vapour permeability of the films were not statistically significant ($p > 0.05$) in relation to the heating temperature of the ADM gluten solution. Herald et al. made similar observations and reported that there was no significant difference in WVP, measured with a 55% RH gradient, for ethanol cast gluten films when the solution was heated to 40 or 80°C (Herald et al. 1995). Numerous studies (Domenek et al. 2002, Angellier-Coussy et al. 2011, Schofield et al. 1983) show that the fraction of SDS-soluble wheat gluten protein decreases with increasing processing temperature due to conformational changes and intermolecular cross-linking by disulfide interchange reactions (Schofield et al. 1983). Therefore, the negligible effect of heating temperature was unexpected given that an increase in intermolecular cross-linking by disulfide interchange reactions was anticipated to reduce the WVP of the film (Angellier-Coussy et al. 2011) by increasing the "tightness" of the protein network forming the film barrier (Gontard, Guilbert & Cuq 1993, Gennadios, Weller & Testin 1993, Park, Chinnan 1995).

Angellier-Coussy et al. reported that wheat gluten films thermoformed at 120°C had 30% lower WVP than those processed at 80°C attributed to decreased chain mobility, which in turn decreased the ability of the proteins to rearrange when water was absorbed from the water vapour permeating the film (Angellier-Coussy et al. 2011). Since Angellier-Coussy et al. obtained WVP measurements with 8% standard deviation for thermoformed films (Angellier-Coussy et al. 2011) and 16% standard deviation was obtained for films cast at 70°C (Table 27), it is hypothesized that the difference in film formation method (thermoformed versus cast) may affect the film quality and thus the large deviation seen for WVP measurements. This difference may help explain the lack of statistically significant differences ($p > 0.05$) in WVP obtained in this work for water cast gluten films with different solution heating temperatures (Table 27).

4.5.1.3 Effect of ADM Gluten Solution pH

The WVP of films obtained from ADM gluten solutions adjusted to pH 4 and pH 11 are shown in Table 28.

Table 28 - Average WVP of ADM Gluten Films Made from Gluten Solutions Adjusted to pH 4 and pH 11

pH of Gluten Solution	WVP (g.mm/ (day.m ² .atm)) (Average \pm Standard Deviation)	Number of Measurements, n
11	341 \pm 55	16
4	382 \pm 38	3

There was no statistically significant difference in WVP for films prepared from solutions at different pH values ($p \geq 0.05$). This lack of difference was unexpected considering the drastic difference in physical appearance of the two film types (chapter 4.3.1 Film Surface Morphology). One might expect that the film prepared at pH 4, that was heterogeneous and had indentations, would have a higher WVP than the films prepared at pH 11 due to the increased surface area available (in an irregular surface compared to a flat surface) for contact with water vapour, and proposed by Olabarrieta et al. to explain increased oxygen permeability for ethanol cast gluten films (Olabarrieta et al. 2006). However, Olabarrieta et al. also reported no significant difference in WVP (with an 11% RH gradient) for ethanol cast gluten films prepared from gluten solutions adjusted to pH 4 and 11, commenting that the larger amount of voids and capillaries in the heterogeneous pH 4 film only produced small (not statistically significant) differences between the WVP for pH 4 and pH 11 films (Olabarrieta et al. 2006). The absence of statistically significant differences between films cast at pH 4 and 11 observed in this research and reported in the literature suggest that WVP methodology may not be accurate enough to examine the effects of changes in the pH of the casting solution.

4.5.2 Effect of Wheat Gluten Source

The water vapour permeability of gluten films in relation to solution heating temperature, solution pH, and wheat source is given in Table 29. Film thickness is also presented in Table 29.

Table 29 - WVP and Thickness of Gluten Films according to Gluten Solution Temperature, pH and Wheat Source

Solution Temperature (°C)	Solution pH	Wheat Source	WVP [g.mm/(day.m ² .atm)] Average ± Standard Deviation (n=3)	Thickness (mm) Average ± Standard Deviation (n=3)
70	11	ADM	394 ± 56	0.185 ± 0.009
		Old Wonder	370 ± 94	0.217 ± 0.017
		New Wonder	319 ± 42	0.210 ± 0.010
80	11	ADM	345 ± 56	0.190 ± 0.008
		Old Wonder	439 ± 130	0.213 ± 0.023
		New Wonder	292 ± 42	0.207 ± 0.012
100	11	ADM	322 ± 15	0.205 ± 0.018
		Old Wonder	338 ± 41	0.233 ± 0.012
		New Wonder	349 ± 49	0.203 ± 0.009
70	4	ADM	964 ± 95	0.283 ± 0.017
		Old Wonder	895 ± 155	0.254 ± 0.009
		New Wonder	814 ± 123	0.247 ± 0.021

Unlike the initial ADM gluten film study (section 4.5.1), a statistically significant increase in the WVP of the pH 4 films was observed compared to the pH 11 films, irrespective of gluten type ($p < 0.05$). The difference is likely because, compared to section 4.5.1, films presented in Table 29 were prepared subsequently where more care was taken to select the most identical sections for all three samples taken from each film. Given the limited size of each film, locating three identical sections in one film required that the film be consistent across the majority of the surface and thus reflected the quality of the film preparation. It is believed that the higher content of voids and capillaries in the heterogeneous pH 4 film compared to the smooth pH 11 film observed in this study (chapter 4.3.1 Film Surface Morphology) and reported by Olabarieta et al. (Olabarieta et al. 2006) caused the measurable differences in WVP of the most recently prepared films but that practice and fine tuning of the film preparation procedure and the WVP sample preparation are important to see such differences.

There was neither a statistically significant difference in WVP with increasing solution heating temperature nor a statistically significant difference in WVP between wheat sources ($p \geq 0.05$). As mentioned in section 4.5.1, either the WVP method or the film casting method (or both) may have too much variability to examine the effects of solution heating temperature for water cast gluten films.

For all wheat gluten sources, gluten solutions prepared at pH 4 produced significantly thicker films than at pH 11 with $p < 0.05$ (Table 29). However, the thickness for pH 4 and pH 11 films is a

macroscopic property that does not reflect details of the film surface morphology where pH 4 films were heterogeneous and uneven with thinner clear spots and thicker beige hills, while the pH 11 films were smooth and homogeneous (chapter 4.3.1 Film Surface Morphology). Measurements of the thickness of the pH 4 films with a calliper reflected the thicker beige hills which did not account for the thickness of the thinner clear spots. Therefore, it is believed that the change in thickness reflects the film preparation methodology. Since WVP estimates were standardized by thickness estimates (Appendix 1), then WVP should also reflect the film morphology and the preparation methodology.

4.5.3 Conclusions

When WVP was initially investigated with commercial ADM wheat gluten (Whetpro80) films, no statistically significant differences ($p > 0.05$) were observed by varying the gluten solution pH or temperature or selecting a different casting surface. It was concluded that either the WVP method or the film casting method (or both) may be too variable to measure the effect of film formulation and preparation parameters. When a subsequent set of films were produced from three different wheat sources (ADM, new Wonder, and old Wonder), the films cast from a pH 4 gluten solution had statistically significantly higher WVP values ($p < 0.05$), irrespective of wheat gluten source, compared to films cast from a pH 11 gluten solution. The successful measurement of a difference between WVP of pH 11 and pH 4 films was attributed to better control of the film formulation and preparation methodology, which produced more uniform films and reduced the experimental error (reflected as lower standard deviation) for a given film. However, the WVP difference resulting from adjusting solution pH was attributed to the increased surface area available in an irregular film surface that occurred for pH 4 film, compared to the regular films for pH 11. Lastly, the film thickness and WVP both reflect the film preparation methodology and, since WVP estimates were standardized by film thickness, WVP should not be influenced by the film thickness.

4.6 Film Swelling

Swelling ratios of wet to dry film sample mass after 1 hour of soaking and after 24 hours of soaking are presented in Table 30.

Table 30 - Swelling Ratios for Film Samples Soaked for One Hour or Twenty-Four Hours

Film Preparation Parameters (all prepared at pH 11)		Swelling Ratio, q (wet mass/dry mass)	
Temperature (°C)	Glycerol	After 1 h Soak	After 24 h Soak
70	Yes	3.01 ± 0.03	2.13 ± 0.04
80	Yes	3.00 ± 0.14	2.20 ± 0.05
100	Yes	3.29 ± 0.05	2.43 ± 0.04
70	No	6.98 ± 0.35	4.56 ± 0.09

The swelling ratio (q) provided a quantitative measurement for film behaviour when exposed directly to water. The q ratio always decreased from 1 hour to 24 hours of soaking such that the 24 h samples had a q ratio of approximately 2/3 that of the 1 hour soak samples. Based on experimental work of the solubility of fish myofibrillar protein films containing glycerol, Cuq et al. attributed the mass of sample dissolved in the soak water to water soluble glycerol and to low molecular weight protein chains (Cuq et al. 1997). However, Irissin-Mangata et al. hypothesized that wheat gluten films containing glycerol may have a lower glycerol solubility because of cross-linking in the protein film, which traps some of the glycerol molecules in the protein film (Irissin-Mangata et al. 2001). According to Day et al., wheat gluten is fairly insoluble in water because water is polar and it increases the non-covalent interactions between protein segments, causing aggregation at pH 7 (Day et al. 2009). Depending on the type of amino acid side groups, water will interact with neighbouring amino acid side groups by means of hydrophobic, van der Waals, and/or electrostatic interactions, as well as H-bonds (Day et al. 2009). Over a 24 hour prolonged soaking time, the film would have time to become fully hydrated. Therefore, it is hypothesized that the decrease in q observed here, after an additional 23 h of soaking, could be attributed to a combination of glycerol and gluten dissolving in the soak water over time.

When the temperature of the gluten solution was increased to 100°C, the film swelling ratio was only slightly higher at 1 h and 24 h compared to the films prepared at 70°C (after accounting for standard error). This slight increase in swelling ratio was different than the results reported by Domenek et al. for thermoformed gluten films (24 h water soak), where film swelling decreased upon temperature

increase and was related to increased cross-linking and improved protein structure (Domenek et al. 2004). The opposite results suggest that film preparation method plays a major role in film cross-linking and the associated extent of film swelling.

For films cast without glycerol at 70°C, swelling ratios at 1 and 24 hours were at least twice those for films cast with glycerol, suggesting that glycerol affected the degree of swelling in the film. Pommet et al. and Domenek et al., observed 24 hr swelling ratios for films thermoformed without glycerol that were lower compared to films thermoformed with glycerol, supporting that the film preparation method (cast versus thermoformed) has a major effect on the swelling behavior of the films in water (Pommet et al. 2005, Domenek et al. 2004).

To ascertain the approximate quantity of mass lost over 24 hours, total solids estimates were obtained from the soak water (Table 31).

Table 31 - Total Solids Content of the Film Soaking Water after 24 h (Dried at 100°C)

Film Preparation Parameters (all prepared at pH 11)		Total Solids Content $\left(\frac{\text{Dissolved Solid Mass}}{\text{Soak Liquid Mass}} \times 100\right)$ (%)	Total Solids Dry Mass (mg)
Temperature (°C)	Glycerol		
70	Yes	0.031 ± 0.005	2.9 ± 0.9
80	Yes	0.011 ± 0.002	1.6 ± 0.1
100	Yes	0.013 ± 0.001	1.7 ± 0.1
70	No	0.0254 ± 0.0003	3.5 ± 0.2

Some film mass dissolved in the soak water (Table 31). The initial mass of the film samples conditioned at 50% RH before soaking had an average mass of 19 mg. Therefore, the 1.6 to 3.5 mg of oven dried sample recovered from the soak water represents an average of 13% of the initial film sample mass. The total solids results (Table 31) indicate that the lower film swelling ratio observed after 24 hours soaking (Table 30) was partially due to film mass dissolving in the soak water. However, because of the differences in moisture content estimates of the oven dried samples and the film sample conditioned at 50% RH, it is not possible to determine if all the decrease in q after 24 hours soaking was due to film constituents dissolving in the soak water.

Absorbance measurements at 280 nm were obtained for the 24 hour soak water to ascertain the total protein content in the soak water. The total protein mass in the soak water was determined (Table 32) based on a BSA calibration curve (Appendix 10).

Table 32 - BSA Equivalent Total Protein Mass in Film Soaking Solution after 24 h using Absorbance at 280 nm

Film Preparation Parameters (all prepared at pH 11)		Total Protein Mass Estimate (mg)
Temperature (°C)	Glycerol	
70	Yes	41 ± 5
80	Yes	25 ± 3
100	Yes	32 ± 1
70	No	77 ± 7

The protein mass in the soak water, determined by absorbance (Table 32), was larger than when the protein mass was determined by total solids (Table 31). The difference may be due to limitations of the balance used to measure total solids since it could not measure past the 4th decimal digit, potentially limiting the accuracy of the dry solids masses measured. In addition, the use of BSA as the protein for the absorbance calibration curve may impact the accuracy of the total protein mass calculation since BSA and the various proteins in wheat gluten do not share similar protein mass, size, or physical properties.

4.6.1 Conclusions

The swelling ratio of gluten films after 24 h soaking was always approximately 2/3 lower than after 1 h of soaking, which was attributed to a combination of film components dissolving in the soak water over time. When the temperature of the gluten solution was increased to 100°C, the swelling ratio was nearly the same at 1 hour and at 24 hours compared to the films prepared at 70°C. Since this result contrasts with those of Domenek et al. for thermoformed gluten films, the film preparation method affected the film stability and its swelling behavior. The films cast without glycerol at 70°C had swelling ratios, at 1 and 24 hours, that were at least twice those of the film cast with glycerol. The reduced film swelling ratio over 24 hours soaking was associated with the solubilisation of some film components as deduced from the total solids content of the soaking solution, 13% of the original film sample dissolved in the water during the 24 h soak. Total protein estimate of the soaking solution obtained by absorbance at 280 nm indicated that some of the mass dissolved in the water after 24 h was likely protein.

5 Conclusions

Although WVP did not vary significantly with the casting surface, the films cast on a silicone surface were less hydrophobic than the films cast on a glass surface coated with silicone grease (contact angles of 80.6° and 91.1° respectively). FTIR analysis of the top of gluten film surfaces revealed the presence of silicone for the films cast with a silicone grease coating, likely resulting in the observed increase in surface hydrophobicity.

Although WVP did not vary significantly with gluten solution temperature, an increase from 70 to 80 or 100°C in the temperature of the gluten solution produced significant changes in the film surface hydrophobicity deduced from water contact angle measurements, according to the wheat gluten source. The highest surface hydrophobicity for the top and bottom surfaces of the films occurred at 70°C for films produced with wheat gluten from old Wonder wheat (contact angles of 68.5° and 93.1° respectively) and 80°C for films produced with new Wonder wheat (contact angles of 63.4° and 84.3° respectively). The films from ADM gluten were most hydrophobic on the top film surface when the gluten solution was heated to 100°C (contact angle of 79.5°) but were most hydrophobic on the bottom surface when the gluten solution was heated to 80°C (contact angle of 92.0°). These experimental results are higher than published values for ethanol cast gluten films cast at 70°C and pH 11 (55°).

Changes in the film protein tryptophan conformation were also correlated with temperature based on fluorescence spectroscopy measurements. As the temperature of the gluten solution was increased, there was an increase in the blue shift for the tryptophan peak of the films. The tryptophan peaks is very sensitive to changes in polarity and/or its local environment, demonstrating that the change in the preparation method created a change in either tryptophan environment or the conformation of surrounding protein segments.

When the gluten solution was heated to 100°C, there was an increase in film surface roughness which was particularly evident when compared to films cast at temperatures of 70 or 80°C, irrespective of the wheat gluten source. The films produced from ADM gluten exhibited the most drastic change with raised bumps of aggregated protein for the 100°C films compared to smooth surfaces for films produced at 70 or 80°C. The swelling ratio of films incubated in water during 24 hours was not significantly affected by the increase in temperature of the gluten solution, with only a slight increase for those at 100°C. The above observations suggest that some molecular level changes do occur as a

result of increasing the temperature of the gluten solution; however, over the temperature range studied, these are not drastic changes in the final film properties.

Films cast from pH 4 gluten solutions produced much more heterogeneous and bumpy surfaces compared to the smooth homogeneous films produced from pH 11 gluten solutions. Furthermore, the WVP increased significantly for films cast from pH 4 gluten solutions compared to pH 11, averaging a WVP change from 361 g.mm/(day.m².atm), at pH 11, to 891 g.mm/(day.m².atm), at pH 4, across the three wheat sources. The experimental WVP results at pH 11 are lower than published WVP values for ethanol cast gluten films heated to ~76°C and at basic pH (490 g.mm/(day.m².atm)). In contrast, the experimental WVP results at pH 4 are higher than published WVP values for aqueous gluten films cast at pH 4 and 70°C (23.3 g.mm/(day.m².atm)). However, these WVP values for gluten films are both still much higher than the values for plastic films like nylon and polystyrene, at 7.5 and 3.9 g.mm/(m².day.atm) respectively. WVP differences were observed between pH 4 and pH 11 across all gluten sources. However, only Wonder films exhibited a consistent hydrophobicity trend. That is, most Wonder films cast from pH 4 gluten solutions had a higher hydrophobic than films at pH 11 (average contact angles of 79° and 86° on top and bottom respectively at pH 4, and average contact angles of 64° and 86° on top and bottom respectively at pH 11). These experimental results tend to be similar to or higher than published contact angle values for gluten films cast at 70°C and pH 4 (54 - 80°).

These superior film properties (a smoother, more homogeneous film, with lower water vapor permeability) for films cast from pH 11 gluten solutions are believed to occur because a higher degree of protein aggregation was induced in pH 11 films compared to pH 4. Intrinsic fluorescence spectroscopy showed differences in tryptophan peak intensity between the pH 4 and 11 films, suggesting that other changes in protein conformation also occurred as pH was modified from pH 4 to pH 11.

The effect of pH on the viscosity of the glycerol – water – gluten solution was evaluated. Gradual viscosity increase was observed with increasing pH from pH 7.7 up to pH 11, leveling off as pH 11 was approached. This change in viscosity was attributed to increased protein denaturation and increased intermolecular interactions and the resulting aggregation.

The effect of pH on gluten protein association in aqueous solution at pH 7.7 and pH 11 was investigated by SPR using a SAM surface. The gluten in the pH 7.7 solution exhibited a much greater affinity for the SAM surface than the gluten in pH 11 solution, which is believed to result from

increased electrostatic repulsion between the negatively charged gluten proteins and the SAM surface. In contrast, hydrophobic attractive forces and electrostatic attractions dominated at pH 7.7.

Films prepared with commercial gluten were the most hydrophobic for all solution temperature adjustments (contact angle range of 76.4 - 79.5° on the top surface and 75.4 - 92.0° on the bottom surface) but Wonder gluten films produced at pH 4 were more hydrophobic (new and old Wonder contact angles of 77.9 and 80.6° respectively on the top surface and 89.5 and 82.9° respectively on the bottom surface). The Wonder gluten films were more sensitive to changes in temperature (average contact angle variation of 14° on top and 22° on bottom) and pH (average contact angle variation of 16° on top and 10° on bottom), while the commercial gluten films generally had a smaller variation in hydrophobicity with temperature (contact angle variation of 3.1° on top and 16.6° on bottom) and pH change (contact angle variation of 1.4° on top and 6.5° on bottom). The differences in film hydrophobicity are believed to result from differences in gluten extraction method according to scale. Differences in properties of the wheat sources were observed by intrinsic fluorescence measurements of the films with a higher tryptophan peak intensity for commercial gluten films compared to Wonder gluten films.

Commercial and Wonder gluten sources could be distinguished according to film surface morphology. Wonder gluten films had dark flecks dispersed across the surface and a fine, grainy, rough texture. In contrast, commercial gluten films were much smoother containing little to no dark flecks. The dark flecks in the new Wonder gluten films were much more evenly distributed across the film surface, suggesting that the age and/or gluten extraction method also affected the gluten characteristics. The gluten type did not affect the film WVP.

The WVP and contact angle results obtained for each film type according to temperature, pH, and gluten source demonstrates that WVP and contact angle are not related. This indicates that the film surface hydrophobicity relative to the *liquid* form of water does not provide an indication of the degree of film permeability to water in *vapour* form.

The smoothest, most homogeneous and most hydrophobic gluten films with the lowest water vapour permeability, 345 and 292 g.mm/(day.m².atm) respectively for commercial gluten and new Wonder gluten, were produced when the gluten solution was adjusted to pH 11 and the temperature adjusted to 80°C. When gluten films were prepared from old Wonder gluten, a temperature of 70°C and pH 11 was required to produce the smoothest, most homogeneous and most hydrophobic gluten films with the lowest water vapour permeability (370 g.mm/(day.m².atm)).

These results demonstrate that wheat gluten films produced from some Ontario cultivars have water vapour barrier properties similar to films prepared with commercial wheat gluten, illustrating the potential for gluten films as an alternative use for Ontario wheat cultivars. The use of a silicone tray casting surface represents an important improvement to the film preparation method, improving film quality before and after peeling the dry film off the casting surface. The use of the "green" solvent, to prepare wheat gluten films was shown to be a viable replacement for the traditional ethanol solvent, even resulting in lower WVP gluten films than literature values for ethanol cast gluten films. However, further research is needed to reduce the WVP of gluten films enough to make them marketable replacements to plastic food packaging.

6 Future work

The study of a 90°C gluten solution temperature may further improve water vapour barrier properties of gluten films compared to a 80°C gluten solution without exhibiting raised bumps of protein aggregates (as occurred for 100°C films) and so could maintain an aesthetically pleasing homogeneous, smooth film surface. The study of less basic pH conditions such as pH 9 or 10 should be studied because lower pH in the film casting solution would reduce the alkaline nature of the film and likely improve its palatability in edible food packaging applications. In addition, combining wheat gluten protein with proteins from other sources could be explored because linkages between gluten and other protein types could decrease the water vapour permeability of the film protein network (as observed with the addition of keratin for Gennadios et al. (Gennadios, Weller & Testin 1993)) while still maintaining the good gas barrier properties that gluten films are known for.

Approaches could also be explored as to how to cast clear gluten films without using a two day extraction process to separate glutenin and gliadin fractions, as making the gluten film clear would improve its appearance and result in improved product marketability. Since pH 4 films exhibited a heterogeneous morphology, pH 4 gluten solution conditions may be conducive to separation during the film casting process.

SPR and viscosity studies of the gluten solution properties should be made at pH 4 in order to determine how protein interactions in solution relate to and produce the dried film properties with pH in this research. The time allotted for the association phase in SPR experiments should also be extended because the preliminary SPR results did not allow enough time for the SPR signal to plateau during the association phase. Extending the association phase would verify that no other interactions between the gluten solution and the SAM surface takes place over a longer period of time, thus providing a better understanding of pH 11 gluten interactions with the SAM surface.

The role of glycerol addition in gluten solution should be investigated by SPR experiments as means to investigate the nature of glycerol gluten interactions in the solution. TGA experiments with glycerol containing films cast at incremental stages of the film preparation could help in identifying which stages of the film making procedure contribute to increasing the thermal stability of the gluten and glycerol network, based on changes in TGA curve properties (1% onset) and temperature shifts of DTGA peaks.

Quantitative surface roughness measurements according to film formulation and preparation should be obtained using an Optical Profiler as the semi-transparent nature of the films limit the amount of

information provided by microscopy imaging. Quantitative surface roughness measurements would allow for better interpretation of WVP results because surface roughness increases the surface area available to interact with water vapour and is therefore believed to contribute to increased water vapour permeability.

References

- AACC International. "Method 38-10.01. Gluten -- Hand Washing Method" in *Approved Methods of Analysis, 11th Ed.* AACC International, St. Paul, MN, U.S.A.
- ADM 2012, , *ADM Vital Wheat Gluten*. Available:
<http://www.adm.com/en-US/products/Documents/ADM-Vital-Wheat-Gluten.pdf> [2012, 07/30].
- Ang, S., Kogulanathan, J., Morris, G., K k, M., Shewry, P., Tatham, A., Adams, G., Rowe, A. & Harding, S. 2010, "Structure and heterogeneity of gliadin: a hydrodynamic evaluation", *European Biophysics Journal*, vol. 39, no. 2, pp. 255-261.
- Angellier-Coussy, H., Gastaldi, E., Gontard, N. & Guillard, V. 2011, "Influence of processing temperature on the water vapour transport properties of wheat gluten based agromaterials", *Industrial Crops and Products*, vol. 33, no. 2, pp. 457-461.
- Arentz-Hansen, E.H., McAdam, S.N., Molberg, Kristiansen, C. & Sollid, L.M. 2000, "Production of a panel of recombinant gliadins for the characterisation of T cell reactivity in coeliac disease", *GUT*, vol. 46, pp. 46-51.
- ASTM Standard D1653, 2003 (2008) *Standard Test Methods for Water Vapor Transmission of Organic Coating Films*, ASTM International, West Conshohocken, PA.
- Audic, J. & Chaufer, B. 2010, "Caseinate based biodegradable films with improved water resistance", *Journal of Applied Polymer Science*, vol. 117, no. 3, pp. 1828-1836.
- Barrett, D.A., Power, G.M., Hussain, M.A., Pitfield, I.D., Shaw, P.N. & Davies, M.C. 2005, "Protein interactions with model chromatographic stationary phases constructed using self-assembled monolayers", *Journal of Separation Science*, vol. 28, no. 5, pp. 483-491.
- Barth, A. 2007, "Infrared spectroscopy of proteins", *BBA - Bioenergetics*, vol. 1767, no. 9, pp. 1073-1101.
- Bekkers, A.C., Van Dijk, A., de Boef, E., Van Swieten, E., Robillard, G. & Hamer, R.J. 1996, "HMW glutenins:structure–function relationships step by step", *Gluten 96 - Proc. 6th Int. Wheat Gluten Workshop*Royal Australian Chemical Institute, North Melbourne, Australia, September 1996, pp. 190.
- Belton, P.S. 1999, "Mini review: On the elasticity of wheat gluten", *Journal of cereal science*, vol. 29, no. 2, pp. 103-107.
- Blanch, E.W., Kasarda, D.D., Hecht, L., Nielsen, K. & Barron, L.D. 2003, "New insight into the solution structures of wheat gluten proteins from raman optical activity", *Biochemistry*, vol. 42, no. 19, pp. 5665-5673.

- Bonomi, F., Mora, G., Pagani, M.A. & Iametti, S. 2004, "Probing structural features of water-insoluble proteins by front-face fluorescence", *Analytical Biochemistry*, vol. 329, no. 1, pp. 104-111.
- Chen, L., Reddy, N., Wu, X. & Yang, Y. 2012, "Thermoplastic films from wheat proteins", *Industrial Crops & Products*, vol. 35, no. 1, pp. 70-76.
- Chiou, B., Robertson, G.H., Roof, L.E., Cao, T., Jafri, H., Gregorski, K.S., Imam, S.H., Glenn, G.M. & Orts, W.J. 2010, "Water absorbance and thermal properties of sulfated wheat gluten films", *Journal of Applied Polymer Science*, vol. 116, no. 5, pp. 2638-2644.
- Cho, S.-W., Gällstedt, M. & Hedenqvist, M.S. 2010, "Effects of glycerol content and film thickness on the properties of vital wheat gluten films cast at pH 4 and 11", *Journal of Applied Polymer Science*, vol. 117, no. 6, pp. 3506-3514.
- Commodity Futures and Equity Analytics 2000, , *Types of Wheat*. Available: http://www.commodityseasonals.com/types_of_wheat.htm [2012, Sept 4].
- Cuq, B., Gontard, N., Cuq, J. & Guilbert, S. 1997, "Selected functional properties of fish myofibrillar protein-based films as affected by hydrophilic plasticizers", *Journal of Agricultural and Food Chemistry*, vol. 45, no. 3, pp. 622-626.
- Davis, J.P. & Copeland, R.A. 2000, "Protein engineering" in *Kirk-Othmer Encyclopedia of Chemical Technology* John Wiley & Sons, Inc. ,
- Day, L., Xu, M., Lundin, L. & Wooster, T.J. 2009, "Interfacial properties of deamidated wheat protein in relation to its ability to stabilise oil-in-water emulsions", *Food Hydrocolloids*, vol. 23, no. 8, pp. 2158-2167.
- de Bruijn, H.E., Altenburg, B.S.F., Kooyman, R.P.H. & Greve, J. 1991, "Determination of thickness and dielectric constant of thin transparent dielectric layers using surface plasmon resonance", *Optics Communications*, vol. 82, no. 5-6, pp. 425-432.
- Domenek, S., Brendel, L., Morel, M. & Guilbert, S. 2004, "Swelling behavior and structural characteristics of wheat gluten polypeptide films", *Biomacromolecules*, vol. 5, no. 3, pp. 1002-1008.
- Domenek, S., Morel, M., Bonicel, J. & Guilbert, S. 2002, "Polymerization kinetics of wheat gluten upon thermosetting. A mechanistic model", *Journal of Agricultural and Food Chemistry*, vol. 50, no. 21, pp. 5947-5954.
- Dou, B., Dupont, V., Williams, P.T., Chen, H. & Ding, Y. 2009, "Thermogravimetric kinetics of crude glycerol", *Bioresource technology*, vol. 100, no. 9, pp. 2613-2620.
- Eco Chemie B.V. 2006, *Autolab ESPRIT/SPRINGLE User manual: Surface Plasmon Resonance*, , Utrecht, Netherlands.
- Exova 2012, , *FTIR - Fourier Transform Infra Red*. Available: <http://www.wcaslab.com/tech/tbftir.htm> [2012, 07/2012].

- Fu, B. & Sapirstein, H. 1996, "Procedure for isolating monomeric proteins and polymeric glutenin of wheat flour", *Cereal Chemistry*, vol. 73, no. 1, pp. 143-152.
- Gällstedt, M., Mattozzi, A., Johansson, E. & Hedenqvist, M.S. 2004, "Transport and tensile properties of compression-molded wheat gluten films", *Biomacromolecules*, vol. 5, no. 5, pp. 2020-2028.
- Gennadios, A., Weller, C.L. & Testin, R.F. 1993, "Modification of physical and barrier properties of edible wheat gluten-based films", *Cereal Chem.*, vol. 70, pp. 426-429.
- Genot, C., Tonetti, F., Montenaygarestier, T., Marion, D. & Drapron, R. 1992, "Front face fluorescence applied to structural studies of proteins and lipid-protein interactions of viscoelastic food-products .2. Application to wheat gluten", *Sciences des Aliments*, vol. 12, no. 4, pp. 687-704.
- Georget, D.M.R. & Belton, P.S. 2006, "Effects of temperature and water content on the secondary structure of wheat gluten studied by FTIR spectroscopy", *Biomacromolecules*, vol. 7, no. 2, pp. 469-475.
- Gómez-Martínez, D., Barneto, A.G., Martínez, I. & Partal, P. 2011, "Modelling of pyrolysis and combustion of gluten-glycerol-based bioplastics", *Bioresource technology*, vol. 102, no. 10, pp. 6246-6253.
- Gontard, N., Guilbert, S. & Cuq, J. 1992, "Edible wheat gluten films: Influence of the main process variables on film properties using response surface methodology", *Journal of Food Science*, vol. 57, no. - 1, pp. 190.
- Gontard, N., Guilbert, S. & Cuq, J.L. 1993, "Water and glycerol as plasticizers affect mechanical and water vapor barrier properties of an edible wheat gluten film", *J. Food Sci.*, vol. 58, no. 1, pp. 206-211.
- Gu, Y. & Jérôme, F. 2010, "Glycerol as a sustainable solvent for green chemistry", *Green Chemistry*, vol. 12, no. 7, pp. 1127-1138.
- Guimarães, G.C., Coelho Júnior, M.C. & Garcia Rojas, E.E. 2009, "Density and kinematic viscosity of pectin aqueous solution†", *Journal of Chemical & Engineering Data*, vol. 54, no. 2, pp. 662-667.
- Hager, A., Vallons, K.J.R. & Arendt, E.K. 2012, "Influence of gallic acid and tannic acid on the mechanical and barrier properties of wheat gluten films", *Journal of Agricultural and Food Chemistry*, vol. 60, no. 24, pp. 6157-6163.
- Hamer, R.J. & Vliet, T.V. 2000, "Understanding the structure and properties of gluten: An overview" in *Wheat Gluten*, eds. P.R. Shewry & A.S. Tatham, The Royal Society of Chemistry, Cambridge, U.K., pp. 125.
- Heiss, R. 1959, "Shelf-life determinations", *Modern Packag.*, vol. 31, pp. 119-126.

- Herald, T.J., Gnanasambandam, R., McGuire, B.H. & Hachmeister, K.A. 1995, "Degradable wheat gluten films: Preparation, properties and applications", *Journal of Food Science*, vol. 60, pp. 1147.
- Hernández-Muñoz, P., Kanavouras, A., Ng, P.K.W. & Gavara, R. 2003, "Development and characterization of biodegradable films made from wheat gluten protein fractions", *Journal of Agricultural and Food Chemistry*, vol. 51, no. 26, pp. 7647-7654.
- Hofmann, S. 2006, "Surface and interface analysis" in *Kirk-Othmer Encyclopedia of Chemical Technology* John Wiley & Sons, Inc., .
- Hsia, C.C. & Anderson, O.D. 2001, "Isolation and characterization of wheat ω -gliadin genes", *TAG Theoretical and Applied Genetics*, vol. 103, no. 1, pp. 37-44.
- Huang, X. & Cloutier, S. 2008, "Molecular characterization and genomic organization of low molecular weight glutenin subunit genes at the Glu-3 loci in hexaploid wheat (*Triticum aestivum* L.)", *Theoretical and Applied Genetics*, vol. 116, no. 7, pp. 953-966.
- Ignagni, N. 2011, *Engineering Applications of Surface Plasmon Resonance: Protein-Protein and Protein-Molecule Interactions*.
- Irissin-Mangata, J., Bauduin, G., Boutevin, B. & Gontard, N. 2001, "New plasticizers for wheat gluten films", *European Polymer Journal*, vol. 37, no. 8, pp. 1533-1541.
- Ishida, H. & Lee, Y. 2001, "Synergism observed in polybenzoxazine and poly(ϵ -caprolactone) blends by dynamic mechanical and thermogravimetric analysis", *Polymer*, vol. 42, no. 16, pp. 6971-6979.
- Jerez, A., Partal, P., Martinez, I., Gallegos, C. & Guerrero, A. 2005, "Rheology and processing of gluten based bioplastics", *Biochemical engineering journal*, vol. 26, no. 2-3, pp. 131-138.
- Kaali, P., Momcilovic, D., Markström, A., Aune, R., Czel, G. & Karlsson, S. 2010, "Degradation of biomedical polydimethylsiloxanes during exposure to in vivo biofilm environment monitored by FE-SEM, ATR-FTIR, and MALDI-TOF MS", *Journal of Applied Polymer Science*, vol. 115, no. 2, pp. 802-810.
- Kayserilioğlu, B.Ş., Bakir, U., Yilmaz, L. & Akkaş, N. 2003, "Drying temperature and relative humidity effects on wheat gluten film properties", *Journal of Agricultural and Food Chemistry*, vol. 51, no. 4, pp. 964-968.
- Kerton, F.M. 2009, *Alternative solvents for green chemistry*, RSC Publishing, Cambridge, UK.
- Kohler, P., KeckGassenmeier, B., Wieser, H. & Kasarda, D.D. 1997, "Molecular modeling of the n-terminal regions of high molecular weight glutenin subunits 7 and 5 in relation to intramolecular disulfide bond formation", *Cereal Chem.*, vol. 74, pp. 154-158.
- KRÜSS GmbH. 2004, *DSA1 v 1.9 Drop Shape Analysis for DSA100, User Manual*, , Hamburg, Germany.

- Lafiandra, D., Masci, S., DOvidio, R. & Margiotta, B. 2000, "The genetics of wheat gluten proteins; An overview" in *Wheat Gluten*, eds. P.R. Shewry & A.S. Tatham, The Royal Society of Chemistry, Cambridge, UK, pp. 3.
- Lagrain, B., Goderis, B., Brijs, K. & Delcour, J.A. 2010, "Molecular basis of processing wheat gluten toward biobased materials", *Biomacromolecules*, vol. 11, no. 3, pp. 533-541.
- Lakowicz, J.R. 2006, *Principles of fluorescence spectroscopy*, Springer, New York.
- Lambourne, J., Tosi, P., Marsh, J., Bhandari, D., Green, R., Frazier, R. & Shewry, P.R. 2010, "Characterisation of an s-type low molecular weight glutenin subunit of wheat and its proline and glutamine-rich repetitive domain", *Journal of cereal science*, vol. 51, no. 1, pp. 96-104.
- Lang, C.A. 1958, "Simple microdetermination of kjeldahl nitrogen in biological materials", *Analytical Chemistry*, vol. 30, no. 10, pp. 1692-1694.
- Larré, C., Desserme, C., Barbot, J. & Gueguen, J. 2000, "Properties of deamidated gluten films enzymatically cross-linked", *Journal of Agricultural and Food Chemistry*, vol. 48, no. 11, pp. 5444-5449.
- Lefebvre, J., Pruska-Kedzior, A., Kedzior, Z. & Lavenant, L. 2003, "A phenomenological analysis of wheat gluten viscoelastic response in retardation and in dynamic experiments over a large time scale", *Journal of cereal science*, vol. 38, no. 3, pp. 257-267.
- Lehninger, A.L., Nelson, D.L. & Cox, M.M. 2004, "Chapter 3: Amino Acids, Peptides, and Proteins" in *Lehninger's Principles of Biochemistry* Worth Publishers, New York, pp. 80.
- Lens, J.P., de Graaf, L.A., Stevels, W.M., Dietz, C.H.J.T., Verhelst, K.C.S., Vereijken, J.M. & Kolster, P. 2003, "Influence of processing and storage conditions on the mechanical and barrier properties of films cast from aqueous wheat gluten dispersions", *Industrial Crops and Products*, vol. 17, no. 2, pp. 119-130.
- Li, Y., Xia, Q., Shi, K. & Huang, Q. 2011, "Scaling behaviors of α -zein in acetic acid solutions", *The Journal of Physical Chemistry B*, vol. 115, no. 32, pp. 9695-9702.
- Liu, C., Tellez-Garay, A.M. & Castell-Perez, M.E. 2004, "Physical and mechanical properties of peanut protein films", *Lebensmittel-Wissenschaft und -Technologie*, vol. 37, no. 7, pp. 731-738.
- Maleki, A., Lafitte, G., Kjoniksen, A.L., Thuresson, K. & Nystrom, B. 2008, "Effect of pH on the association behavior in aqueous solutions of pig gastric mucin", *Carbohydrate research*, vol. 343, no. 2, pp. 328-340.
- Marcuzzo, E., Peressini, D., Debeaufort, F. & Sensidoni, A. 2010, "Effect of ultrasound treatment on properties of gluten-based film", *Innovative Food Science and Emerging Technologies*, vol. 11, no. 3, pp. 451-457.
- Marsh, K. & Bugusu, B. 2007, "Food packaging—roles, materials, and environmental issues", *Journal of Food Science*, vol. 72, pp. 39-55.

- Massey, L.K. 2003, *Permeability Properties of Plastics and Elastomers: A Guide to Packaging and Barrier Materials, 2nd Ed.* Plastics Design Library / William Andrew Publishing, Norwich, NY, USA.
- Mastromatteo, M., Chillo, S., Buonocore, G.G., Massaro, A., Conte, A. & Del Nobile, M.A. 2008, "Effects of spelt and wheat bran on the performances of wheat gluten films", *Journal of Food Engineering*, vol. 88, no. 2, pp. 202-212.
- McHugh, T., Avenabustillos, R. & Krochta, J. 1993, "Hydrophilic edible films - modified procedure for water-vapor permeability and explanation of thickness effects", *Journal of Food Science*, vol. 58, no. 4, pp. 899-903.
- Mendichi, R., Fisichella, S. & Savarino, A. 2008, "Molecular weight, size distribution and conformation of glutenin from different wheat cultivars by SEC-MALLS", *Journal of cereal science*, vol. 48, no. 2, pp. 486-493.
- Micard, V., Morel, M.-., Bonicel, J. & Guilbert, S. 2001, "Thermal properties of raw and processed wheat gluten in relation with protein aggregation", *Polymer*, vol. 42, no. 2, pp. 477-485.
- Mohamed, A., Finkenstadt, V.L., Gordon, S.H., Biresaw, G., Palmquist, D.E. & Rayas-Duarte, P. 2008, "Thermal properties of PCL/gluten bioblends characterized by TGA, DSC, SEM, and infrared-PAS", *Journal of Applied Polymer Science*, vol. 110, no. 5, pp. 3256-3266.
- Mojumdar, S., Moresoli, C., Simon, L. & Legge, R. 2011, "Edible wheat gluten (WG) protein films", *Journal of Thermal Analysis and Calorimetry*, vol. 104, no. 3, pp. 929-936.
- Montgomery, D.C. 2009, "2.4 Inferences about the differences in means, randomized designs" in *Design and Analysis of Experiments, 7th Ed.*, 7th ed edn, Wiley, Hoboken, NJ, pp. 34-45.
- Muensri, P., Kunanopparat, T., Menut, P. & Siriwattanayotin, S. 2011, "Effect of lignin removal on the properties of coconut coir fiber/wheat gluten biocomposite", *Composites Part A*, vol. 42, no. 2, pp. 173-179.
- Olabarrieta, I., Cho, S., Gällstedt, M., Sarasua, J., Johansson, E. & Hedenqvist, M.S. 2006, "Aging properties of films of plasticized vital wheat gluten cast from acidic and basic solutions", *Biomacromolecules*, vol. 7, no. 5, pp. 1657-1664.
- Pareyt, B. & Delcour, J.A. 2008, "The role of wheat flour constituents, sugar, and fat in low moisture cereal based products: A review on sugar-snap cookies", *Critical reviews in food science and nutrition*, vol. 48, no. 9, pp. 824-839.
- Park, H.J. & Chinnan, M.S. 1995, "Gas and water vapor barrier properties of edible films from protein and cellulosic materials", *Journal of Food Engineering*, vol. 25, no. 4, pp. 497-507.
- Pascat, B. 1986, "Study of some factors affecting permeability" in *Food Packaging and Preservation, Theory and Practice*, ed. M. Mathlouthi, Elsevier Applied Science, London, pp. 6-24.
- Patnaik, P. 2004, "Thermal Analysis" in *Dean's Analytical Chemistry Handbook, Second Edition* McGRAW-HILL: New York, New York, USA.

- Peiris, R.H., Hallé, C., Budman, H., Moresoli, C., Peldszus, S., Huck, P.M. & Legge, R.L. 2010, "Identifying fouling events in a membrane-based drinking water treatment process using principal component analysis of fluorescence excitation-emission matrices", *Water research*, vol. 44, no. 1, pp. 185-194.
- PerkinElmer, I. 2010, , *Thermogravimetric Analysis (TGA) - A Beginner's Guide*. Available: http://www.perkinelmer.com/CMSResources/Images/44-74556GDE_TGABeginnersGuide.pdf [2012, Sept 11].
- Pommet, M., Redl, A., Guilbert, S. & Morel, M.H. 2005, "Intrinsic influence of various plasticizers on functional properties and reactivity of wheat gluten thermoplastic materials", *Journal of cereal science*, vol. 42, no. 1, pp. 81-91.
- Reeves, C.D. & Okita, T.W. 1987, "Analyses of alpha/beta-type gliadin genes from diploid and hexaploid wheats", *Gene*, vol. 52, pp. 257.
- Sánchez, A.C., Popineau, Y., Mangavel, C., Larré, C. & Guéguen, J. 1998, "Effect of different plasticizers on the mechanical and surface properties of wheat gliadin films", *Journal of Agricultural and Food Chemistry*, vol. 46, no. 11, pp. 4539-4544.
- Schofield, J.D., Bottomley, R.C., Timms, M.F. & Booth, M.R. 1983, "The effect of heat on wheat gluten and the involvement of sulphhydryl-disulphide interchange reactions", *J.Cereal Sci.*, vol. 1, pp. 241-253.
- Shewry, P.R., Halford, N.G., Belton, P.S. & Tatham, A.S. 2002, "The structure and properties of gluten: An elastic protein from wheat grain", *Philosophical Transactions: Biological Sciences*, vol. 357, no. 1418, Elastomeric Proteins: Structures, Biomechanical Properties and Biological Roles, pp. pp. 133-142.
- Skinner, D. & Bellinger, B. 2010, "Exposure to subfreezing temperature and a freeze-thaw cycle affect freezing tolerance of winter wheat in saturated soil", *Plant and Soil*, .
- Sluiter, A., Hames, D., Payne, C., Ruiz, R., Scarlata, C., Sluiter, J., Templeton, D. & Wolfe, J. 2008, *Determination of Total Solids in Biomass and Total Dissolved Solids in Liquid Process Samples - Laboratory Analytical Procedure*.
- Song, Y. & Zheng, Q. 2009, "Structure and properties of methylcellulose microfiber reinforced wheat gluten based green composites", *Industrial Crops & Products*, vol. 29, no. 2-3, pp. 446-454.
- Song, Y. & Zheng, Q. 2008, "Network formation in glycerol plasticized wheat gluten as viewed by extensional deformation and stress relaxation: Final conclusions", *Food Hydrocolloids*, vol. 22, no. 4, pp. 674-681.
- Stevenson, S.G., You, S., Izydorczyk, M.S. & Preston, K.R. 2003, "Characterization of polymeric wheat proteins by flow field-flow fractionation/MALLS", *Journal of Liquid Chromatography & Related Technologies*, vol. 26, no. 17, pp. 2771-2781.
- Stothard, P. 2000, "The sequence manipulation suite: JavaScript programs for analyzing and formatting protein and DNA sequences.", *Biotechniques*, vol. 28, pp. 1102-1104.

- Stuart, B. 2005, "Infrared Spectroscopy" in *Kirk-Othmer Encyclopedia of Chemical Technology* John Wiley & Sons, Inc., .
- Sugiyama, T., Rafalski, A., Peterson, D. & Soll, D. 1985, "A wheat HMW glutenin subunit gene reveals a highly repeated structure", *Nucleic Acid Res.*, vol. 13, pp. 8729.
- Tanada-Palmu, P.S. & Grosso, C.R.F. 2005, "Effect of edible wheat gluten-based films and coatings on refrigerated strawberry (*Fragaria ananassa*) quality", *Postharvest Biology and Technology*, vol. 36, no. 2, pp. 199-208.
- Tatham, A.S., Mifflin, B.J. & Shewry, P.R. 1985, "The beta-turn conformation in wheat gluten proteins: Relationship to gluten elasticity", *Cereal Chem.*, vol. 62, pp. 405-412.
- Tatham, A.S. & Shewry, P.R. 1995, "The S-poor prolamins of wheat, barley and rye", *Journal of cereal science*, vol. 22, no. 1, pp. 1-16.
- Tatham, A.S., Shewry, P.R. & Mifflin, B.J. 1984, "Wheat gluten elasticity: a similar molecular basis to elastin?", *FEBS letters*, vol. 177, no. 2, pp. 205-208.
- Thomson, N.H., Miles, M.J., Popineau, Y., Harries, J., Shewry, P. & Tatham, A.S. 1999, "Small angle X-ray scattering of wheat seed-storage proteins: α -, γ - and ω -gliadins and the high molecular weight (HMW) subunits of glutenin", *Biochimica et Biophysica Acta (BBA)/Protein Structure and Molecular Enzymology*, vol. 1430, no. 2, pp. 359-366.
- Tunc, S., Angellier, H., Cahyana, Y., Chalier, P., Gontard, N. & Gastaldi, E. 2007, "Functional properties of wheat gluten/montmorillonite nanocomposite films processed by casting", *Journal of Membrane Science*, vol. 289, no. 1-2, pp. 159-168.
- Ukai, T., Matsumura, Y. & Urade, R. 2008, "Disaggregation and reaggregation of gluten proteins by sodium chloride", *Journal of Agricultural and Food Chemistry*, vol. 56, no. 3, pp. 1122-1130.
- Van Der Borgh, A., Goesaert, H., Veraverbeke, W.S. & Delcour, J.A. 2005, "Fractionation of wheat and wheat flour into starch and gluten: overview of the main processes and the factors involved", *Journal of cereal science*, vol. 41, no. 3, pp. 221-237.
- van Dijk, A.A., van Swieten, E., Kruize, I.T. & Robillard, G.T. 1998, "Physical characterisation of the N-terminal domain of high-molecular-weight glutenin subunit Dx5 from wheat", *Journal of cereal science*, vol. 28, no. 2, pp. 115-126.
- Veraverbeke, W.S. & Delcour, J.A. 2002, "Wheat protein composition and properties of wheat glutenin in relation to breadmaking functionality", *Critical reviews in food science and nutrition*, vol. 42, no. 3, pp. 179-208.
- Vogler, E. 1998, "Structure and reactivity of water at biomaterial surfaces", *Advances in Colloid and Interface Science*, vol. 74, pp. 69-117.
- Wang, Q., Crofts, A.R. & Padua, G.W. 2003, "Protein-lipid interactions in zein films investigated by surface plasmon resonance", *Journal of Agricultural and Food Chemistry*, vol. 51, no. 25, pp. 7439-7444.

- Wrigley, C.W. 2000, "Wheat and Other Cereal Grains" in *Kirk-Othmer Encyclopedia of Chemical Technology* John Wiley & Sons, Inc., .
- Wyatt, P.J. 1993, "Light scattering and the absolute characterization of macromolecules", *Analytica Chimica Acta*, vol. 272, no. 1, pp. 1-40.
- Yarimkaya, S. & Basan, H. 2007, "Swelling behavior of poly(2-hydroxyethyl methacrylate-co-acrylic acid-co-ammonium acrylate) hydrogels", *Journal of Macromolecular Science, Part A*, vol. 44, no. 9, pp. 939-946.
- Zalm, E.E.J.v.d., Goot, A.J.v.d. & Boom, R.M. 2010, "Influence of sodium chloride on shear flow induced starch–gluten separation from Soissons wheat dough", *Journal of Food Engineering*, vol. 99, no. 3, pp. 366-372.
- Zandomeneghi, M. 1999, "Fluorescence of cereal flours", *Journal of Agricultural and Food Chemistry*, vol. 47, no. 3, pp. 878-882.

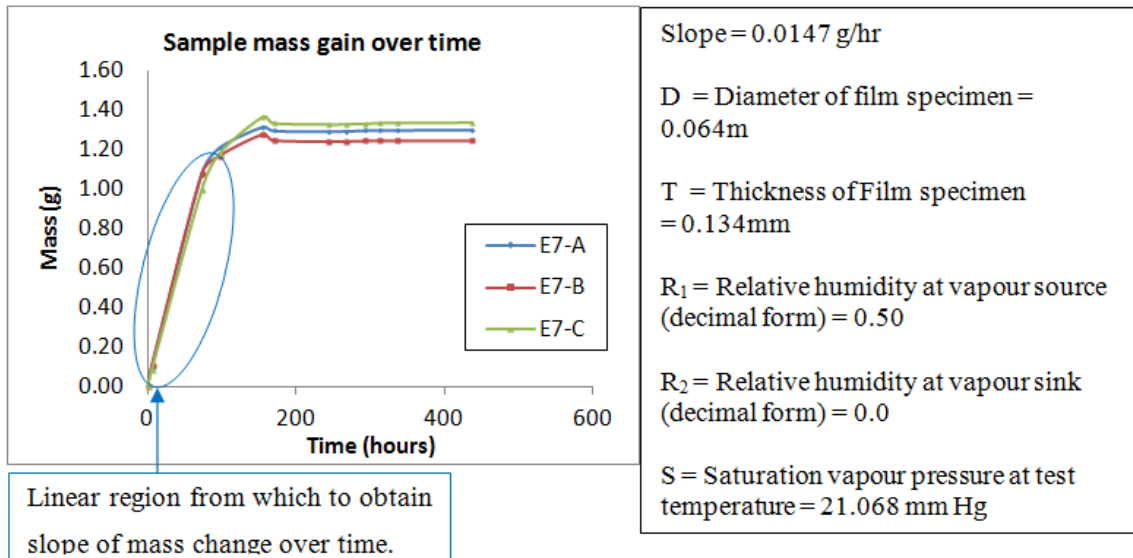
Appendix 1 – WVP Sample Calculation (metric units)

WVP was calculated using the following equation:

$$WVP = \frac{\text{Slope} \times T \times 760 \frac{\text{mmHg}}{\text{atm}}}{A \times (S \times (R_1 - R_2))}$$

Where the slope is the linear region in the graph of sample-mass versus time, T is the film thickness (mm), A is the surface area (m²) available for water vapour permeation, S is the known saturation vapour pressure (mmHg) at the test temperature (23 °C), and R₁ and R₂ are the relative humidity decimal values for the vapour source and the vapour sink respectively. The 760 mmHg/atm is a unit conversion factor.

Sample Data set



Estimation of the slope

The ASTM D1653 (ASTM Standard D1653, 2003 (2008)) says “When a straight line adequately fits the plot of at least four properly spaced points, a nominally steady state exists and the slope of the straight line is the rate of water vapour transmission.” Therefore, the slope was taken from a minimum of 4 data points forming a straight line and always starting with the first point to be the closest to time zero while being part of the other points producing the straight line. Further, when the slope of the line remained constant after the 4th data point, the slope was taken using as many additional points as possible without compromising the linearity of the line (Typically this meant up to around 150 or 250 hours).

When a data set did not have at least 4 data points to produce a straight line for times shorter than 200 h, this data set was not considered for WVP estimates which was reflected in the number of samples, n, listed in the WVP summary tables (normally n=3 for each film).

Calculation Steps

1. Calculate test area of film specimen (film area available for water vapour transfer):

$$Area = \pi \left(\frac{D}{2}\right)^2 = 3.14 \times \left(\frac{0.064m}{2}\right)^2 = 0.003 m^2$$

2. Calculate Water Vapour Transmission (WVT) rate:

$$WVT = \frac{Slope}{A} = \frac{0.0147 \frac{g}{hr} \times \frac{24hr}{1day}}{0.003 m^2} = 117.6 \frac{g}{m^2 \times 1 day}$$

3. Calculate Δp :

$$\Delta p = S \times (R_1 - R_2) = 21.068 mm Hg \times (0.50 - 0.0) = 10.534 mm Hg$$

4. Calculate Water Vapour Permeability (WVP) rate:

$$WVP = \frac{WVT}{\Delta p} = \frac{117.6 \frac{g}{m^2 \times 1 day}}{10.534 mm Hg} = 11.2 \frac{g}{m^2 \times 1 day \times mm Hg}$$

5. Calculate Water Vapour Permeability Rate with film thickness included, WVP_t (not part of ASTM):

$$\begin{aligned} WVP_t &= WVT \times T \times 760 \frac{mmHg}{1 atm} = 11.2 \frac{g}{m^2 \times 1 day \times mm Hg} \times 0.134 mm \times 760 \frac{mmHg}{1 atm} \\ &= 1136.5 \frac{g \times mm}{m^2 \times 1 day \times atm} \end{aligned}$$

Appendix 2 – Reported FTIR Peaks for Wheat Gluten, Glycerol, and Water

Table 33 – Major FTIR Gluten Protein Peaks according to Literature

Vibration Type	Wavenumber (cm ⁻¹)	Reference
Amide 1 (C=O stretching, N-H vibration)	~1650, broad (1580-1720)	(Olabarrieta et al. 2006, Ukai, Matsumura & Urade 2008, Chiou et al. 2010, Muensri et al. 2011, Georget, Belton 2006, Mojumdar et al. 2011)
Amide 2 (NH bending and CN stretching)	~1542, broad (1480-1575)	(Olabarrieta et al. 2006, Cho, Gällstedt & Hedenqvist 2010, Muensri et al. 2011, Georget, Belton 2006, Mojumdar et al. 2011)

Table 34 – Major FTIR Glycerol and Water Peaks of Gluten Films according to Literature

Vibration Type	Wavenumber (cm ⁻¹)	Reference
C-C-O stretch or CH ₂ twist of glycerol	850 (850-856)	(Olabarrieta et al. 2006, Cho, Gällstedt & Hedenqvist 2010, Mojumdar et al. 2011)
OH stretching (due to Water/glycerol and/or EtOH molecules)	3200-3800	(Mojumdar et al. 2011)

Table 35 – Major FTIR Peaks Characteristic of Proteins (Barth et al. ((Barth 2007))

Peak Name	Vibration Type	Wavenumber (cm ⁻¹)
Amide A	NH stretch	3300 (3310-3270)
Amide B	NH stretch	3070 (3100-3030)
Amide 1	C=O stretch, CN out-of phase stretch, CCN deformation, NH in plane bend	1650 (1600-1700)
Amide 2	Combined out of phase bends for: NH in-plane bends, CN stretch, some CO in-plane bends, CC and NC stretch	1550
Amide 3	In-phase NH bending, CN stretching, and some CO in-plane bending and CC stretching	(1400-1200)

Appendix 3 – Typical Amino Acid Sequences for Various Wheat Gluten Protein Classes

Below, are typical amino acid sequences for each wheat gluten protein type. Each wheat protein shown has a different amino acid sequence for its primary structure; however, some similarities are visible between the different types. For example, parts of the starting, repeating, and ending sequences of the α/β , γ , and ω gliadins share similarities. Also the B, C, and D type LMW classes of wheat protein share similarities in their repeating sequences. Note that different sources of wheat can also possess sequence differences.

Alpha/beta type gliadin amino acid sequence (Reeves, Okita 1987):

```

1 mktflilall aivattatta vrvvpvppqp qnpsqpqqqr qvplvqqqaf pggqqqfppq
61 qppqpqqpfp sqqpylqlqp fpqpqpfppq lpypppppfs pqqpypqqqp qypqqqqpis
121 qqqqqqqqqq qqqqqqqqqq qqilpqilqg qlipcrdvvl qqhniahars qvlqqstyqp
181 lqqllccqqlw qipeqsrcqa ihnvvhaiil hqqqqqqqps sqvslqqppq qypsgqgffq
241 psqqnpqaag svqqqqlpqf eeirnlalqt lprmcnvyip pycstttapf gifgtn
  
```

Gamma-Gliadin (Arentz-Hansen et al. 2000)

```

1 mniqvdpvsg vpwpqqqpf qphqpfqsqq qatfpqqqat fphqppqqfs qpqqppqqfi
61 qpqqppqtyp qrpqqpfpqt qppqqpfpqs qppqqpfpqp qqafpqqqqp qqsfpqqqps
121 liqqslqqql npcknflqq ckpvsllvss wsmilprsdq qvmrqqccqg laqipqqqlq
181 aaihsivhsi imqqeqqeqr qgvqilvpls qqqqvqggtl vqgggiqqp qpaqlevirs
241 lvlqtlatmc nvyvppycst irapfasiva giggqyr
  
```

Omega-Gliadin (Hsia, Anderson 2001)

```

1 mktflifvll amamkiataa relnpsnkel qspqqsfisy qapfpqqpyp qppypsqqpy
61 psqqpfptpq qafpeqsqqp ftqpqqptpi qppqpfpqqp qppqpfpqp qppfpwqpqq
121 pfpqtqqsfp lppqqpfpqq pppqpfpqq l pfpqqseqii pqqllqqpfp l qppqpfpqqp
181 qppfpqpqqp ipvqpqqsfp qqsqqsqppf aqqqqlfpe l qppipqqppq pfp lppqpfp
241 pppqpfpfpq qppqsfpqqp qppypqqqpy gssltsigqg
  
```

HMW glutenin amino acid sequence (Sugiyama et al. 1985):

```

1 makrlvlfva vvvalvalt v aegeaseqlq cerelgelqe relkacqgvm dqqlrdisp
61 chpvvvsppa gqyeqqivvp kggfsypget tppqqlqqri fwgipallkr yypsvtspq
121 vsyppgqasp qrpqgqgqpg qgqqsqgqg gyytspqqp gqwwqpeqgq pgyyptspq
181 pqqllqppaq qppqgqgqg qppqgqgqg ptssqlppg lqppaqqgqg qppqgqgqg
241 qppqgqgqg qppqgqgqg qppqgqgqg qlgqgqgqg pttllqsgqg ppyyptslq
301 qlgqgqsgyy ptspqppqg qppqqlqppa qgqgqgqg gqppqgqgqg qppqgqgqg
361 qgqppgyypts pqqsgqgqpg yyptssqapt qsqppqgqg gqavqgqgq qppqgqgqg
421 qgqppgyypts plqsgqgqpg yytspqqsg qgqppqqlq saqqgkqgqg qgqgqgqgq
481 qgqppqgqg qgqppqgqpg yytspqqsg qgqppqgqg pqqgqppgyy tsslqppqgq
541 pgydptspqq pqqgqgqgq qppaqqgqg qlaqqgqgq paqvqqgqg aqqgqgqgq
601 qgqgqgqgq gqppaqqgqg qppqgqgqg qppqgqgqg gqpwyyptsp qesgqgqgq
661 qwqppqgqg qgqgqgqg tsslqgqg qgyyptslq pqqgqgqg qgsgqgqgq
721 yptspqlsg qarpqgqlq gqgqgqypt spqqsgqgq lqqwlpqgq qgyyptslq
781 qtgqgqgqg qgqgyyssh vsvehqaas kvakaqqllaa qlpamcrleg gdalsasq
  
```

B-type LMW-s Glutenin (Huang, Cloutier 2008)

```

1 mktflifall avaatsaiag ienshipgle kpsqqqlpl qatllshqqq qpvaqqpppf
61 pqqppcsqqq qplsqqqqp pfsqqppfs qqqqpsfsq qpppfsqqq pfsqqqqpvi
121 pqqpsfsqqq lppfsqqqp fsqqqqpvlp qpppfsqqq pilpqqppfs qqqqqpvlp
181 qqipfvhpsi lqqllnpckvf lqqqcsppvam pqlarsqml qssschvmq qccqqlppip
241 qqsryeara iysiilqeq qvqgsiqs qppqqlgac vsppqqqsq qlgqqppqqq
  
```

301 laqgtflqph qiaqlevmts ialrilptmc rvnvplyrtrt tsvpfdvgtg vgay

B-type LMW-m Glutenin (Huang, Cloutier 2008)

1 mktflifall aiaatsaiaq metsrvpgle kpwqqqplpp qqppcsqqq qpfpqaaqpi
61 iilqqspfsq qqqpvlpqqq pviilqppf sqaqqpvlpq qppfsqqqqq qqqqqppfs
121 qqqqpvlpq ppfsqqqpp fsqqqqpssq qppfpqqhq qfqqqipvvq psvlaqlnpc
181 kvflqqqcsh vamsqrlars qmwqqsschv mqqqccqqlp qipeqsrsea iraiivysiil
241 qeqqqgfvqp qqqqppqsgq gvsqhqqqsq qqqqlgqcsf qppqqlqqlg qppqqaaqpa
301 giflqphqis qlevmtsial rtlptmcgvn vplyssttim pfsigtgvvg y

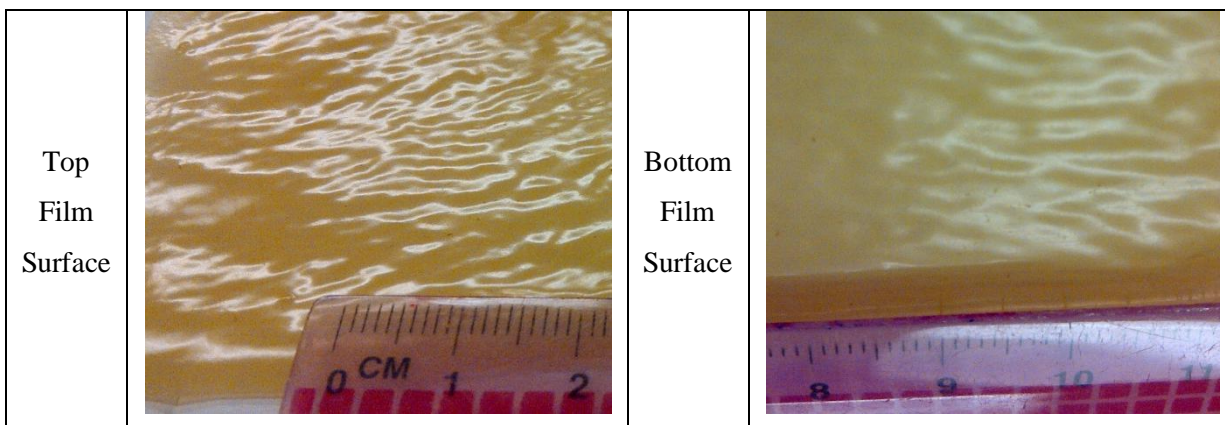
C-type LMW Glutenin

no sequence provided on NCBI database

D-type LMW Glutenin (Snegaroff - not published). Available on NCBI Protein Database/ GenBank CAR82265.1.

1 marqlnpsnk elsqpqsfs hqqqpfqqp ypqqypsq pypsqpft pqpqfqqsq
61 qpftqpqqpt plqqqpfpq qppqqppf qppqpfwqp qppfpqtqqs flqqqpfp
121 qppqpfpqp qlqfpqqpeq iipqqpppf llesqqpfpq qppqpfqpq qlipmqppq
181 fpqqsqqsq pfpqpqqflp elqqpqpqq qppfplqqq pfpqqsqppf pqqppqpcpl
241 qppqpfpqp qppfpqqppq pfpqqppf plrpqqpfsq qppqsqqsf qppqqppqp
301 silqqppfl qppqqlsqql eqtisqqppq pfpqqphqp qppqqpppy ssltsidg

Appendix 4 - Images of top and bottom surfaces of gluten film cast on a glass tray with a silicone release layer



The film is much smoother on the bottom surface than the top surface at the large (camera) scale but the eye can easily see the parallel lines on the bottom of the film (as described in chapter 4.3.1 Film Surface Morphology).

Appendix 5 - Gluten Preparation Method Comparison

Preparation Method provided by Dr. Loo-Sar Chia (University of Guelph, Guelph, ON) for the Gluten Preparation of old Wonder Gluten:

Gluten – Hand wash method (AACC approved method)

Objective

Starch, water-soluble pentosans, and water-soluble proteins can be removed from wheat flour by manipulating the dough in water, using the AACC approved “Hand washing method”, (Method 38-10.01) (AACC International.). The total wet or dry gluten is expressed as a percent of sample.

(When you wash the soft wheat, be very careful and use a slow flow of tap water or else you will wash away all the gluten especially at the beginning. Once you obtain a sponge type of texture, it will be easier to handle.)

Procedure

1. Weigh 25 g flour into mortar and add sufficient ice cold water to form a firm dough ball. Hand-knead dough and incorporate fines into a ball. Let dough stand in water at room temperature for 60 min.
2. Knead dough gently in stream of cold tap water over cheesecloth (No name, China) until starch and all soluble matter are removed. When much of the starch has been removed, the gluten ball will become darker and will take on a web-like structure.
3. To determine whether the gluten is approximately starch-free, let 1 or 2 drops of wash water, obtained by squeezing, fall into a beaker containing perfectly clear water. If starch is present, cloudiness appears.
4. Let gluten thus obtained by washing stand in water 1 hr, press as dry as possible between the hands, roll into a ball, place in pre-weighed flat-bottom dish, and weigh as moist gluten.
5. Freeze dry it and store at -80°C

Crude gluten will be used for casting film.

New Wonder wheat gluten was prepared in the same manner except for the following modification:

In step 2, after kneading the sample in cold tap water for 20 to 30 minutes, the sample was placed in the bowl of a Kitchen-Aid mixer with cold water and the dough hook attachment was used to knead the sample for 1 h, where the water was replaced every 15 min to remove the starch precipitates.

Appendix 6 - ADM Whetpro 80 Data Sheet

ADM PRODUCT DATA SHEET

WHETPRO® 80 VITAL WHEAT GLUTEN

GENERAL DESCRIPTION

WHETPRO®80 is a natural high protein, free-flowing powder extracted from premium quality Canadian wheat flour. Careful, enzyme-free processing, and stringent quality control procedures, guaranty a consistent, high-quality product. WHETPRO®80 is a highly functional vital wheat gluten for use in food systems requiring improved binding strength, increased ingredient carrying capacity and restructuring. It is also useful for adjusting the protein-carbohydrate ratio in flour to any desired level and for strengthening the "hinge" in buns and rolls. WHETPRO®80 helps prevent breakage in pretzels and other snack products without toughening the eating quality.

PRODUCT CHARACTERISTICS

- Excellent water absorption.
- A natural high protein.
- Forms a viscoelastic dough, absorbing about two parts water to one part gluten.
- Readily mixes with other dry ingredients and is easily handled and stored.
- Increases baking tolerances with increased absorption, mixing time tolerance, and fermentation tolerance.

INGREDIENT LIST

100% Vital Wheat Gluten

SUGGESTED APPLICATIONS

- Flour milling
- Baked goods
- Breakfast cereals
- Pasta fortification
- Breadings and batters
- Meat, meat analogs
- Surimi products
- Pet foods and aquaculture

TYPICAL COMPOSITIONAL ANALYSIS – Dry Basis

Protein (88% min. Nx6.25)	89
Protein (80% min. Nx5.7)	81
Moisture (8% max.)	6.0
Fat, EE (1.0% max.)	0.6
Ash (1.0% max.)	0.9
Water Absorption %	170
Reconstitution Time (20 seconds max.)	13

MICROBIOLOGICAL ANALYSIS- Maximum

Standard Plate Count	1 000/g
Yeast & Mold	100/g
E.coli	<10/g
Salmonella	Negative/25 g
Staphylococci	<10/g

TYPICAL PHYSICAL PROPERTIES

Color	Cream
Granulation:	100
thru 45 USBS, %	min 75
thru 80 USBS, %	min 70
thru 100 USBS, %	44
Bulk Density: packed, lb/ft ³	34
loose, lb/ft ³	



ARCHER DANIELS MIDLAND COMPANY, 995 MILL STREET, MONTREAL, QUEBEC, CANADA, H3C 1Y5
 TELEPHONE: 800-561-3715 OR 514-937-9937 FAX: 514-937-9578 www.adm.com

The information contained herein is correct to the best of our knowledge. The recommendations or suggestions contained in this bulletin are made without guarantee or representation as to results. We suggest that you evaluate these recommendations and suggestions in your own laboratory prior to use. Our responsibility for claims arising from breach of warranty, negligence, or otherwise, is limited to the purchase price of the material. Freedom to use any patent owned by ADM or others is not to be inferred for any statement contained herein.

Code 6006-C

PDS/01/2011

Appendix 7 - Total Protein Content Sample Calculation for Kjeldahl Method

The equation to calculate total protein content from the Kjeldahl method is:

$$Protein (\%) = \frac{Abs_{sample} - Abs_{Blank}}{B} * d_1 * d_2 * d_3 * 5.70 * \frac{1}{wt_{initial\ dry\ sample}} * 100$$

Where

$$\frac{Abs_{sample} - Abs_{Blank}}{B} * d_1 * d_2 * d_3 * 5.70 = Protein [\mu g]$$

Abs_{sample} = absorbance recorded for sample

Abs_{Blank} = absorbance recorded for blank (prepared without adding the protein)

B = slope of calibration curve in 1/ μ g

d₁ = dilution in volumetric flask = 100

d₂ = dilution to fit in calibration curve $\left(\frac{600\mu L + 200\mu L}{200\mu L}\right) = 4$

d₃ = switch from 5 ml test tube scale colorimetric assay to 250 μ L 96-well plate scale $\left(\frac{5000\mu L}{250\mu L}\right) = 20$

wt_{initial dry sample} = the recorded mass of the initial dry sample in μ g

The 5.7 x factor is the nitrogen to protein conversion factor specific to wheat (Genot et al. 1992)

Sample Data Set

Abs_{sample} = (0.363+0.365+0.359)/3 = 0.3623 \pm 0.003 (average of 3 absorbance measurements \pm standard deviation)

Abs_{Blank} = (0.226+0.228)/2 = 0.227 \pm 0.001 (average of 2 absorbance measurements \pm standard deviation) Here n=2 instead of n=3 because a mistake was made on 1 of the 3 wells.

d₁ = 100

d₂ = $\left(\frac{600\mu L + 200\mu L}{200\mu L}\right) = 4$

d₃ = $\left(\frac{5000\mu L}{250\mu L}\right) = 20$

wt_{initial dry sample} = 16100 μ g

Calculation of Slope B and Estimation of Associated Error

B is obtained from the standard calibration curve where Abs_{Blank} is subtracted from each standard absorbance value (Table 36) and plotted against the standard concentrations (Figure 18).

Table 36 - Kjeldahl Standard Absorbances as a function of Concentrations

Sample	Concentration (μg)	Absorbance \pm Standard Deviation	Absorbance minus Blank \pm Error *
Blank	0	0.22700 ± 0.001	0.00000 ± 0.002
Standard 20%	0.1	0.26867 ± 0.001	0.04167 ± 0.002
Standard 40%	0.2	0.32233 ± 0.006	0.09533 ± 0.007
Standard 60%	0.3	0.38067 ± 0.009	0.15367 ± 0.010
Standard 80%	0.4	0.43433 ± 0.010	0.20733 ± 0.011
Standard	0.5	0.48467 ± 0.003	0.25767 ± 0.004

* Error is combined with standard deviation from blank absorbance (0.001): add 0.001 to each standard deviation value from the absorbance column to get the new error values.

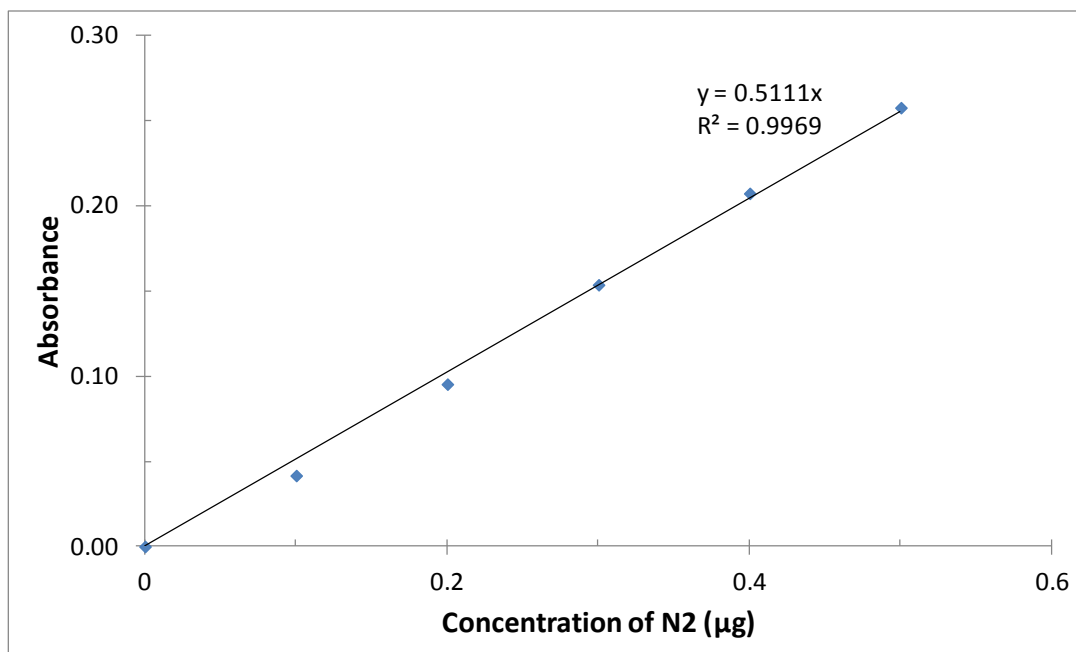


Figure 18 - Kjeldahl Absorbance as a function of Concentrations

From the line equation (Figure 18) we have the slope $B = 0.5111$.

Error of the slope, B, can be approximated by taking the difference between B (0.5111) and the slope using the worst case "Absorbance minus Blank" values at concentrations 0.1 μg and 0.5 μg :

At concentration $x = 0.1 \mu\text{g}$, change $y = 0.04167$ to $y = 0.04167 - 0.002 = 0.03967$

At concentration $x = 0.5 \mu\text{g}$, change $y = 0.25767$ to $y = 0.25767 + 0.004 = 0.26167$

The worst case slope is therefore: 0.5342

Error of slope $B = 0.5342 - 0.5111 = 0.0231 \sim 0.02$

Therefore, $B = 0.51(11) \pm 0.02 \mu\text{g}^{-1}$

Calculation of Percent Protein Content and Estimation of Associated Error

Protein (%)

$$\begin{aligned}
 &= \frac{Abs_{sample} - Abs_{Blank}}{B} * d_1 * d_2 * d_3 * 5.70 * \frac{1}{wt_{initial\ dry\ sample}} * 100 \\
 &= \frac{0.3623 - 0.2270}{0.5111 * \mu\text{g}^{-1}} * 100 * 4 * 20 * 5.70 * \frac{1}{16100 \mu\text{g}} * 100 \\
 &= 75.0\%
 \end{aligned}$$

The error is based on standard deviation of absorbance values, error of slope B ($0.02 \mu\text{g}^{-1}$), and balance errors for the initial dry sample mass (200 μg)

Error (%)

$$\begin{aligned}
 &= \left(Error(Abs_{sample}) + Error(Abs_{Blank}) \right) * Error(B) * Error(wt_{initial\ dry\ sample}) * 100\% \\
 &= (0.003 + 0.001) * 0.02 \mu\text{g}^{-1} * 200 \mu\text{g} * 100\% \\
 &= 1.8\% \sim 2\%
 \end{aligned}$$

Appendix 8 - Viscosity Sample Calculation

Sample Data Set

Efflux time = 134.44 s

Viscometer constant = 0.01439 cSt/s

Sample Calculation

Kinematic Viscosity

= efflux time x Viscometer constant

= 134.44 s x 0.01439 cSt/s

= 1.93459 cSt

~1.93 cSt

Appendix 9 - TGA Estimating 1% Onset of Degradation

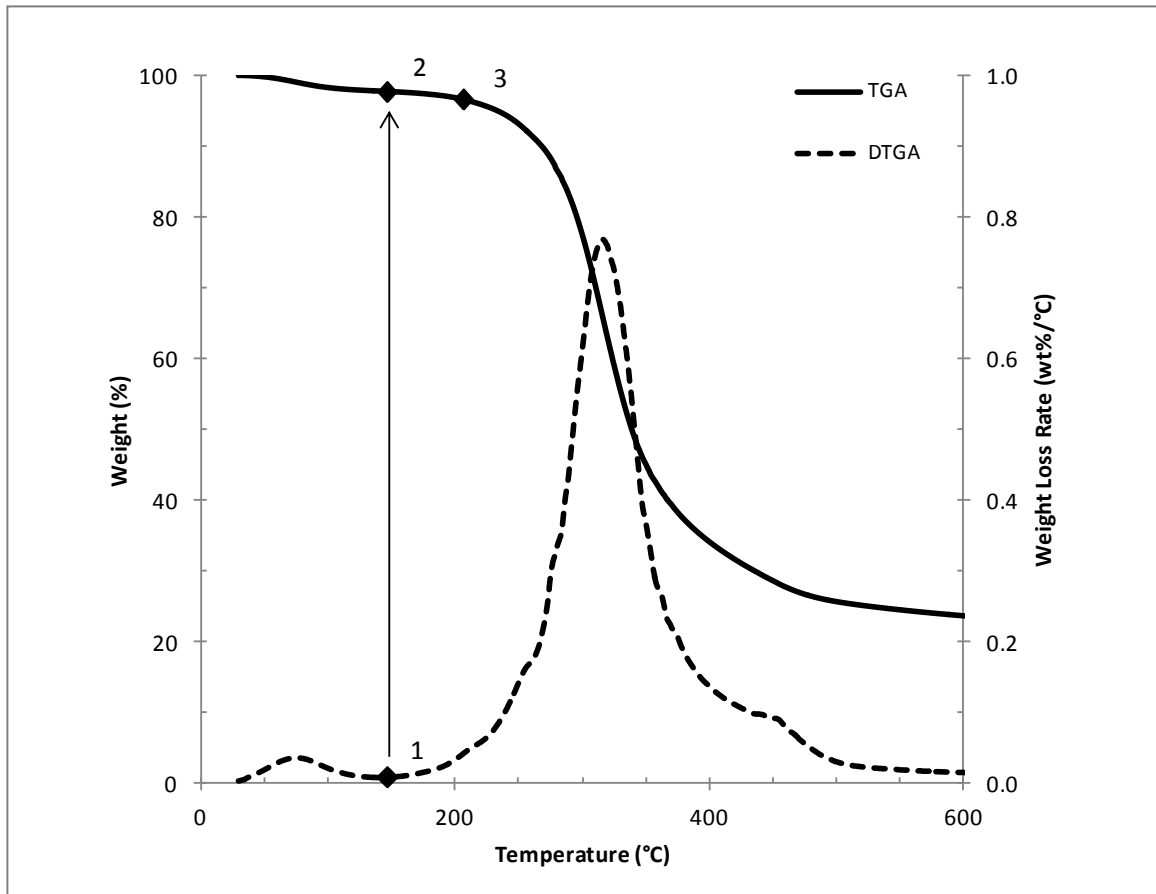


Figure 19 - Sample Data Set: TGA and DTGA curves for Wonder Wheat Gluten

The DTGA minimum occurring directly *after water evaporation* is located at 141.3°C (Figure 19, point 1) and also corresponds to a weight percent of 96.83% on the TGA curve (Figure 19, point 2). To determine the temperature at 1% weight loss *beginning after water evaporation*, 1% is subtracted from 96.83%, to yield 95.83% (Figure 19, point 3). The temperature, at 95.83% on the TGA curve is 202.97°C (Figure 19, point 3).

Therefore, temperature at 1% onset of degradation = 203.0°C

Appendix 10 - Film Swelling Sample Calculations

Swelling Ratio

Sample data set with film sample prepared at 70°C, pH 11:

Mass of sample before soaking, conditioned at 23°C, 50% RH = 0.0176 g

Mass of sample after 24 h soak in water = 0.0368 g

$$\begin{aligned}q &= \frac{mass_{swollen}}{mass_{dry}} \\ &= \frac{0.0368 \text{ g}}{0.0176 \text{ g}} \\ &= 2.09\end{aligned}$$

Total Solids

Sample data set with film sample prepared at 70°C, pH 11 and soaked 24 h:

Mass of aluminum pan = 0.9859 g

Mass of aluminum pan + aqueous sample = 8.4481g

Mass of aluminum pan + solid sample = 0.9879 g

Mass of solid sample (total solids dry mass)

$$\begin{aligned}&= (\text{Mass of aluminum pan + solid sample}) - \text{Mass of aluminum pan} \\ &= 0.9879 \text{ g} - 0.9859 \text{ g} \\ &= 0.0020 \text{ g} = 2.0 \text{ mg}\end{aligned}$$

Mass of liquid sample

$$\begin{aligned}&= (\text{Mass of aluminum pan + aqueous sample}) - \text{Mass of aluminum pan} \\ &= 8.4481\text{g} - 0.9859 \text{ g} \\ &= 7.4622 \text{ g}\end{aligned}$$

Total solids content

$$\begin{aligned}&= \left(\frac{\text{Dissolved Solid Mass}}{\text{Soak Liquid Mass}} \times 100 \right) \\ &= \left(\frac{0.0020 \text{ g}}{7.4622 \text{ g}} \times 100 \right) \\ &= 0.027 \%\end{aligned}$$

All data was measured in duplicate (n=2) and standard error was calculated for each film type.

BSA Calibration Curve, Protein Concentration Estimate and Total Mass Estimate

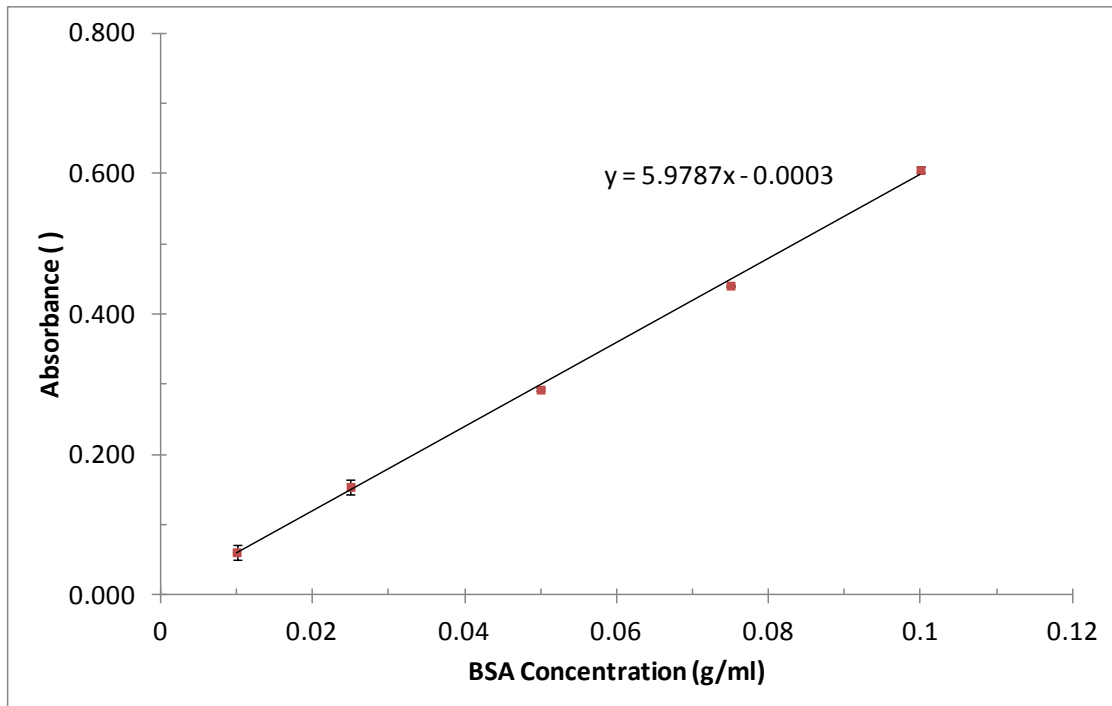


Figure 20 - BSA Calibration Curve for Wheat Gluten Concentration Estimate (vertical error bars are shown on graph but are very small)

Sample calculation of wheat gluten concentration estimate:

Absorbance t1 = 0.134

Absorbance t2 = 0.1325

Average absorbance = 0.133

Gluten concentration estimate (using BSA calibration curve)

= (average absorbance - intercept) / line slope

= $(0.133 - (-0.0003)) / (5.9787 \text{ g/ml})$

= 0.0223 g/ml

Total gluten mass estimate (using BSA calibration curve)

= Concentration estimate * sample volume

= 0.0223 g/ml * 2ml

= 0.0447 g = 44.7 mg